CHEMICAL INHIBITION OF RNA VIRUSES REVEALS REDD1 AS A HOST DEFENSE FACTOR

APPROVED BY SUPERVISORY COMMITTEE

_____
Beatriz Fontoura, Ph.D.

_____
Michael Roth, Ph.D.

_____
Michael White, Ph.D.

_____
Lawrence Lum, Ph.D.

# ACKNOWLEDGMENTS

I would like to acknowledge everyone who in some way helped me complete this work. In particular, I would like to thank my mentor, Beatriz Fontoura, who mentored and guided me throughout these five amazing years. Also, I would like to thank my Graduate Committee, Dr. Lawrence Lum, Dr. Michael Roth, and Dr. Michael White for their continuous support and valuable advice. Many thanks to current and past members of the Fontoura lab who helped carry this project and without whom none of these would have been possible.

También me gustaría darle las gracias a mi Hermosa Esposa, Yazmin Carrasco. Con tu amor, apoyo, y constante impulso me llevaste cada día a no solo ser mejor persona sino también a ser mejor esposo, hijo, tío, y todo lo demás. Este Mayo pasado después de unos cuantos años de noviazgo nos unimos en unión matrimonial y empezó una nueva etapa en nuestras vidas. Solo espero que en el futuro que nos espera juntos continúes estando tan orgullosa de mí como yo lo estoy de ti. A tu lado y con tu amor se que los obstáculos que la vida ponga en nuestro camino los podremos superar porque nos tenemos el uno al otro. Gracias por todo lo que me das Amor, solo espero hacerte tan feliz como tú me haces a mí. TE AMO MI VIDA!

A mis padres, José y Margarita Mata, muchas gracias por darme la vida y por todo su amor y apoyo. Gracias por la cantidad de burritos de barbacha, por los jugos Jumex, por la cantidad de besos y abrazos que por 28 años me han brindado. Gracias por ser los mejores padres que cualquier persona pudiera pedir, estoy tan orgulloso de ser su

hijo. Gracias a mis hermanos Pancho, Tito, y Perla por su amor, apoyo incondicional, y por las enseñanzas como niño y como adulto. Mis sobrinos Alexa, Cuchifleto Veloz, Diego Mata Canales, Grecia “La Vaca”, Dominique “La Gallinita”, y a nuestro hermoso ahijado Emiliano gracias por haber traído a mi vida tanta felicidad, su Titillo siempre en todo momento estará a su lado. También gracias a mi Suegra, Bertha Bañuelos, por haber dado luz a la mujer más hermosa del universo y por el amor y apoyo que me brindo desde el primer día que puse un pie en su hogar.

GRACIAS FAMILIA, LOS AMO

# CHEMICAL INHITION OF RNA VIRUSES REVEALS REDD1 AS A HOST DEFENSE FACTOR

by

MIGUEL ANGEL MATA

DISSERTATION

Presented to the Faculty of the Graduate School of Biomedical Sciences

The University of Texas Southwestern Medical Center at Dallas

In Partial Fulfillment of the Requirements

For the Degree of

DOCTOR OF PHILOSOPHY

The University of Texas Southwestern Medical Center at Dallas

Dallas, Texas

August, 2013

CHEMICAL INHIBITION OF RNA VIRUSES REVEALS REDD1 AS A HOST DEFENSE FACTOR

MIGUEL ANGEL MATA, Ph.D.

The University of Texas Southwestern Medical Center at Dallas, 2013

BEATRIZ FONTOURA, Ph.D.

Influenza (flu) is a contagious infectious respiratory illness. The flu can cause from mild to life-threatening illness. The current therapeutic intervention strategies to prevent or treat influenza infection are not sufficient in the event that a pathogenic virus strains reaches pandemic proportions. Therefore, the development of anti-influenza therapeutic modalities is critical to respond to a future influenza pandemic.

In this study, a chemical genetics approach was taken to identify inhibitors of NS1, a major influenza A virus virulence factor that inhibits host gene expression. A high-throughput screen of 200,000 synthetic compounds identified small molecules that

reversed NS1-mediated inhibition of host gene expression. A counterscreen for suppression of influenza virus cytotoxicity identified naphthalimides that inhibited replication of influenza virus and vesicular stomatitis virus (VSV). The mechanism of action occurs through activation of REDD1 expression and concomitant inhibition of mammalian target of rapamycin complex 1 (mTORC1) via TSC1–TSC2 complex. The antiviral activity of naphthalimides was abolished in *REDD1*$^{-/-}$ cells. Inhibition of REDD1 expression by viruses resulted in activation of the mTORC1 pathway. *REDD1*-/- cells prematurely upregulated viral proteins via mTORC1 activation and were permissive to virus replication. In contrast, cells conditionally expressing high concentrations of REDD1 downregulated the amount of viral protein. Whole animal studies revealed *REDD1*-/- mice are highly susceptible to virus infection. Influenza infection of *REDD1*-/- mice results in decreased TLR7 and MHC class II expression by dendritic cells and macrophages. In addition, excessive inflammatory cell infiltration in the lungs of *REDD1*-/- infected mice was observed. Preliminary evidence suggests a potential defect in NF-κB signaling upon influenza virus infection in REDD1 deficient mice. Thus, REDD1 is a new host defense factor, and chemical activation of REDD1 expression represents a potent antiviral intervention strategy.

Our studies also reveal passage immortalization of *REDD1*-/- MEFs require loss of the type I IFN response pathway as these cells are unable to induce the expression of interferon genes and interferon inducible genes when challenged with synthetic dsRNA. In contrast, primary or SV40 large T antigen transformed *REDD1*-/- MEFs activate a type I IFN response when exposed to synthetic dsRNA.

**TABLE OF CONTENTS**

## PUBLICATIONS

Kuss SK, **Mata MA**, Zhang L, and Fontoura BMA. (2013) Nuclear Imprisonment: Viral Strategies to Arrest Host mRNA Nuclear Export. *Viruses* 5: 1824-1849.

**Mata MA**, Satterly N, Versteeg GA, Frantz D, Wei S, Williams N, Schmolke M, Pena-Llopis S, Brugarolas J, Forst CV, White MA, Garcia-Sastre A, Roth MG, and Fontoura BMA. (2011) Chemical inhibition of RNA viruses reveals REDD1 as a host defense factor. *Nature Chemical Biology* 7: 712-719

Link N, Chen P, Lu WJ, Pogue K, Chuong A, **Mata MA**, Checketts J, and Abrams JM. (2007) A collective form of cell death requires homeodomain interacting protein kinase. *Journa of Cell Biology*, 178(4): 567-574

## LIST OF FIGURES

## LIST OF ABBREVIATIONS

| | |
|---|---|
| IAV | Influenza A virus |
| VSV | Vesicular stomatitis virus |
| REDD1 | Regulated in development and DNA Damage protein 1 |
| NS1 | Non-structural protein 1 |
| Poly(I:C) | Polyinosine-polycytidylic acid |
| DMSO | Dimethyl sulfoxide |
| 5’-ppp RNA | 5’-triphosphorylated RNA |
| ATP | Adenosine triphosphate |
| PBS | Phosphate buffered saline |
| FBS | Fetal bovine serum |
| Tet | Tetracycline |
| GFP | Green fluorescent protein |
| DMEM | Dulbecco’s Modified Eagle Medium |
| IFN | Interferon |
| NF-κB | Nuclear factor kappa B |
| GSEA | Gene Set Enrichment Analysis |
| HBEC | Human bronchial epithelial cells |
| SAR | Structure Activity Relationship |
| MDCK | Madin-Darby canine kidney |
| RLU | Relative light units |
| LN | Natural log |
| DIC | Differential interference contrast |

| | |
|---|---|
| h.i.p. | Hours post infection |
| PFU | Plaque forming units |
| SeV | Sendai virus |
| HAU | Hemagglutination units |
| C.P.M. | Counts per minute |
| HCV | Hepatitis C virus |
| QPCR | Real Time PCR |
| Act D | Actinomycin D |
| CQ | Chloroquine |
| GAP | GTPase activating protein |
| m.o.i. | Multiplicity of infection |
| P/M | Polysome/monosome ratio |
| DC | Dendritic cell |
| APC | Antigen presenting cell |
| MFI | Mean fluorescence intensity |
| MHC | Major histocompatibility complex |
| BAL | Broncoalveolar lavage |
| ELISA | Enzyme-linked immunosorbent assay |
| Con A | Concanavalin A |
| PRR | Patter Recognition Receptors |
| CHX | Cyclohexamide |
| h.p.t. | Hours post-transfection |
| dsRNA | Double stranded RNA |

# CHAPTER ONE
# Introduction and Literature Review

## *Influenza A virus, a global threat*

Human influenza virus (flu) is a highly infectious respiratory illness. A wide variety of respiratory signs and symptoms can arise ranging from cough, sore throat, and rhinitis to abrupt onset of fever and myalgia. Influenza illness is cleared 3-7 days after infection for the average healthy individual. However, existing medical conditions can exacerbate what is an otherwise uncomplicated illness leading to secondary bacterial pneumonia, sinusitis, or contribute to infections with other viral or bacterial pathogens (1). Seasonal epidemics occur every year during the fall/winter months due to the continuous accumulation of mutations in the viral genome, specifically in the coding sequences of two surface viral glycoproteins, hemaglutinin (HA) and neuraminidase (NA), which are normally recognized and neutralized by the host immune system. This process of antigenic drift allows the virus to evade the host's pre-existing immunity, leading to the emergence of pathogenic strains to which humans are immunologically naïve. Such a strain surfaced in 1918 and caused the Spanish influenza pandemic. It is estimated that between 1918 and 1919 more than 50 million people perished worldwide (2). Most recently, in 2009, a flu outbreak, categorized as Swine flu, was reported by the U.S. Center for Disease Control and Prevention (CDC). By the end of the Swine flu pandemic, more than 40,000 laboratory-confirmed cases and 302 deaths were reported in the United States, making it the first pandemic of the 21$^{st}$ century (3).

Influenza A virus genome is comprised of eight individual gene segments (4). Genome segmentation facilitates reassortment of influenza A virus (IAV) subtypes generating a virus with a genome composed of segments from one or more virus subtypes to which the population lacks immunity. The influenza strain that caused the 2009 Swine flu outbreak originated from a triple reassortment event in which genomic material from swine, avian, and human influenza virus combined to produce an infectious virus to which no pre-existing immunity was present in the human population (5).

Seasonal influenza infections are responsible for ~20,000 deaths annually in the United States (6) and up to one million deaths worldwide (7). Annual influenza epidemics, in the United States alone, account for an estimated $10 billion in U.S. dollars in direct medical costs (8). Currently, protective measures for preventing or treating influenza infections include vaccination and antiviral agents. Immunoprophylaxis remains the most effective preventive strategy against influenza infection. Based on the data generated from the U.S. Influenza Surveillance System that determines which influenza viruses are circulating and which are most likely to cause the most illness during the next influenza season, trivalent influenza vaccines are produced to administer to the general population each year. At present, three FDA-approved seasonal vaccines are administered in the United States (9). Due to the viral genetic diversity and rapid rate of mutation of influenza virus, constant re-formulation of vaccines occurs every year. The 2009 Swine flu represented a case in which no immunologically matched vaccines were available for the circulating virus strain due to the triple reassortment event which generated this novel agent (5) . In the event of a pandemic, the number of vaccines available would be inadequate and could take months to generate a protective

immunoprophylactic against a novel influenza virus strain (7). Thus, the use and development of anti-viral drugs represents a critical therapeutic strategy for preventing and treating influenza. Two classes of clinically-approved anti-influenza drugs have been developed: amantadine and neuraminidase inhibitors. Amantadine was the first chemical compound reported to inhibit influenza virus replication (10). These agents interfere with viral uncoating and genome release inside the host by blocking the activity of the viral M2 ion channel which is required for the early phase of the replication cycle (11). Due to the rapid emergence of drug-resistant influenza virus strains and central nervous system side effects, amantadine use for the treatment of influenza is limited (12). The second class of clinically approved anti-influenza agents, neuraminidase inhibitors, block progeny virion release from infected cells, thus preventing infection of surrounding host cells and halts the spread of the virus. These anti-viral agents inhibit the enzymatic activity of the viral NA protein, whose activity is necessary for the detachment of the progeny virions from infected host cells (13). Unlike amantadines, neuraminidase inhibitors are well tolerated by humans and can be administered to prevent or treat influenza virus infections (12). However, the emergence of influenza virus resistant strains to neuraminidase inhibitors has raised concerns about the limited therapeutic intervention strategies available to prevent and treat influenza (7). These examples highlight the importance for developing additional anti-influenza therapeutic modalities to improve our capacity to respond to a potential influenza pandemic.

An alternative strategy to antiviral drugs that target key viral protein function(s) is to therapeutically target host cellular factors that are essential for influenza virus replication but are not cytotoxic at the effective concentrations. This new class of

therapeutic modalities that safely target the host can limit the emergence of drug-resistant virus strains because it's more difficult for the virus to adapt and evolve to changes in the molecular architecture of the host. Hundreds of human host factors necessary for influenza virus replication have been identified via genome-wide RNA interference (RNAi) and genetic screens (14-16). The vast amount of information gathered has resulted in an explosion of candidate genes available for therapeutic targeting and has shed light on previously uncharacterized host-pathogen interaction networks. Of particular interest to this study, pharmacological inhibition or silencing the expression of the conserved serine/threonine kinase mammalian target of rapamycin complex 1 (mTORC1) resulted in the inhibition of influenza virus replication (15). The mechanism by which inhibition of mTORC1 leads to a reduction in virus replication was not determined (15).

***The mammalian target of rapamycin (mTOR)***

First described in the budding yeast, target of rapamycin (TOR) has been identified in mammals, algae, slime mold, plants, worms, and flies (17). In mammals, TOR protein is known as the mammalian target of rapamycin (mTOR). This evolutionary conserved serine/threonine kinase is a central regulator of cell growth, proliferation, and metabolism. Its importance in cellular homeostasis is highlighted by evidence demonstrating genetic deletion of TOR in a number of eukaryotes (worms, flies, and mice) results in impaired cell growth and proliferation leading to developmental arrests (17). Isolated from the bacterium *Streptomyces hygroscopicus*, rapamycin, a potent

secondary metabolite capable of inhibiting the proliferation of mammalian cells (17), has shown to be an indispensable experimental tool to dissect the role TOR plays during growth and development. Mechanistically, Heitman and colleagues first demonstrated rapamycin-mediated inhibition of TOR in *S. cerevisiae* requires the cellular cofactor FKBP12 (18).

In mammals, mTOR is part of two distinct complexes: the rapamycin-sensitive mTOR complex 1 (mTORC1) and the rapamycin-insensitive mTOR complex 2 (mTORC2). Each complex is composed of different subunits. mTORC1 is composed of five components including: mTOR kinase, the regulatory-associated protein of mTOR (Raptor), the mammalian lethal with Sec13 protein 8 (mLST8), the proline-rich AKT substrate 40kDa (PRAS40), and DEP-domain-containing mTOR-interacting protein (Deptor) (19). mTORC2 is compose of six components including: mTOR, the rapamycin-insensitive companion of mTOR (Rictor), the mammalian stress-activated protein kinase interacting protein (mSIN1), the protein observed with Rictor-1 (Protor-1), mLST8 and Deptor (19). In contrast to mTORC1, little is known about the cellular functions of mTORC2. Cytoskeletal organization and activation of the serine/threonine kinase AKT, a kinase involved in cell survival and proliferation, are two a biological processes that have been demonstrated to be regulated by mTORC2 (19). On the other hand, mTORC1 has been shown to positively regulate growth, development, immunity, protein and lipid synthesis, mitochondrial metabolism and biogenesis, and to limit catabolic process such as autophagy (19) (Figure 1).

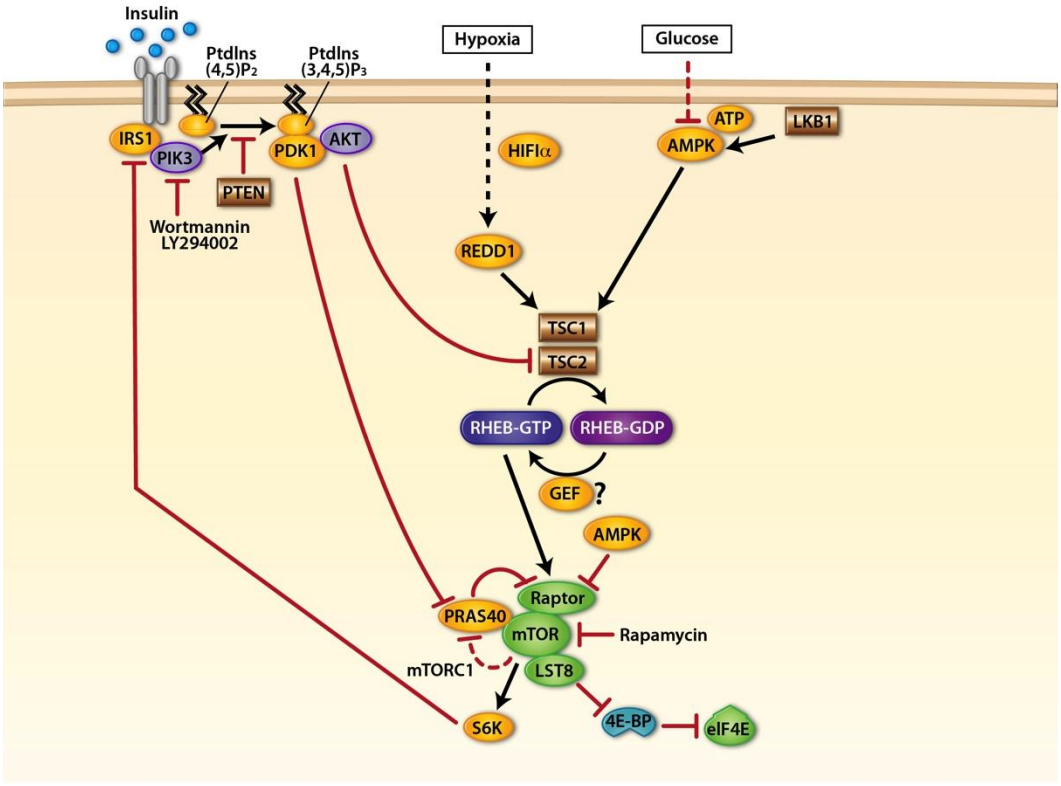


**Figure 1. mTORC1: master regulator of cell growth, proliferation, and metabolism.** The mTORC1 signaling pathway integrates multiple environmental signals to regulator growth and metabolism. Upon insulin detection, the PI3K/AKT pathway promotes the activation of mTORC1 leading to S6K activation and inactivation of 4E-BPs, both regulators of protein synthesis. Under a number of environmental conditions, such as limited growth factors, oxygen, amino acids, and glucose levels, the mTORC1 pathway is downregulated in an effort to limit energy-consuming cellular process. In turn, the autophagy pathway is activated in an effort to re-establish cellular balance by providing biological material to maintain energy-demanding processes.

***Cellular processes governed by the mTORC1 signaling pathway***

Protein synthesis is a highly regulated cellular process controlled by the mTORC1 signaling pathway. Two of the most extensively studied mTORC1 substrates regulate mRNA translation, p70 S6k (S6K) and eukaryotic initiation factor 4E-binding protein 1 (4E-BP1) (Figure 1). Hypophosphorylated 4E-BP1 binds and sequesters the translation initiation factor eIF-4E from the cap-dependent complex, thus preventing cap-dependent mRNA translation (20). mTORC1-mediated phosphorylation of 4E-BP1 results in the dissociation and release of eIF-4E restoring cap-dependent translation (17). S6K activation, via mTORC1-dependent phosphorylation, promotes protein synthesis by acting on several substrates. Phosphorylation and degradation of the programmed cell death 4 (PDCD4) protein mediated by S6K releases PDCD4 inhibitory activity on eIF4A, an RNA helicase involved in unwinding secondary structures in the 5' UTR of mRNAs (21). In addition, activation of S6K by mTORC1 results in its recruitment to the exon-junction complex (EJC), a multiprotein structure involved in mRNA surveillance, mediated by the S6K binding partner and substrate SKAR (22-23). Phosphorylation of several mRNA-binding proteins was observed upon S6K loading onto the EJC and this coincided with efficient spliced-mRNA translation (22). Finally, through an unknown mechanism, mTORC1 positively regulates the translation of a subset of transcripts containing a 5'-tract of oligopyrimidine (5'-TOP) sequence, found on many mRNAs including those encoding components of the translational machinery (24). Translation of these transcripts would likely result in a general increase in translation.

Activation of mTORC1 in nutrient-rich conditions stimulates anabolic processes while restricting catabolic pathways. An important catabolic pathway in health and

disease is autophagy, the process of degrading cellular components, including proteins and organelles, via lysosomal degradation to recycle macromolecules (25). mTORC1 dependent phosphorylation of the autophagy initiators autophagy-related gene 13 (ATG13) and unc-51-like kinase 1 and 2 (ULK1/2) inhibits autophagy by blocking the nucleation of the complex required for autophagosome formation (26). In contrast, starvation-induced or pharmacological inhibition of mTORC1 with rapamycin results in hypophosphorylation of ATG13 and ULK1/2 leading to autophagosome formation and lysosomal fusion (26).

mTORC1 integrates multiple extracellular and intracellular signals such as growth factors, nutrient availability, cellular energy, and stress conditions to regulate cell growth and proliferation. Upregulation of mTORC1 by growth factors occurs via the PI3K/AKT pathway (Figure 1). In response to insulin, phosphatidylinositol-3,4,5-phosphate (PIP3) levels rise at the plasma membrane leading to recruitment of PDK1 and AKT. At the plasma membrane, PDK1 and mTORC2 phosphorylate and activate AKT (27). Downregulation of this pathway is achieved by reduction in PIP3 levels by the tumor suppressor PTEN (17). Following activation, AKT directly phosphorylates the tuberous sclerosis tumor suppressor proteins 2 (TSC2) protein, a subunit of the TSC1/TSC2 heterodimeric complex that acts as a negative regulator of the mTORC1 signaling pathway, which disrupts TSC1 and TSC2 interaction leading to mTORC1 activation (28). The TSC1/TSC2 complex act as a GTPase-activating protein (GAP) towards the small GTPase Ras homologue enriched in the brain (Rheb), a known mTORC1 interacting partner (29). Rheb, in its GTP state, directly associates and

activates mTORC1 (30). Conversion of Rheb-GTP to Rheb-GDP, mediated by the TSC1/TSC2 complex, leads to the downregulation of mTORC1 activity (29) (Figure 1).

In addition, amino acid levels have been shown to modulate mTORC1 activity independent of the TSC1/TSC2 complex (31). When amino acids are abundant, the Rag proteins, four small GTPases RagA/B and RagC/D, associate with the mTOR complex 1 subunit Raptor resulting in the activation of mTORC1(32). A complex found on the lysosomal membrane and composed of three proteins (Mp1, p14, and p18), termed the Ragulator, was shown to activate mTORC1 by interacting and recruiting the Rag proteins to the lysosome where mTORC1 associates with its activator Rheb (33). In amino acids starving conditions, mTORC1 remains cytoplasmic, the Rag proteins fail to associate with Raptor, and the activity of mTORC1 is downregulated as it fails to translocate to the lysosome where Rheb is localized (32).

Under unfavorable conditions, including low oxygen conditions (hypoxia), mTORC1 activity is downregulated to limit energy-demanding processes and maintain cellular homeostasis (34). Brugarolas and colleagues demonstrated hypoxia-mediated downregulation of mTORC1 activity not only required an intact TSC1/TSC2 complex but also require the hypoxia-inducible gene regulated in development and DNA damage (*REDD1* or *DDIT4*) (35). Genetic deletion of REDD1 leads to increase mTORC1 activity under hypoxic conditions, while REDD1 overexpression is sufficient to inhibit mTORC1 activity in a TSC1/TSC2 complex dependent manner (35-36).

***mTORC1 and cancer***

mTORC1 regulates key cellular signaling pathways that are commonly found to be deregulated in human cancers, suggesting a potential role for mTOR in cancer. In fact, disruption of positive and negative mTORC1-regulators has been implicated in tumor development. Germline mutations to the *TSC1* or *TSC2* genes (a heterodimeric complex responsible for negatively regulating mTORC1 activity) results in the tuberous sclerosis complex (TSC) syndrome, a genetic disease characterized by benign tumors in a number of tissues including kidney, brain, heart, lung and skin that can progress to malignancy (37). This relationship between TSC and the mTORC1 pathway represented the first link of mTOR with cancer. Also, mutations in the tumor suppressor phosphatase and tensin homolog (*PTEN*) gene, a negative regulator of mTORC1, are commonly found in a variety of human cancers including prostate, breast, lung, bladder, melanoma, renal carcinoma, and others (38). Because PTEN is a known negative regulator of AKT, an oncoprotein with aberrant activity in several cancers and a well-characterized positive regulator of mTORC1, recent models suggests hyperactive AKT stimulates mTORC1 activity to drive tumor formation (38-39). This suggest mTORC1 may be a suitable target for anti-cancer therapy (40). The role of rapamycin has expanded from the laboratory setting into the clinic. The clinical potential of rapamycin and rapalogues (rapamycin analogues such as sirolimus, evorolimus and temsirolimus) is being evaluated for the treatment of cancer (17). Rapamycin analogues have shown ant-tumor activities in some patients with renal clear cell carcinoma and breast cancer (41).

***mTORC1 and viruses***

Pathogens have developed strategies to modulate host signaling pathways important for growth and survival in order to establish an environment that can support virus replication and assembly. A host pathway often exploited by nearly all DNA and RNA viruses is the PI3K/AKT/mTOR pathway, a signaling network that governs cell survival, growth, and regulates protein synthesis (42-43). The human herpesvirus 8 (Epstein—Barr virus), implicated in several human pathologies, encodes the viral LMP1 protein that modulates the PI3K/AKT/mTOR pathway by stimulating AKT activation via LMP1 association to the p85 subunit of PI3K to control cell survival (44). Adenovirus is another human pathogen that requires activation of the mTOR pathway for virus replication in primary cells (45). Adenovirus-meditated activation of the mTOR pathway requires the viral encoded protein E4-ORF1 and E4-ORF4 (45). From the RNA virus world, influenza A virus and vesicular stomatitis virus (VSV) also modulate the mTOR pathway. Pharmacological inhibition or RNAi-mediated depletion of mTOR activity results in inhibition of influenza virus replication (15), while mTOR activity is elevated in VSV-infected cells (46). These examples highlight the crosstalk between viruses and signaling pathway deregulated in cancer, and show understanding how viruses manipulate host cellular processes will not only provide valuable information regarding key points of virus vulnerability that can be exploited for therapeutic intervention but can also reveal information about the regulation of these pathways by the host.

***Identification and regulation of the mTORC1 inhibitor, REDD1***

Regulated in development and DNA damage response 1 (REDD1), also known as DNA-damage-inducible transcript 4 (DDIT4), dexamethasone-induced gene 2 (Dig2) and RTP801 is localized at human chromosome 10q24.33. *REDD1* encodes a 232 amino acid protein with no identifiable structural /functional motifs, and highly unstable protein with a predicted half-life of less than 5 minutes (47-50). The mechanism of REDD1 degradation to restore mTORC1 signaling has been proposed to occur via the ubiquitin-proteasome degradation pathway mediated by the CUL4A-DDB1-ROC1-β-TRCP E3 ligase complex (51). Subcellular localization studies reveal REDD1 is localized to the cytoplasm and mitochondria. In support of REDD1 localization to the mitochondria, a yeast two-hybrid screen revealed several mitochondrial proteins to be REDD1-interacting partners (52). Further biochemical characterization of these interactions is required. While expressed at low levels, REDD1 is present in most tissues (47, 50). Three independent research laboratories first described REDD1 as cellular protein induced under a number of environmental stress conditions including hypoxia, ionizing radiation (IR)-induced DNA damage, and glucocorticoid hormone treatment (47-48, 53). Recently, two independent groups reported the generation of *REDD1* deficient mice (54-55). Genetic deletion of *REDD1* results in no obvious developmental defects and mice reproduce normally.

REDD1 is induced by the hypoxia-inducible factor 1 (HIF-1), a transcription factor involved in modifying the transcriptional landscape by promoting the transcription of genes with a HIF responsive element (HRE) sequence during anaerobic conditions to promote adaptation and survival (47, 56). REDD1 mRNA expression increased 14-fold

and 37-fold following 4 and 6h of hypoxia, respectively (47). Closer examination of the *REDD1* promoter region revealed a functional HRE element and more importantly, *HIF1-*$\alpha$ null embryonic stem cells failed to upregulated *REDD1* expression under hypoxic conditions (47). The hypoxia mimetic, cobalt chloride ($CoCl_2$), was also shown to strongly induce *REDD1* in mammalian cells, further demonstrating the link between hypoxia and REDD1 (57-58). Sequence analysis showed human *REDD1* is a part of an evolutionary conserved family of protein with orthologs found in mouse, zebrafish, rat, *Drosophila*, and *Xenopus*, which are poorly conserved at the N-terminus but show strong evolutionary sequence conservation at their C-termini (47-48, 59).

Subsequent studies showed that mammalian cells exposed to ionizing radiation (IR), a common DNA damaging-agent, and glucocorticoid hormone treatment strongly upregulated *REDD1* mRNA expression levels (48, 53). REDD1 induction by IR is dependent on the tumor suppressor protein p53, as *TP53* null cells failed to induce *REDD1* after IR (48). In support of the role p53 plays in the regulation of *REDD1* expression, a functional p53-responsive element was identified on the *REDD1* promoter sequence (48). Interestingly, etoposide, a topoisomerase inhibitor known to cause DNA damage and promote apoptosis, was also reported to induce *REDD1* expression (53). In addition, *REDD1* induction was detected 30 minutes following glucocorticoid treatment, a commonly used immunosuppressive, and this upregulation was blocked by and the glucocorticoid receptor antagonist RU486 and by the transcriptional inhibitor actinomycin D (53). This study also reported that *REDD1* may function as an anti-apoptotic factor as REDD1 overexpression lead to a significant reduction in the glucocorticoid-induced cell death in a murine T-cell lymphoma cell line (53).

Later, studies in *Drosophila* provided molecular evidence of the function of *REDD1* under cellular stress conditions. Reiling and Hafen identified two *Drosophila* genes, s*cylla* and *charybdis*, that when overexpressed in an enhancer/promoter screen resulted in the inhibition of the "bulging eye" phenotype in a *Drosophila* line carrying active PDK1/AKT signaling (60). Overexpression of *scylla* and *charybdis* individually results in decrease organ size in the adult fly with no effect on cell number. In contrast, loss of both genes resulted in a ~20% increase in body weight (60). Sequence analysis showed *REDD1* is the *scylla* and *charybdis* mammalian orthologue. Compromised larval development was observed when *scylla*/*charybdis* double mutant larvae where exposed to hypoxic conditions, suggesting both genes are important for survival under this environmental stress condition (60). *Scylla* was also shown to be a transcriptional target of the *Drosophila* HIF-1 factor induced under hypoxic conditions, similar to its mammalian orthologue, *REDD1* (47, 60). Subsequent genetic studies demonstrated that *scylla* acts upstream of the TSC1/TSC2 complex and biochemical approaches showed that *scylla* overexpression decreased S6K activity, a well-characterized target of TOR (60). This study for the first time showed that downregulation of the TOR pathway under hypoxic conditions required the *REDD1* orthologues *scylla* and *charybdis* and demonstrated *REDD1* acts as a negative regulator of cell growth.

The characterization of *scylla* and *charybdis* as TOR negative regulators in *Drosophila*, lead Brugarolas and colleagues to examine whether *REDD1* was involved in the hypoxia-mediated downregulation of mTOR (35). Loss of *REDD1* failed to downregulate the mTORC1 pathway under low oxygen conditions and this required an intact TSC1/TSC2 complex as depletion of TSC2 via RNAi blocks mTORC1 inhibition

by REDD1. Importantly, ectopic expression of REDD1 is sufficient to downregulate mTORC1 activity in various cell types (35). Recently, it was proposed that the mechanism by which REDD1 inhibits mTORC1 activity is by directly binding and dissociating the inhibitory 14-3-3 proteins bound to TSC2 as a result of AKT-dependent phosphorylation, thereby restoring the TSC1/TSC2 complex and its inhibitory activity on mTORC1 (61-62). However, structure and functional analyses of REDD1 and 14-3-3 proteins have challenged these observations (59).

Other environmental conditions have also been shown to induce *REDD1* expression. Two widely used compounds known to induce endoplasmic reticular (ER) stress, tunicamycin and thapsigargin, have been shown to robustly induce *REDD1* expression in multiple murine and human cell lines (53, 57, 63). ER-stress mediated induction of *REDD1* required the protein kinase RNA (PKR)-like ER kinase (PERK) and activating transcription factor 4 (ATF4) to downregulate mTORC1 activity (57, 63). REDD1 can also be upregulated by high cell confluency and ablation of HIF-1$\alpha$ and the SP1 transcription factors via RNAi blocks this induction (58). Additionally, REDD1 has been shown to be involved in the regulation of reactive oxygen species (ROS), which regulate many signal transduction events involved in proliferation to survival and found in a number of disease states (47-48, 64). REDD1 overexpression suppressed ROS generation and protected a human epithelial breast carcinoma and a rat adrenal gland tumor cell line from ROS-mediated apoptosis, through a mechanism yet to be elucidated (47). On the contrary, in neuron-like terminally differentiated rat cells and U937 leukemic cells REDD1 ectopic expression was sufficient to promote apoptosis (47, 52). ROS exposure was also shown to robustly induce the expression of human REDD1 under

the control of ATF4 resulting in the downregulation of mTORC1 activity (57). These observations suggest that under certain environmental conditions and cell types REDD1 functions as a pro-apoptotic and anti-apoptotic cellular factor. A recent study reported that genetic ablation of *REDD1* results in elevated HIF-1 levels, switch to glycolytic metabolism, and increased mitochondrial ROS production (50). These effects are a direct result of *REDD1* genetic deletion as reconstitution of REDD1 into *REDD1-/-* cells significantly decreased cellular ROS levels (50). Cellular fractionation studies reveal REDD1 is localized in the mitochondria and reconstitution of REDD1 bearing mutations to the mitochondrial-targeting motif fail to target it to the mitochondria and to decrease the elevated ROS levels in REDD1 knockout cells (50). These observations indicate that REDD1 may regulate mitochondrial metabolism.

Importantly, REDD1 is induced by interferon-α (IFN-α) (65), a type I IFN that has potent antiviral and antiproliferative effects (66). Chimpanzees were inoculated with IFN-α to measure the transcriptional response to this potent cytokine (65). IFN-α treatment induced *REDD1* mRNA levels eight hours post-treatment compared to vehicle treated liver samples (65). In support of this report, REDD1 ectopic expression in a hepatocellular carcinoma (Huh-7) cell line before infection with hepatitis C virus resulted in reduction of HCV replication (67).

In sum, these observations suggests REDD1 is an IFN-stimulated gene (ISG) with antiviral activity against HCV and demonstrated that it is an important stress-response gene as various cellular stress conditions induce its expression resulting in modulation of the mTORC1 pathway and likely other cellular signaling networks as well.

Similar to *Drosophila's scylla* and *charybdis* genes, humans have two REDD genes that share 67% sequence conservation, REDD1 and REDD2 ( also known as DDIT4L or RTP801L) (36, 47-48, 59, 68). In human macrophages, treatment with the hypoxia mimetic desferrioxamine results in REDD2 transcriptional upregulation (68), whereas others have reported that low oxygen levels fail to induce REDD2 expression at the transcription level (47). While in mouse embryonic fibroblast is not detected, REDD2 ectopic expression in MEFs and HEK293 cells results in the inhibition of mTORC1 activity, as measured by S6K phosphorylation (35-36), and requires the TSC1/TSC2 complex (36).

***REDD1 in cancer***

An increasing body of evidence suggests REDD1 may play a role in tumor suppression. Loss-of-function mutations of negative regulators of the mTORC1 pathway have been implicated in a number of human cancers (38). Studies show REDD1 may function as a pro-apoptotic cellular factor (47, 52). REDD orthologs in *Drosophila* have growth-suppressive properties as expression of *scylla* and *charybdis* genes resulted in reduced organ size (60). Under condition of increased TOR activation (i.e. TSC1 or TSC2 genetic mutants) FOXO levels (a family of transcription factors known to function as tumor suppressors) are upregulated in *Drosophila* and mammalian cells leading to expression of genes that restrict growth such as *scylla* and *REDD1* (69). It is conceivable mutations to the FOXO family of transcription factor or to target genes with growth-restricting abilities could further aggravate the TSC syndrome. In addition, soft agar

colony formation assays, which measure proliferation, suggest that *REDD1* is important for anchorage-independent growth inhibition as greater number of colonies were observed in cells lacking *REDD1* under hypoxic conditions (61). In addition, the expression of REDD1 transcripts was significantly downregulated in 8 of 27 human primary breast carcinoma specimens (~30%) compared to specimen-matched normal breast tissue (61). Furthermore, REDD1 has been shown to negatively regulate HIF-1 expression levels in an mTORC1-independent manner (50). Often tumors must adapt to environments in which oxygen and nutrients are limited. A key regulator of these types of microenvironments is the HIF-1 transcription factor. HIF-1 role in tumor development is highlighted by the von Hippel-Lindau (VHL) hereditary cancer syndrome in which loss-of-function mutations to the tumor suppressor VHL, a key subunit of the HIF-1$\alpha$ oxygen dependent E3 ubiquitin ligase degradation complex, results in increase HIF-1$\alpha$ expression and the formation of a number of human tumors including renal cell carcinomas and pancreatic islet cell tumors (56, 70). Genetic deletion of *REDD1* leads to increase mitochondrial ROS and HIF-1$\alpha$ stabilization independent of mTORC1 (50). These observations suggest REDD1 through mTORC1-dependent and –independent mechanisms may restrict growth and proliferation of cells under anaerobic microenvironments.

***The innate immune response to virus infection***

Host invasion by pathogens, such as viruses, triggers a diverse array of immune responses that facilitates pathogen clearance. Host recognition of conserved pathogen

molecular determinants, known as pathogen-associated molecular patterns (PAMPs), by extracellular, compartmentalized, or cytosolic patter recognition receptors (PRRs) represents the first line of defense against pathogens that leads to the activation of innate immune response. This response results in the production of proinflammatory cytokines and the activation of a type I interferon (IFN) response, a critical signaling pathway with potent antiviral and antiproliferative effects (71). Viral PAMPs (such as single and double stranded RNA) are sensed by the following PRRs: cytosolic RIG-I like receptors (RLRs) and extracellular/membrane bound Toll-like receptors (TLRs) (72).

***RIG-I-Like receptors and innate immunity***

The RLRs family of DExD/H box RNA helicases, composed of the retinoic-inducible gene 1 (RIG-I), melanoma differentiation associated gene 5 (MDA5) and laboratory of genetics and physiology 2 (LGP2). RLRs recognize various types of viral RNA and signal to downstream effectors leading to the induction of proinflammatory cytokines and the production of type I IFN by infected cells which will induce the expression of a battery of genes to promote a number of cellular responses from virus inhibition and clearance to apoptosis of infected cells (66). RIG-I and MDA5 share three structural domains: at the N-terminus, two caspase activation and recruitment domains (CARD) are involved in downstream signaling and found in proapoptotic signaling proteins, a central RNA helicase domain with RNA-binding ability, and at the C-terminus a repressor domain only involved in the autoregulation of RIG-I (73-75). RLRs have been shown to discriminate between viruses and types of RNAs recognized based on their

structural features. RIG-I was originally identified as a cytosolic sensor for polyinosine-polycytidylic acid (poly(I:C)), a synthetic analog of viral dsRNA, that upon binding dsRNA triggered an IFN response (76) (Figure 2). Subsequent molecular characterization of RIG-I revealed uncapped, 5'-triphosphorylated RNA (5'-ppp RNA) generated by viral polymerases is the bona fide RIG-I substrate that induces its activation and downstream signaling (77). To date, a variety of viruses have been reported to be recognized by RIG-I including: Rhabdovirus (negative sense, single stranded RNA; Vesicular Stomatitis Virus), Orthomyxovirus (negative sense, single stranded RNA; Influenza virus), and Flavivirus (positive sense, single stranded RNA; hepatitis C virus) (78-82). RIG-I loss-of-function mutations result in permissiveness to hepatitis C virus (HCV) replication (81). Additionally, viruses have developed strategies to inhibit RIG-I mediated induction of an innate immune response. RIG-I mediated induction of IFN response has been shown to be inhibited at least in part by HCV non-structural proteins 4B and 34A (NS4B and NS3/4A, respectively) (83). Influenza virus NS1 protein blocks RIG-I activation and signaling in part by 1) sequestering viral dsRNA and 2) binding and forming and inhibitory complex with RIG-I and downstream signaling components (84). Mice lacking *RIG-I* are highly susceptible to infection (78). MDA5, on the other hand, was originally identified as an IFN responsive gene involved in the IFN-mediated terminal differentiation of human melanoma cells and as a cellular factor potentially involved in programmed cell death (85-86). Similar to RIG-I, MDA5 recognizes specific types of RNA structures. Induction of type I IFN response occurs by high-molecular-weight synthetic dsRNA poly(I:C) (HMW poly(I:C)) mediated activation of MDA5 (78, 87-88) (Figure 2). MDA5 has been shown to be essential for recognition of

encephalomyocarditis picornavirus, a positive sense, single stranded RNA virus (78, 87). Compared to control mice, *MDA5-/-* mice are highly susceptible to picornavirus infection (78). MDA5 is also the target of several virus-encoded proteins to block IFN signaling and evade the host immune response. The V proteins of paramyxoviruses (i.e simian virus 5 and Sendai virus) directly associate and form an inhibitory complex with MDA5; thereby inhibiting type I IFN response (89-90). Also, the HCV NS3/4A protein was found to block MDA5 signaling through an unknown mechanism (79). Structurally, LGP2 has a functional RNA-binding helicase domain but lacks the CARD domains (73). Whether LGP2 functions as a negative or positive regulator of RLRs is controversial (73, 79, 91).

Upon binding viral or synthetic RNA through the helicase domain, RIG-I and MDA5 undergo modifications that lead to their signaling activation. Activation of RLRs results in the CARD domain exposure and subsequent CARD domain-mediated association with the signaling adaptor molecule mitochondrial antiviral signaling protein (MAVS; also known as IPS-1, Cardif, and VISA), localized to the outer mitochondrial membrane (92-95) (Figure 2). HCV NS3/4A has been shown to inhibit the virus-induced type I IFN response by targeting and inactivating MAVS (94), yet another clever mechanism by which HCV blocks the host innate immune response. The cellular localization of MAVS to the mitochondria is critical for its antiviral signaling activity as targeted localization to the ER or plasma membrane compromised its function (92). Thus, the mitochondria not only plays a critical role in metabolism and program cell death, but also represents a signaling platform essential for innate immune signaling in response to viral infection. Association of RLRs to MAVS results in the recruitment of numerous

innate immune signaling molecules giving rise to the MAVS signalosome (96). Two key downstream components of the innate immune pathway which are activated by members of the MAVS signalosome are the IκB kinase-ε (IKKε) and TANK-binding kinase-1 (TBK1) (96). Activation of IKKε and TBK1 was shown to result in the phosphorylation and subsequent activation of the antiviral response transcription factors interferon regulatory factor 3 and 7 (IRF3 and IRF7) (97-98) (Figure 2). In their inactive state, IRF3 and IRF7 are restricted to the cytoplasm and, following virus infection, IRF3 and IRF7 are phosphorylated leading to the formation of IRF3 homodimer or IRF3-IRF7 heterodimer which translocates to the nuclei of infected cells where they bind and activate the expression of type I IFN genes (i.e. IFN-α/β) as well as IFN-inducible genes (such as RIG-I and MDA5) (99-103). Highlighting their critical role in type I IFN induction, mice deficient in *IRF7* and *IRF3* are more vulnerable to virus infection than their wildtype littermates (104). IFN-α/β produced and secreted from virus infected cells binds to the type I IFN receptors leading to the activation of the JAK/STAT signaling pathway resulting in the amplification of the IFN production and expression of interferon stimulated genes (74, 105-108).

The MAVS signalosome, in a IKKε and TBK1-independnet manner, drives proinflammatory cytokine production through activation of the transcription factors nuclear factor-kappa B (NF-κB) (93). The NF-κB family consists of five members found as homodimer or heterodimers in most cells (109). The family of NF-κB transcription factors is involved in numerous cellular processes from cellular differentiation and proliferation to the development of tissues involved in the mammalian immune response

pathways (110). In the absence of stimulus, NF-κB associates with NF-κB-inhibitory proteins (IκB) that sequester the transcription factor in the cytoplasm (109). Following stimulation, the IκB proteins undergo phosphorylation by the IKK complex resulting in their degradation via the ubiquitin-mediated proteasomal pathway (111). The IKK complex is composed of three subunits IKKα, β, and Nemo which are required for NF-κB dimer activation (109) (Figure 2). Following degradation of the IκB proteins, NF-κB is released and efficiently translocates to the nucleus where it binds to the promoter region of target genes with κB sites, such as proinflammatory and immunoregulatory genes: tumor necrosis factor alpha (TNF-α), interleukin 1 (IL-1), IL-6, IL-12, and IL-18 (72, 109) (Figure 2). Recognition of exogenous dsRNA results in the formation of the MAVS signalosome on the mitochondria where FADD, an innate immune signaling molecule and member of the signalosome, triggers proinflammatory cytokine production (93). Truncation mutants or genetic deletion of FADD results in impaired inflammatory cytokine production and susceptibility to virus infection (93, 112). In response to dsRNA, FADD associates with caspase-8 and caspase-10. The cleavage products are necessary for NF-κB activation as cells lacking caspase-8 are impaired in their ability to drive the production of proinflammatory and immunoregulatory cytokines in a dsRNA-dependent manner (113).

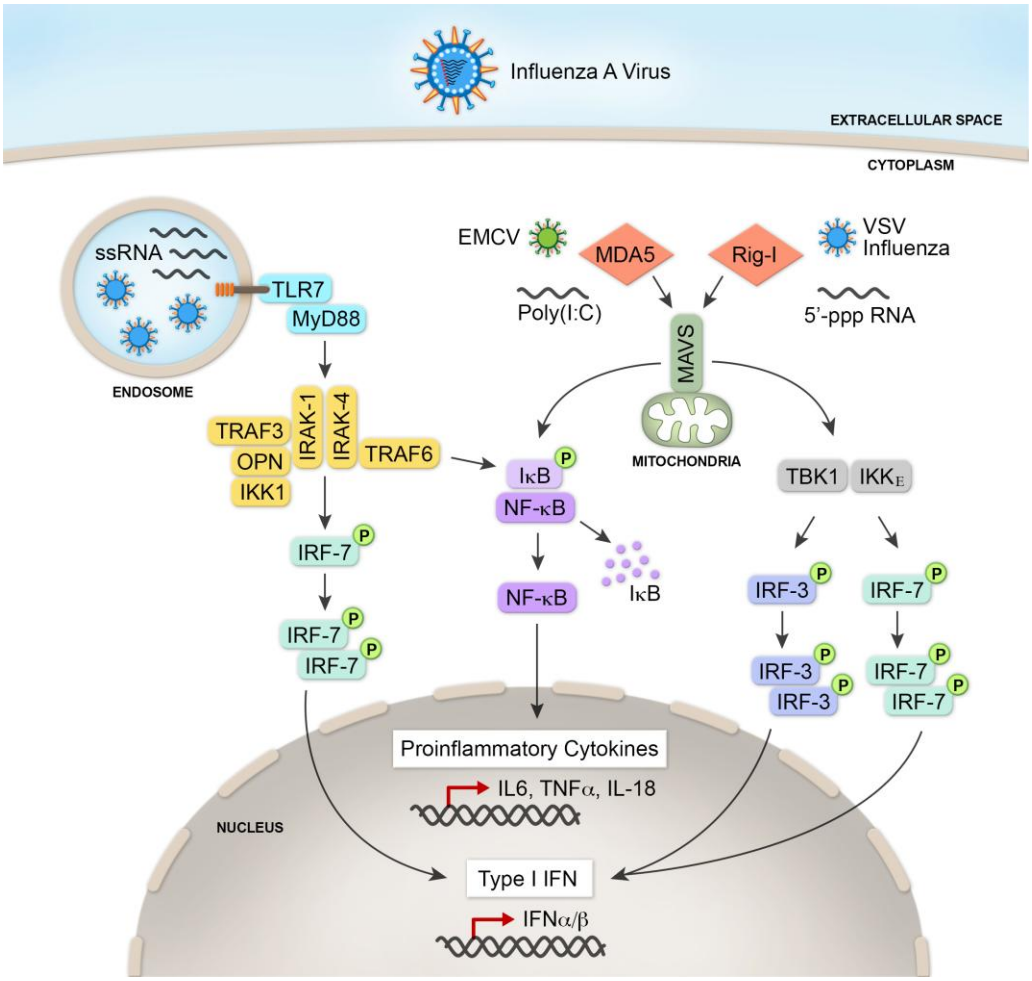


**Figure 2. PRR-mediated activation of type I IFN and proinflammatory cytokine production.**
PRRs activation by virus PAMPs leads to the recruitment immune signaling molecules which signal to downstream effectors inducing an innate immune response. In an IRF3 or IRF7-depedent manner type I IFN genes (IFN-α/β) are express, while proinflammatory cytokines are induced in an NF-κB- dependent manner.

***Toll-like receptors and innate immunity***

The TLR family of patter recognition receptors is composed of 13 members of which TLR3, 7/8, and 9 are localized to the late endosome/lysosome compartment and recognize viral genomic material (72). In particular to this study, TLR7 was shown to recognize and mediate an innate immune response against single stranded RNA virus (i.e. influenza virus) as *TLR7-/-* influenza virus infected cells fail to induce a type I IFN response and proinflammatory cytokine production (114-115). TLR7 signaling following ligand binding (ssRNA) requires the adaptor molecule MyD88 for proinflammatory cytokine, such as IL-6, IL-12, IL-1B, and type I IFN production (114-117) (Figure 3). Association of MyD88 to the cytoplasmic portion of TLR7 results in the recruitment of various immune signaling co-factors giving rise to an immune signaling complex (72). Once associated to MyD88, IRAK-4 phosphorylates and activates IRAK-1 leading to its association to TRAF6 (118). In a TRAF6-dependent manner, NEMO and TAK1, both critical regulators of the IKK complex required for degradation of IκB proteins, undergo post-translational modifications required for downstream signaling (119-120). Phosphorylation and activation of the β subunit of the IKK complex by TAK1 leads to the degradation of the IκB proteins resulting in the induction of proinflammatory and immunomodulatory genes following NF-κB nuclear translocation (120-121) (Figure 2).

Induction of type I IFN response after virus-mediated TLR7 activation has been shown in plasmacytoid dendritic cells (pDC). Plasmacytoid dendritic cells, a specialized antigen presenting cell of the immune system responsible for virus-induced production of systemic type I IFN, detects influenza virus genomic material via TLR7 following virus mediated endosomal acidification (114-115, 122). Activation of type I IFN response by

TLR7 in pDCs requires IRF7, a transcription factor that is highly expressed in pDCs but not in conventional dendritic cells (123-124). IRF7 was shown to form a complex with MyD88 and TRAF6, components of the signaling complex required for TLR7 mediated induction of the innate immune response (125-126). As described earlier, IRF7 activation and nuclear translocation is phosphorylation dependent. Two kinases have been reported to phosphorylate and activate IRF7. IRAK1, a member of the TLR7-MyD88 complex, was reported to phosphorylate IRF7 and IRAK1 loss results in impaired IRF7 activation (127). On the other hand, the $\alpha$ subunit of the IKK complex was also shown to serve as an IRF7 kinase (128). Dimerization and nuclear translocation of active IRF7 drives the expression of type I IFN genes.

This highly complex and integrated signaling cascade initiated by recognition of viral PAPMs results in the establishment of an antiviral state in the cell that serves to limit and facilitate virus clearance.

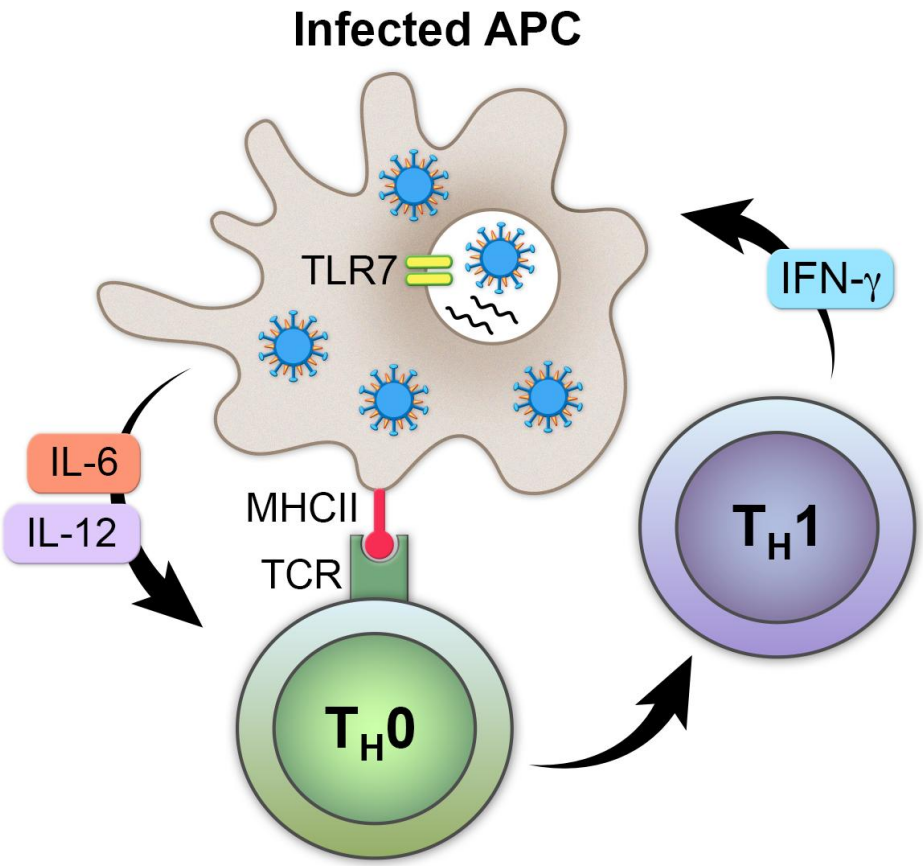


**Figure 3. APCs recognize influenza virus via TLR7, produce immunoregulatory cytokines and activate naïve T-lymphocytes.**
APCs recognition of influenza virus is mediated by TLR7. APCs proteolytically process virus antigens and load them onto MHC class II molecules for antigen presentation and subsequent activation of naïve T-lymphocytes.

***Intimate relationships between the innate immune system and the mTORC1 pathway***

A growing body of evidence suggests the mTORC1 pathway regulates the type I IFN response pathway. Studies in pDC, reveal interferon production in response to synthetic DNA or virus infection is sensitive to pharmacological inhibition of mTORC1 activity with rapamycin or depletion of mTORC1 downstream target S6K (129). Translational control of the IFN transcription factor *IRF7* mRNA was also shown to be regulated by the mTORC1 pathway (130). Genetic deletion of the mTORC1 downstream targets 4E-BP1 and 2 increased *IRF7* mRNA translation resulting in higher IFN-α/β production (130). 4E-BPs are negative regulator of mRNA translation and mTORC1-mediated phosphorylation releases this repressive activity leading to the translation of a subset of transcripts. Mechanistic studies reveal 4E-BPs represses *IRF7* mRNA translation in part through a structural element found on the 5'UTR of *IRF7* transcripts. In support of the *in vitro* observations, *4E-BP1* and *2* double knockout mice produce large amounts of type I IFN and are more resistant to VSV infection than their wildtype littermates (130). Finally, MEFs and mice lacking the mTORC1 downstream target S6K, a positive regulator of protein synthesis, are more susceptible to virus infection partially due to a defect in type I IFN production (131). These observations indicate the mTORC1 pathway is a critical regulator of the innate immune system and highlights the complex nature of this signaling network.

***Biology of influenza A virus***

Influenza A virus (IAV) is a segmented, negative-strand RNA virus that belongs to the family *Orthomyxoviridae* (4). IAV can be further classified into subtypes based on the antigenicity of their surface glycoproteins hemaglutinin (HA) and the neuraminidase (NA). For example, the H1N1 1918 Spanish influenza virus has a HA subtype 1(H1) and an NA subtype 1 (N1). To date, 16 HA subtypes and 9 NA subtypes have been identified, and only three HA subtypes (H1, H2, and H3) and two NA subtypes (N1 and N2) have been reported to cause human disease (4). IAVs have been isolated from many animal hosts, such as humans, birds, horses, dogs and pigs.

Influenza A virions are composed of host-cell lipid membrane with HA and NA glycoproteins projecting from the virion surface (4). Matrix protein 2 (M2) is an ion channel that also projects from the membrane. Underneath the membrane, the structural matrix protein 1 (M1) encloses the genomic material. Inside the M1 layer, the viral RNA genome is coated with several proteins forming a structure known as the viral ribonucleoprotein (vRNP) complex which includes: the non-structural protein 2 (NS2), nucleoprotein (NP), and the heterotrimeric RNA-dependent RNA polymerase PB1, PB2, and PA subunits to ensure efficient virus transcription, replication and packaging (132).

IAV genome consist of eight negative sense, single stranded viral RNA (vRNA) segments coiled into a hairpin structure (133). The viral RNA genome encodes at least eleven proteins, several vRNA segments encoding more than a single protein. The polymerase B2 (PB2), polymerase B1 (PB1), and polymerase A protein (PA), and the polymerase basic protein 1-fram2 (PB1-F2) are encoded by the three largest vRNA segments. PB1, PB2 and PA are the main components of the active RNA-dependent

RNA polymerase complex, while the PB1-F2 protein has been implicated as a pro-apoptotic protein during influenza virus infection (134) . Three separate segments encode NP and the surface glycoproteins HA and NA, while the two matrix proteins (M1 and M2) are encoded by one single vRNA segment and are generated by alternative splicing. One segment encodes the non-structural protein 1 (NS1) and mRNA splicing gives rise to the NS2 protein (135).

The HA spikes on the surface of IAV bind to host cell surface receptors containing an α-2,6-linked or an α-2,3-linked *N*-acetylneuraminic (sialic) acid present in human tracheal epithelial cells (4). This represents the first stage in the virus replication cycle. Following attachment, virus gains entry into the host cell via receptor-mediated endocytosis (136). Then, fusion of endosomal and viral membranes takes place, a process that is critical for virus entry. The acidity of endosomal compartments is crucial for the release of viral RNPs into the cytoplasm. First, the HA protein undergoes conformational changes in the acidic environment which leads to the fusion of the viral and endosomal membranes (137). The M2 transmembrane ion channel pumps $H^+$ ions from the endosome into the virion which causes acidification and the low pH disrupts internal protein-protein interactions resulting in the release of viral RNPs (vRNP) into the cytoplasm. Following release into the cytoplasm, the vRNPs associate with karyopherin alpha via the nuclear import signals (NLS) found on the NP viral protein and translocate the viral RNAs to the host nucleus (138). The viral RNAs will then become the template for viral mRNA synthesis, which will be translated into viral proteins. In addition, the viral RNAs will be converted to cRNA, which will generate vRNA that will be incorporated into new viral particles (139). For the viral polymerase to initiate viral RNA

synthesis, a primer with a 5'-terminal methylated caps structure is needed. Plotch and colleagues found that capping of vmRNAs is mediated by a unique "cap-snatching" mechanism where the 5'-cap of host cellular transcripts is cleaved by an influenza virus endonuclease (140). Recent evidence suggests the cap-snatching endonuclease activity of influenza virus resides in the PA subunit of the viral polymerase complex (141). Polyadenylation of viral mRNA is carried out by the RNA polymerase from a stretch of uracil residues encoded in the vRNA (59, 142).

Export of vmRNA is an important step during influenza virus life cycle. Once vmRNA is capped and polyadenylated, it can translocate to the cytoplasm where the host translational machinery synthesizes viral proteins from the vmRNA templates. One proposed mechanism of vRNP export involves the association of the NP protein, a component of vRNPs, with the cellular export factor CRM1 and through this interaction vRNPs are exported to the cytoplasm (143). Furthermore, pharmacological inhibition of the CRM1 activity by the natural product leptomycin B results in the accumulation of NP protein in the nuclei of virus infected cells (143). Others suggested viral proteins M1 and NS2 mediate nuclear export of vRNPs (144-145). This raises the possibility that different components of the vRNPs may contribute to the recruitment of components of the nuclear mRNA export machinery for efficient translocation of vRNPs to the cytoplasm.

Fully infectious virus particles are achieved by the incorporation of the eight different vRNA segments into virions. Incorporation of vRNA segments into virions is not a random process. In fact, a unique sequence on the coding region of the NA vRNA segment was discovered to drive the incorporation of viral RNA segment into virions (146). Identification of these sequences on other vRNA segments that allow

incorporation into virions have yet to be identified but this provides a mechanism by which vRNAs are selectively incorporated into virions to generate a fully infectious particle. Once all segments are incorporated into the virion, budding of the virus takes place. The HA protein, projecting from the virion surface, binds to the sialic acid on the host cell surface until the sialidase activity of the NA protein cleaves off sialic acids from the surface glycoproteins to release the virus progeny and promote spreading of the virus to neighboring uninfected cells (147).

***The multifunctional IAV NS1 protein***

While exploiting host cellular mechanisms that allow for successful virus replication, IAV, with its limited coding capacity, efficiently blocks specific pathways that have detrimental effects to virus replication. A virus encoded protein that modulates many of the virus and host cellular processes to establish an environment suitable for virus replication is the non-structural 1 (NS1) protein. NS1 has an approximate molecular mass of 26kDa and contains two identifiable functional domains: an RNA-binding domain composed of a stretch of 73 amino acids located on the N-terminus, and an effector domain comprised of ~156 amino acids on the C-terminus (148). During virus infection, the intracellular localization of NS1 is predominantly nuclear, but can also be detected in the cytoplasm (149) (Figure 4). Nuclear localization of NS1 is achieved by its interaction with importin-$\alpha$, a nuclear transport factor, via the two nuclear localization signals found on NS1 (149-150). Export to the cytoplasm is achieved by a nuclear export signal found in its effector domain (151).

NS1 protein inhibits host gene expression and signal transduction to promote virus replication and antagonize the host innate immune response. By targeting and blocking export of cellular RNAs at multiple stages of RNA maturation and export, NS1 prevents the nuclear translocation of mRNA that encode antiviral factors, but promotes the export and translation of viral mRNAs. In the nucleus, NS1 has been shown to down-regulate RNA processing by inhibiting the functions of the 3'-end processing machinery. The effector domain of NS1 inhibits 3'-end processing of cellular RNAs by binding and disrupting the 30-kDa subunit of the cleavage and polyadenylation specificity factor (CPSF30) ability to interact with its substrates, resulting in nuclear accumulation of RNAs (152) (Figure 4). Further evidence for NS1 mediated-block of 3'-end processing comes from mutation analysis of the binding site of CPSF30 on the NS1 effector domain which restores CPSF30 activity (153). Influenza virus also targets the poly(A)-binding protein II (PABII), another component of the 3'-end processing machinery. NS1, through its effector domain, physically binds and disrupts the localization and activity of PABII leading to the accumulation of RNAs with short poly(A) tails that fail to be exported to the cytoplasm (154) (Figure 4). Viral RNAs are not affected by the NS1-mediated disruption of the RNA processing because viral transcripts poly(A) tail synthesis is carried out by the viral heterotrimeric polymerase complex (155-156). Therefore, viral mRNAs are efficiently processed and exported to the cytoplasm where they are translated. In addition, NS1 blocks processing and export of host mRNAs by physically interacting and forming an inhibitory complex with mRNA export factors including NXF1, NXT1, RAE1, and E1B-AP5 in a RNA-independent manner (157) (Figure 4). Virus infection studies revealed that cellular poly(A) RNAs are retained in the nucleus

early after infection and this block occurred in parallel with the expression of several viral proteins (157). Further supporting the NS1-mediated inhibition of gene expression, ectopic expression of NS1 resulted in increased nuclear poly(A) RNA retention (157). This inhibition was reverted by expressing NXF1, NXT1, and RAE1 (157). By physically interacting and disrupting the activity of core components of the mRNA export and the 3'-end processing machinery, influenza virus NS1 protein blocks export and maturation of RNAs that may be required to establish an antiviral state during infection (Figure 4).

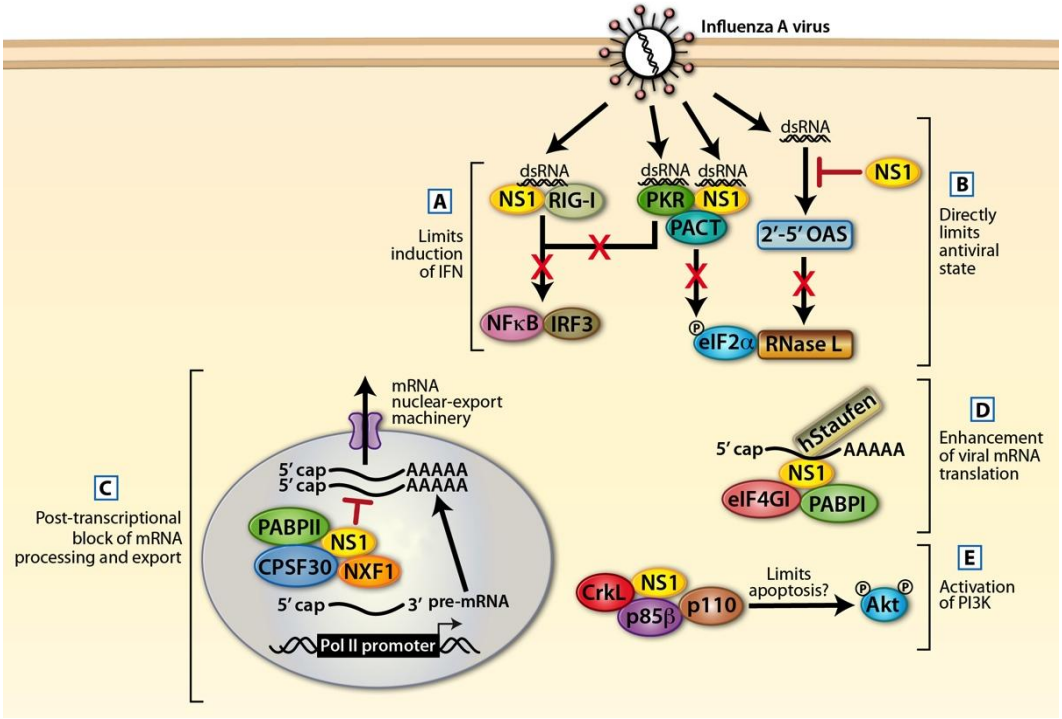


**Figure 4. The multifunctional IAV NS1 protein.**
A) In the cytoplasm, IAV NS1 protein limits the induction of type I IFN response by the host. B) NS1 associates with dsRNA and blocks 2’5’-OAS/RNaseL activation. C) In the nucleus, NS1 blocks host gene expression at the post-transcriptional level by blocking mRNA processing and export. D) IAV NS1 recruits host mRNA factors to enhance viral mRNA translation. E) Activation of the PI3K/AKT pathway in an NS1-dependent manner blocks virus-induced cell death and enhances virus replication.

Cellular localization studies reveal that a pool of NS1 is found in the cytoplasm of virus infected cells. Cytoplasmic NS1 efficiently blocks the host innate immune response at multiple steps. First, NS1 blocks RIG-I-mediated activation of the type I IFN response pathway by 1) binding and sequestering viral dsRNA generated during replication preventing RIG-I activation (158-160), and 2) by directly associating and forming an inhibitory complex with RIG-I and TRIM25, a positive regulator of RIG-I signaling (84, 161) (Figure 4). Secondly, NS1 inhibits the function of the 2'-5'-oligoadenylate synthetase (OAS)/RNaseL system and the protein kinase R (PKR), two cytoplasmic antiviral proteins whose expression is enhanced by dsRNA-mediated activation of the type I IFN pathway (162-163) (Figure 4). Thus, influenza virus inhibits the host's ability to mount an antiviral response by antagonizing type I IFN production via the 26kDa NS1 protein to establish an environment that can support virus replication.

IAV through its viral NS1 protein also regulates the PI3K/AKT/mTORC1 signaling pathway, a key regular of cell growth and proliferation. Pharmacological inhibition of the PI3K/AKT/mTORC1 pathway results in inhibition of IAV replication (15, 164). At the molecular level, IAV NS1 protein stimulated the phosphorylation and activation of AKT by directly binding and promoting PI3K activity (165) (Figure 4). AKT activation was abolished in cells infected with IAV lacking the viral protein NS1 (ΔNS1), demonstrating NS1 is required for PI3K/AKT activation (148, 164). NS1 mediated activation of the PI3K/AKT pathway was later shown to inhibit host pro-apoptotic signaling responses to limit virus-mediated cell death and promote virus proliferation (166) (Figure 4).

Inhibitors of the pyrimidine synthesis pathway have recently gained attention as potential antiviral strategies against IAV. Zhang and colleagues found inhibition of dihydroorotate dehydrogenase (DHODH), an enzyme involved in pyrimidine biosynthesis, down-regulated IAV protein production and replication (167). NS1 was shown to be required for the influenza virus-mediated inhibition of mRNA export as ectopic expression of NS1 alone resulted in the accumulation of host poly(A) RNA in the nucleus of infected cells and virus lacking NS1 (ΔNS1) failed to block mRNA export (167). Subsequently, NS1-mediated inhibition of host gene expression was shown to require an active pyrimidine synthesis pathway as pharmacological inhibition resulted in the release of mRNAs from the nucleus in cells transfected with NS1 alone or in infected cells (167). These observations indicate IAV controls several host pathways to promote virus infection and propagation.

Finally, the introduction of reverse genetics of influenza virus, in which an infectious virus can be assembled from cDNA templates, was critical to examine NS1 functions during virus infection. Virus lacking NS1 (ΔNS1) was shown to be highly attenuated and could only replicate in interferon-deficient systems (168), as ΔNS1 virus fail to inhibit the host innate immune response (84, 161, 169-170).

In sum, these findings underscore the key role of NS1 as a proviral virulence factor and emphasize the need to identify its inhibitors as well as previously unknown host antiviral mechanisms that antagonize its functions.

***Aims of this study***

Antiviral drugs against influenza virus are becoming increasingly ineffective in part due to 1) the rapid rate of mutation of the virus, 2) the increasing viral genetic diversity, 3) the limited number of viral targets for drug development, 4) and resistance to vaccines and clinically approved antiviral drugs. Given the importance of NS1 as a major virulence factor capable of disrupting multiple host cellular pathways, a high throughput screen was performed to identify small molecules that could antagonize NS1 functions. Identification and characterization of compounds with anti-flu activity can shed light on novel signaling pathway regulated by the IAV, provide insight into host antiviral mechanisms, and result in the discovery of new cellular targets for anti-influenza therapeutic modalities.

# CHAPTER TWO
# Materials and Methods
## (Contents of Chapters 2-5 were adapted from *Nature Chemical Biology* 7 (2011))

### Compound screen

The UT Southwestern Compound Library is composed of 200,000 synthetic-drug–like compounds arrayed in DMSO (Sigma) in 384 well plates. HEK 293T cells were transfected with an approximately 10:1 ratio of plasmid pCMV-Luc encoding luciferase and pCAGGS-NS1 encoding NS1 using Lipofectamine2000 (Invitrogen). Cells were transfected with the luciferase plasmid alone as a positive control. After 16 h, cells were dispensed at 5,000 cells per well in 384-well plates. After 1 h, compounds from the library were added to a final concentration of 5 μM in 1% (v/v) DMSO in a one compound per well format. Experimental samples were limited to columns 3 to 22, with controls treated with 1% DMSO in the first and last two columns of wells. Wells in the first column of each plate contained cells transfected with the luciferase plasmid alone; all other wells received cells transfected with both plasmids. Plates were incubated for 22 h at 37 °C in 5% $CO_2$, then cooled to 22 °C, incubated with Bright-Glo luciferase substrate (Promega) for 4 min, then luminescence was recorded. Experiments producing plates with standard (*Z)* scores lower than 0.45 were repeated. Experimental values were normalized to the mean of the luciferase-only control on the same plate. Compounds were ranked by *Z*score, and the 640 compounds with the most positive *Z* scores were selected and retested in the assay at concentrations of 15 μM, 5 μM and 1.7 μM. These compounds were also tested for the ability to prevent cell death of immortalized human

bronchial epithelial cells (HBECs) that had been infected with A/WS/33 influenza virus by measuring cell ATP levels with ATP-lite (PerkinElmer).

**Plasmids used in HTS screen**

Plasmids pCMVLuc expressing luciferase and pGAGGS-NS1 expressing NS1 were used in the compound screen and validation assays.

**Compound half-life**

Compound half-lives were measured in HBECs by LC/MS/MS. Metabolic stability half-life was determined by substrate depletion (171)

**Cell survival and cytotoxicity measurements**

MEFs, HBECs or MDCK cells were seeded in white-walled 96-well plates at a density of $3 \times 10^3$ cells per well, 16 h before compound addition. Compounds dissolved in sterile DMSO (Sigma) at a concentration of 25 mM were diluted to 100 μM in OptiMEM I (Invitrogen) in triplicates. The 100-μM starting dilutions were serially diluted in twofold steps to a final concentration of 0.2 μM. Control experiments, performed in the absence of compound, had the same final concentration of DMSO as compound-treated samples. At the time points depicted in the figures (24 h, 48 h and 72 h), cells were lysed, and ATP levels were measured by luminescence using the Cell Titer-

Glo kit (Promega), following manufacturer instructions. In parallel, cells were also counted at the beginning and at the end of each experiment, and cell survival was quantified by Trypan blue exclusion assay.

**Influenza virus replication**

MDCK cells were infected with various strains of influenza virus depicted in the figures at an m.o.i. of 0.001 p.f.u. per cell for 1 h. Next, cells were washed with PBS and overlaid with OptiMEM containing twofold compound dilutions ranging from 100 μM to 0.8 μM. Samples containing only the same volume of DMSO as the compounds were included. At 30 h after infection, culture medium was collected, and cell debris was removed by centrifugation at 1,000*g* for 10 min and frozen at −80 °C. Viral titers were determined by plaque assay. The experiments conducted with the H1N1/1918 strain were performed in a high-containment (BSL3++) facility.

For experiments performed with U20S cells, cells were plated in 12-well plates in DMEM containing 10% (v/v) FBS (Atlas Biologicals) and incubated overnight. Cells were then incubated in medium containing tetracycline (1 μg $ml^{-1}$) for 2 h to induce REDD1 overexpression. Cells were washed with PBS and infected with A/WSN/1933 or VSV at m.o.i. 2 for 1 h. Tetracycline was again added 1 h after infection, and cell lysates were prepared at various time points after infection, as indicated in Figure 6.

**VSV replication assay**

VSV replication: MDCK cells seeded in 35 mm–diameter dishes were infected with VSV-GFP at m.o.i. 0.001 p.f.u. per cell. At 24 h after infection, supernatants were clarified and used for titration on Vero cells. Fourfold serial dilutions of virus containing supernatants were made in PBS containing serum and antibiotics. Fifty microliters of each dilution were mixed with an equal volume of complete growth medium containing 8,000 Vero cells and incubated at 37 °C for 48 h in 96-well plates. Cells were fixed in 4% (v/v) paraformaldehyde. The number of wells with GFP expression were counted by fluorescence microscopy and subsequently used to calculate relative virus titers. Infection of U2OS cells with VSV was performed in the same manner as influenza virus infection described above.

***In situ* hybridization**

mRNA distribution in MDCK cells infected with influenza virus in the presence or absence of compounds was performed as previously described (157). Influenza proteins were detected with mouse influenza-specific antibody (Biodesign International) and FITC-labeled mouse-specific antibody (Invitrogen).

**Phospho-S6K analysis**

Cells were starved for 18 h and then mock infected or infected as described in the legend of Figure 5. Five percent serum was added to induce S6K phosphorylation in

control lanes. H358 and H1993 cells were treated with 10 μM **3**, and LnCap cells were treated with 30 μM.

**Cell culture**

Human A549, 293T, LnCap, and MDCK cells were obtained from the American Type Culture Collection and cultured in DMEM (Invitrogen) containing 10% fetal bovine serum (Atlas Biologicals) and 1% penicillin/streptomycin (Invitrogen). Female ICR/CD-1 mouse hepatocytes, InVitroGRO HI and HT Medium, and Celsis Torpedo Antibiotic Mix were purchased from Celsis/In Vitro Technologies (Baltimore, MD). The immortalized human bronchial epithelial cells (HBEC) (172)were obtained originally from John Minna (UT Southwestern) and were cultured in keratinocyte serum-free medium (SFM, Invitrogen). H358 and H1993 cells were also obtained from John Minna. REDD1 cells are immortalized mouse embryo fibroblasts according to a 3T3 protocol (59).

**Antibodies**

The following antibodies were used for immunoblot analysis: anti-p70 S6 Kinase rabbit polyclonal (Cell Signaling, MA), anti-P-p70 S6 Kinase (T389)(108D2) rabbit monoclonal (Cell Signaling), anti-NXF1/TAP (Proteintech) and anti-P-Akt (S473) (D9E) rabbit monoclonal antibodies (Cell signaling); α-tubulin and γ-tubulin monoclonal antibody (Sigma); goat polyclonal anti-PB1 antibodies (Santa Cruz Biotechnology).

phospho-4E-BP1 (Thr37/46) (236B4) Rabbit mAb (Cell Signaling Technology); REDD1 (DDIT4) rabbit antibody (Novus Biologicals); β-actin (SIGMA); LC3 rabbit antibody (Novus Biologicals). Monoclonal antibody against Complex II subunit 70 kD (Mito-70 kD) was obtained from Mitoscience. Anti-VSV M protein antibody was generated against recombinant full-length protein. Anti-VSV proteins antibodies were a gift from G. Barber.

**Representative synthetic procedure for the synthesis of naphthalimide analogs**

**Step 1**: Synthesis of 6-(6-chloro-1,3-dioxo-1*H*-benzo[*de*]isoquinolin-2(3*H*)-yl)hexanoic acid. A solution of 4-chloro-1,8-naphthalic anhyrdie (10.0 g, 43 mmol) and 6-aminocaproic acid (5.6 g, 43 mmol) in *N*-methylpyrrolidone (100 mL) was heated to 110 ºC in a 250 mL round bottom flask under an atmosphere of nitrogen. The reaction was monitored by LC/MS for product formation. After 90 minutes at 110 ºC, the reaction was complete consumption of both starting materials. The reaction was cooled to room temperature and then diluted with ethyl acetate (250 mL) and a dilute aqueous NaCl solution (120 mL). The resulting layers were separated and the aqueous layer back-extracted with EtOAc (2 x 100 mL). The combined organic layers were then washed with water (10 x 100 mL) followed by a final brine wash (50 mL) and the dried over anhydrous $Na_2SO_4$. Concentration gave a crude dark solid (9.6 g) which was purified using normal phase silica gel chromatography (50% ethyl acetate in hexanes) to provide the desired naphthalimide as a light yellow amorphous solid (7.7 g, 52% yield). $^1$H NMR ($CDCl_3$) 8.65 (d, 1H), 8.60 (d, 1H), 8.52 (d, 1H) 7.9-7.8 (m, 2H), 4.2 (t, 2H), 2.39 (t,

2H), 1.76 (m, 4H), 1.5 (m, 2H). MS (ESI) 346 (M+H), 368 (M+Na).

**Step 2:** Synthesis of analog **3** [6-(1,3-dioxo-6-(piperidin-1-yl)-1*H*-benzo[*de*]isoquinolin-2(3*H*)-yl)hexanoic acid]. A solution of 6-(6-chloro-1,3-dioxo-1*H*-benzo[*de*]isoquinolin-2(3*H*)-yl)hexanoic acid (74 mg, 0.22 mmol, from **Step 1**) in piperidine (2.0 mL) was heated to 80 ºC in a sealed scintillation vial. The reaction was monitored by LC/MS for product formation. After 105 min, the reaction was complete by evidence of complete consumption of the starting material. The reaction was cooled and diluted with EtOAc (20 mL) and then washed with water (~ 10 x 5 mL) until the aqueous washings were clear. The combined aqueous layers were then acidified with 3N HCl to a pH = 4.0 and then extracted with EtOAc (2 x 50mL). The combined organic layers were washed with brine (5 mL) and dried over $Na_2SO_4$. The crude orange solid obtained after concentration was purified by recrystallization from EtOH to provide **3** as a light orange crystalline solid (40 mg, 46% yield). $^1$H NMR ($CDCl_3$) 8.58 (d, 1H), 8.49 (d, 1H), 8.38 (d, 1H), 7.53 (t, 1H), 7.18 (d, 1H), 4.20 (t, 2H), 3.21 (br m, 4H), 2.35, (t, 2H), 1.80 (m, 4H), 1.75 (m, 7H), 1.49 (m, 2H). MS (ESI) 395 (M+H), 417 (M+Na).

**$^{13}$C NMR (500 MHz, DMSO) of 3:** δ 175.11, 164.17, 163.63, 157.31, 132.88, 131.21, 131.17, 129.76, 126.45, 126.06, 123.12, 115.65, 115.54, 54.63, 34.17, 28.00, 26.73, 26.40, 24.91, 24.54

Purity: 93% at 254 nm

**$^{13}$C NMR (500 MHz, DMSO) of 4:** δ 175.12, 164.16, 163.64, 156.09, 149.45, 132.83, 131.32, 131.13, 130.16, 129.72, 128.75, 126.77, 125.98, 123.21, 116.56, 116.42, 115.81, 53.26, 49.56, 34.17, 28.00, 26.73, 24.91, 20.78

Purity: 91% at 254 nm

**RNA isolation and real-time RT-PCR**

A549 cells were seeded in 35-mm-diameter dishes and infected with A/WSN/1933 virus at an m.o.i. of 0.001 pfu/cell. After one hour, cells were washed and compound-containing medium was overlaid onto the monolayers. At 36 h p.i., the medium was harvested to confirm compound activity by HA assay. From the same wells, total RNA was isolated using TRIzol reagent (Invitrogen) as recommended by the manufacturer. Isolated RNA was treated with 2 U of Turbo DNase (Ambion) at 37°C for 30 min to remove potential genomic DNA contamination. Reverse transcription and real-time RT-PCR was performed by the Mount Sinai Microarray, PCR and Bioinformatics Shared Research Facility as described previously (173). In brief, cDNA was synthesized using Affiniscript RT (Stratagene) in combination with oligo $dT_{18}$ primers (Integrated DNA Technologies) for cDNA synthesis of cellular genes or an influenza virus NP specific primer for cDNA synthesis of viral NP RNA. Real-time PCR was performed using Platinum Taq polymerase (Invitrogen) and SYBR Green I (Molecular Probes) using an ABI 7900HT real-time PCR machine. Primer nucleotide sequences are available upon

request. The results of quantification were normalized to the amount of alpha-tubulin, beta-actin and ribosomal protein S11 mRNA in the same sample. Each PCR was performed in triplicate, and median values and standard deviations were calculated. The amount of RNA was determined with respect to standardized samples and expressed in relative units. A similar assay was performed to measure REDD1 mRNA levels in the absence or presence of actinomycin D (0.5 μg/ml), as described in the legend of Fig. 5a

**Gene expression analysis**

5 X $10^5$ A549 cells, in DMEM media (Gibco) supplemented with 10% FBS (Atlas Biologicals) and 1% penicillin/streptomycin (Gibco), were seeded overnight in 6-well plates. Compound **3,** at 30μM, or DMSO (0.3%) was added for 3 h, and RNA was isolated using the RNeasy Mini Kit (Invitrogen) following the manufacturer's instructions. cDNA was synthesized, labeled, and hybridized to an Illumina HumanRef-8 BeadChip 22K.

After baseline correction and normalization of the expression data from the Illumina bead array, we further filtered the expression profile by omitting entries with a p-value of 0.05 or greater. Fold-changes between test and reference-sets have been calculated. For genes with multiple oligonucleotide probes, fold-changes have been calculated prior to the calculation of averages. Only test and reference pairs for each probe were used when both p-values were at or below the 0.05 cutoff value. We then subjected the post-processed gene expression data to Gene Set Enrichment Analysis (GSEA(174)) using the fold changes as ranks within the *Prerank* algorithm of the GSEA

software (http://www.broadinstitute.org/gsea) with default parameters and 2000 permutations. The curated C2/CP "canonical pathways" set from the Molecular Signature Database at the Broad Institute has been used as reference gene sets for GSEA, consisting of sets of genes known to function in 639 pathways. Two enriched gene sets, corresponding to different branches of the same pathway were selected for further response network analysis:

1. MTORPATHWAY: 23 genes (20 genes enriched) on the mammalian target of rapamycin (mTOR) that senses mitogenic factors and nutrients, including ATP, and induces cell proliferation, from BioCarta (http://www.biocarta.com/pathfiles/h_MTORPATHWAY.asp)
2. IGF1MTORPATHWAY: 20 genes (16 genes enriched) on the growth factor IGF-1 that activates AKT, Gsk3-beta, and mTOR to promote muscle hypertrophy, from BioCarta (http://www.biocarta.com/pathfiles/h_IGF1MTORPATHWAY.asp)

For each pathway, the set of enriched genes was used as seed-nodes for further network analysis. NetworkExpress, discussed below, was used to calculate response networks representing the particular response of enriched genes embedded in the constructed human biochemical network omitting interaction data from iHOP.

**Human biochemical network**

To construct a hybrid *Homo sapiens* interaction and reaction network, protein-protein interactions with directional signal transduction and metabolic reactions were combined. Interaction information from *IntAc*t (175), *NetworKi (143)*, the *Human Protein Reference Database* (*HPRD*(176) and from Palsson's group (H. sapiens Recon1@(145) yielded a network of ~40,000 nodes (genes, proteins and small chemicals) as well as ~200,000 interactions (gene-protein, protein-protein) and reactions (chemical, protein-phosphorylation, etc). In addition, curated information on the influenza virus life-cycle and on host-interactions with influenza factors from the *Reactome* database (177) were included. We have also integrated the human biochemical network above with a larger literature based network available from *iHOP* with 45,041 nodes and 438,567 interactions, which are about 2/3s of 650,000 interactions predicted by Stumpf *et al.*(178). As a third reference network, the Homo sapiens protein interaction network was downloaded from the *BioGRID* database version 2.0.39 (179), which was generated from literature curation of protein interaction data. The data set was filtered to include only direct and physical interactions between human proteins. All loops and duplicate edges were removed. However, duplicate edges from different data sources and different property (e.g., an interaction identified as generic protein-protein interaction in one data-set and predicted as phosphorylation of a protein by a kinase in another data-set) were kept to emphasize the importance/validity of such interactions.

**Network analysis tool**

We have previously developed a computational method to identify response networks in large biological networks based on expression data (180-181). This method and the corresponding computer program NetworkExpress are based on superimposing expression values upon the large network, identifying *k*-shortest paths (182-183) between seed-nodes, scoring the sub-network spanned by the set of *k*-shortest paths that are shorter than a pre-defined maximum weighted length *l*, and finding the best scored sub-network by optimization techniques. We have a variety of scoring functions available, from simple arithmetic or geometric means to different types of correlation functions for time-series correlations, optionally between same time-points or time-forward/backward. The best-scored sub-network refers to the response network of the system under the specific environmental condition measured by the corresponding expression experiment. NetworkExpress also performs a statistical analysis to validate the significance of the identified sub-graph by comparison to randomly sampled sub-networks using a Monte Carlo approach.

**Protein synthesis**

MDCK cells were seeded into 35mm dishes. Fifty μM of **3** or **8** was added for 6, 24, and 48 hours. Cells were pulsed with 100 μCi $^{35}$S-Met for 20 min, harvested, lyzed, and centrifuged at 14,000 x g for 10 min. Supernatant (25μl) was then blotted on Whatman filter paper (approximately 1 square inch) and allowed to dry. The filters were

soaked individually in ice cold 10% TCA for 30 minutes. Filters were then washed for 5 minutes with 1:1 ethyl ether/ethanol, and again in ethyl ether alone for 5 minutes. The filters were air-dried and radiation was measured in a scintillation counter.

**IRF3 Nuclear translocation assay**

Place flamed-coverslip into each well in a 6-well dish. Plate $3X10^5$ cells overnight in 2mL full media. Next day prepare Lipofectamine/poly (I:C) complex by adding 50uL of plain media + 3uL of Lipofectamine 2000 and 50uL of plain media + 1uL of poly IC (1mg/mL) for final 0.5ug/mL. Mix and incubate for at least 20mins. Add the mixture into each of the wells and incubate for 6h. After incubation, rinse with PBS once (does not have to be sterile). Fix 30min with 2% Paraformaldehyde dissolved in PBS. Rinse once with PBS for 10mins. Permeabilize with 0.5% Triton X-100 (dissolved in PBS; 250uL Triton X-100 into 50mL PBS) for exactly 5 minutes at 4ºC. Rinse 2X with PBS for 10mins. Label with primary antibody diluted 1:200 in PBS with 1% high-grade BSA. For each coverslip, place one drop of primary antibody solution on a piece of parafilm inside a humidity chamber. Place coverslip FACE DOWN on top of the drop of primary antibody solution. Seal humidity chamber and incubate at R.T. for 1h. Rinse 3X with PBS for 10mins. Label with secondary antibody diluted 1:200 in PBS with 1% high-grade BSA. Place one drop of primary antibody solution on a piece of parafilm inside a humidity chamber. Place coverslip FACE DOWN on top of the drop of primary antibody solution. Seal humidity chamber and incubate at R.T. for 30mins. Rinse 3X with PBS 10min. Mount coverslips.

**Polysome profiling**

Plate $3.5X10^6$ cells onto a 15cm culture dish overnight. At harvest, the cells should be at no more than 70-80% confluency because cultures approaching 100% confluency tend to slow down general protein translation. Next morning infect cells with influenza WSN strain at an m.o.i. 2. Infect in 7.5mL regular media (no FBS) and incubate at RT for 1h and rock plates every 15mins. After 1h, add 7.5mL regular media + 2% FBS and incubate for 5h. After 6 h.t.p. add 75uL cyclohexamide to 100ug/mL to the media and incubate for 10mins at 37 C (add 75uL of cyclohexamide [20mg/mL]). After cyclohexamide incubation, transfer plate directly on ice. Aspirate the growth medium and wash cells with 10mL ice-cold PBS containing cyclohexamide to 100ug/mL. Aspirate the solution and repeat the wash step. Scrape cells with cell lifter and transfer to a cold 1.5mL eppendorf tube. Centrifuge at 7,000 RPM for 1min 4 C. After centrifugation, aspirate supernatant. Add 500 uL of cold RSB + RNAse inhibitor + cyclohexaminde + protease inhibitor buffer to resuspend pellet. Immediately add 500uL of cold PEB and mix. Freeze rapidly by liquid nitrogen and store at -80 degree. Thaw cells on ice and incubate on ice for 30mins for cell lysis (30sec vortex, 2min on ice). Spin at 10,000g for 10min at 4 C to clear lysates. Carefully load 1mL of the lysate on top of the sucrose gradient. Weigh each tube to verify they are about the same (need to be close enough for ultracentrifuge). Put all the tubes in the SW41 Ti rotor in order to properly balance. Place the SW41 Ti rotor in the rotor bucket and centrifuge at 36,000 RPM for 2h and 10mins at 4 C (Accel MAX, Decel 5). After centrifugation, carefully remove rotor bucket and keep tubes in ice at all times.Collect the gradient from the top into 20 fractions (0.6mL/fraction) in cold eppendorf tubes. For RNA extraction, digest each fraction by

adding 60uL 10% SDS and 6uL Proteinase K (20mg/mL) and incubate 30min at 42 C (can STOP and store fraction at -80 C ). Add 0.6mL of Trizol, mix, and incubate for 5mins at RT. Add (1) 0.2mL of chloroform/1mL of Trizol, (2) 4.5uL of glycol-blue [15ug/mL], and (3) 50uL of sodium acetate, pH 5.5 [3M] for final concentration of 0.1M and shake tube vigorously by hand for 15 sec. Incubate for 3mins at RT and then centrifuge samples at 12,000g for 15mins at 4 C. Remove the aqueous phase of the sample by angling the tube at 45 degrees and pipetting the solution out. Avoid drawing any of the interphase or organic layer into the pipette when removing the aqueous phase. Place aqueous phase into a new tube and add 0.5mL of 100% isopropanol to the aqueous phase/1mL of Trizol. Incubate for 10min at RT and then centrifuge at 12,000g for 10mins at 4 C. Remove the sup, leaving only the RNA pellet. Wash pellet with 1mL 75% ethanol/1mL of Trizol (2X) and vortex sample briefly, then centrifuge the tube at 7,500g for 5mins at 4 C. Discard the sup and air dry the RNA pellet for 15mins. Resuspend RNA pellet in RNase-free water (10uL) by passing the solution up and down several times. Incubate in water bath or heat block set at 55 C for 10mins (if necessary). Check RNA concentration by nano-drop. Run each fraction in a 1.5% agarose gel gel using TAE buffer. Add 10uL of RNA + 5uL 2X RNA loading dye to each tube and load each sample into the wells and run gel. Leftover sample can be stored at -80 C or used for QPCR analysis.

**dsRNA transfections**

Plate $3X10^5$ cells in 6-well dish overnight in 2mL full media. Next day prepare Lipofectamine 2000 – poly (I:C) complex. In 50 uL of serum/antibiotic free media add 4uL of lipofectamine 2000. In 50uL of serum/antibiotic free media add 2uL of HMW poly IC [1mg/mL] (final [ ] of 1ug/mL) for immunoblot analysis or 1uL of HMW poly IC [1mg/mL] (final [ ] of 0.5ug/mL) for QPCR analysis. Or 4uL of 5'ppp RNA [0.5mg/mL] (final [] of 1ug/mL) for immunoblot analysis or 2uL of 5'ppp RNA [0.5mg/mL] (final [] of 0.5ug/mL) for QPCR analysis. Mix both lipofectamine and poly (I:C)/RNA for 20mins at RT. Add mixture directly to plated cells and incubate. After incubation, wash cells twice with PBS and add 2X lysis buffer or 1mL of TriZol for RNA isolation.

# CHAPTER THREE
# Chemical screen identifies inhibitors of pathogenic viruses

## INTRODUCTION

One of the major concerns in the field of influenza virus is the limited therapeutic options as resistance to vaccines arises and the number of clinically approved antiviral drugs is small. Interest into developing novel therapeutics that temporarily target host factors without causing cytotoxicity but are vital for virus life cycle may: (1) significantly reduce the emergence of viral resistance and provide new avenues for the development of antiviral drugs that diminish virus propagation, and (2) provide insight into previously uncharacterized host antiviral mechanisms. As discussed above, NS1 is a major inhibitor of host-immune responses (148). Thus, this "viral weapon" represents a major point of weakness for inhibiting influenza virus infection and propagation. In this study, a chemical genetics approach was used to identify novel antagonists of NS1 protein function(s). These studies resulted in the identification of a number of compounds with the ability to antagonize NS1-mediated inhibition of host gene expression and protected cells from virus-mediated cell death. The work presented here focuses on compound **3**, a chemical entity of the naphthalimide family, which is a stable, non-cytotoxic compound that blocks the replication of various influenza virus strains and VSV. Further characterization revealed **3** reverts the influenza virus-mediated mRNA export blockage and that its antiviral effect is independent of type I IFN response pathway. These studies pointed to a novel host antiviral mechanism, which blocks the replication of two evolutionarily diverse viruses in a type I IFN-independent manner.

## RESULTS

*Naphthalimides antagonize NS1 and influenza virus*

A simple, yet highly sensitive assay was developed to monitor IAV NS1 ability to inhibit host gene expression using a luciferase reporter gene (157). Cells co-transfected with a plasmid encoding NS1 and luciferase showed a ~95% reduction in luciferase activity compared to cells transfected with luciferase plasmid alone (157). This assay was then employed to screen the UT Southwestern Compound Library in a high-throughput manner to identify chemical entities with the ability to revert NS1-mediated inhibition of host gene expression, using luciferase activity as the readout. Human 293-T kidney cells were co-transfected with plasmids encoding NS1 and luciferase; as a positive control, cells were transfected with luciferase plasmid alone. In total, 200,000 small molecules were screened at a concentration of 5μM (Figure 5A,B). The most active compounds with the ability of reverting NS1-mediated inhibition of luciferase expression two standard deviations above the mean were selected (640 chemical entities) for further characterization. These 640 compounds were subsequently tested in a secondary screen for their ability to inhibit influenza virus-mediated cell death of immortalized human bronchial epithelial cells (HBECs) by measuring cell ATP levels (Figure 5A,C). From the secondary screen, 71 compounds were identified, among which one of the most active compounds was 4-[N-4-nitro-(1,8-naphthalimide)]-butanoic acid, from here on referred to as compound **1** (Figure 5D).

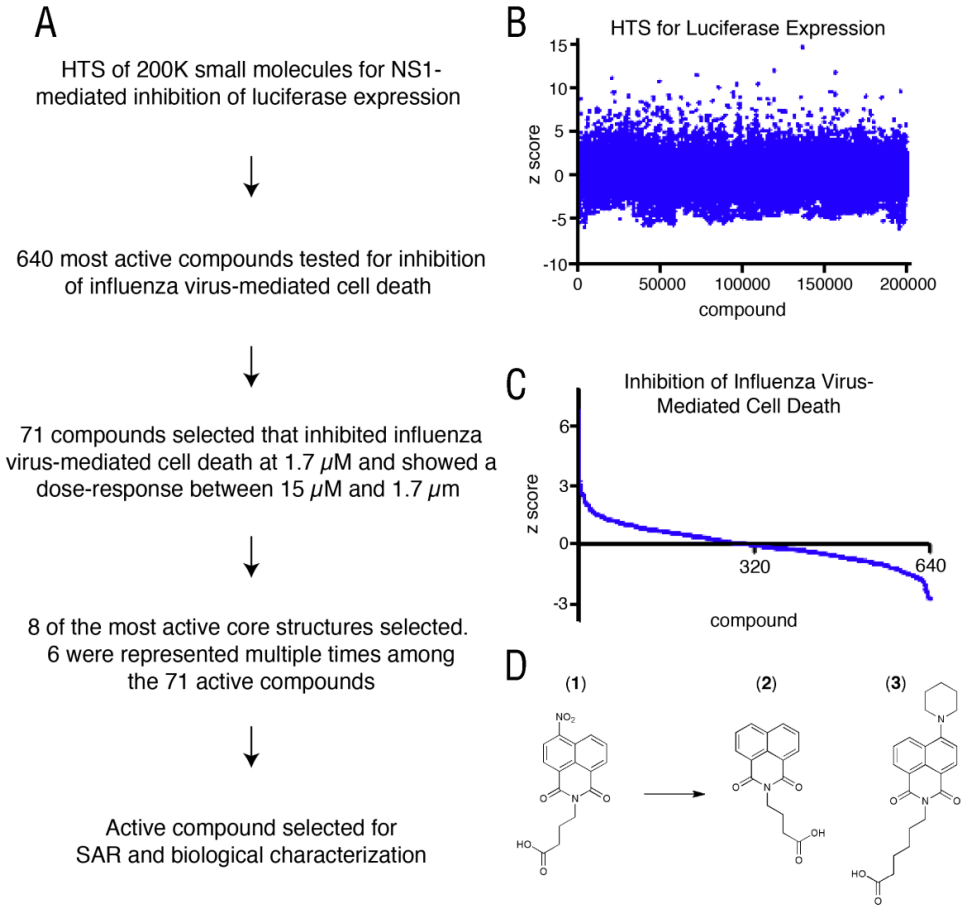


**Figure 5. Identification of small molecules that revert the inhibition of gene expression mediated by the influenza virus NS1 protein and protect cells from virus-induced cell death.**

(A) A flow chart describing primary and secondary screens and hit selection. (B) Luciferase expression in HEK 293Tcells transfected with NS1 and treated individually with 200,000 synthetic compounds (5 μM) was normalized to values for on-plate controls treated with 0.3% DMSO. Values are expressed as Z scores using the mean value and s.d. of the experimental population screened on the same day. Red circle shows compound 1 studied here. (C) Inhibition of influenza virus–mediated cell death. The 640 most active compounds were tested at three concentrations for the ability to inhibit the cytopathic effect of A/WSN/1933 influenza virus infection in HBECs. Z scores for compounds assayed at 1.7 μM are plotted according to activity. (D) The structure of the most active naphthalimide from the primary screen (**1**), an inactive analog (**2**) and a more potent related compound (**3**) are shown.

In collaboration with the UT Southwestern Chemistry Core, compound **1** was selected for Structural-Activity Relationship (SAR) studies to help identify more potent analogs of this bioactive compound. Analogs of compound **1** were each tested for their cytotoxicity and their ability to inhibit influenza virus replication (Figure 6). A few compounds lost antiviral activity upon modification, such as compound **2**, and compounds with more potent activity, such as compound **3**, were identified (Figure 5D and Figure 6).

| Compound | Structure | Cell Toxicity 24 h | Flu Titer 24 h |
|---|---|---|---|
| 1 | 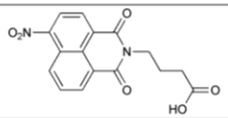 | 1.03 | 0.25 |
| 2 | 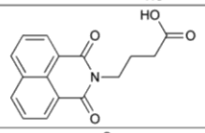 | 1.03 | 1.0 |
| 3 | 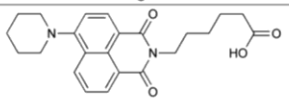 | 0.88 | 0.0005 |
| 5 | 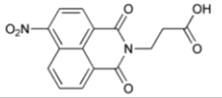 | 0.98 | 0.1 |
| 6 | 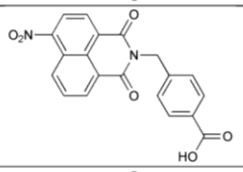 | 0.62 | nd |
| 7 | 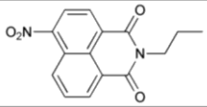 | 0.36 | 0.1 |
| 8 | 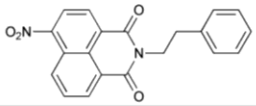 | 0.18 | nd |
| 9 | 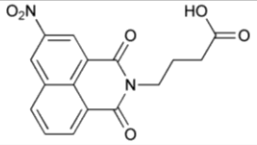 | 0.98 | nd |
| 10 | 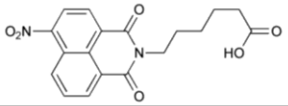 | 0.46 | nd |

**Figure 6. Compound 3 is a more potent inhibitor of influenza virus replication than other 1 analogs**.
To first measure cell toxicity, MDCK cells were treated for 24 h with 20 μM of each compound and ATP levels were measured. Values are normalized to controls treated with DMSO and represent triplicate values that had standard errors less than 10%. From a separate experiment, supernatants of cells infected with A/WSN/1933 influenza virus (m.o.i. 0.001) and treated for 24 h with 20 μM of each compound were subjected to hemagglutination (HA) assays (data not shown) and plaque assays (shown in the table), and values were normalized to that of control cultures treated with DMSO. Plaque assays

were not performed for compounds that exhibited no differences in HA assays (nd). Compound **8** was not tested for virus inhibition due to its rapid cytotoxicity. nd, not determined. Except for **3**, which was synthesized as described above, all the other compounds in this table can be obtained from ChemBridge, ChemDiv, ComGenex, TimTek, and their purities were equal or above 90%.

*Compound **3** is more stable and less cytotoxic than **1***

To demonstrate that the antiviral activity of these compounds was not due to cytotoxic effects, Madin-Darby canine kidney (MDCK) cells were treated with increasing concentrations of compounds **1**, **2**, **3** for 30 hours to determine cell viability by measuring cell ATP levels (Figure 7A). Compound **3** was much less cytotoxic than compound **1** even at high concentrations (Figure 7A). Next, compound stability was assessed by incubating hepatocytes with compounds **1** and **3** and determining the fraction of compound remaining in cells as a function of time by mass spectrometry. As Figure 7B shows, the fraction of compound **1** remaining in treated samples decreases substantially as time progresses. In contrast, compound **3** remains stable through the incubation period (Figure 7B).

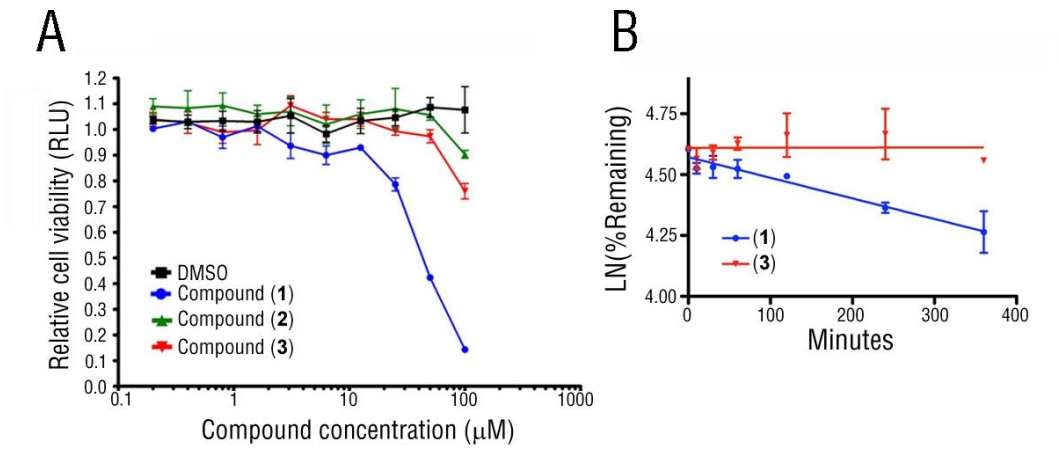


**Figure 7. Compound 3 is less cytotoxic to cells and more stable *in vitro* than 1.** (A) MDCK cells were treated for 30 hours with compounds **1**, **2** and **3** at the various concentrations depicted, and control cells were treated with the same concentration of DMSO as those in the wells containing compound. Cell viability was determined by measuring cell ATP concentrations. RLU, relative light units. (B) The fraction of compound remaining in cells treated with **1** or **3** as a function of incubation time was determined by mass spectrometry. LN, natural log.

*Compound **3** reverts influenza virus-mediated cytotoxicity and mRNA export block*

To determine the effect of compound **3** on the cytopathic effects mediated by influenza virus infection, MDCK cells were infected with influenza A/WSN/1933 virus at a low multiplicity of infection (m.o.i. of 0.001) in the presence or absence of **3**. Widespread cytopathic effects were observed in MDCK cells in the absence of **3** after 48 hours of infection (Figure 8A). In contrast, compound **3** significantly reduced this effect (Figure 8A). Since compound **3** was originally identified for its ability to revert the NS1-mediated inhibition of luciferase reporter expression in the primary screen, we set out to determine if **3** could revert the mRNA export block induced by influenza virus infection. To detect the distribution of host poly(A) RNA in the nucleus and cytoplasm after

influenza virus infection of MDCK cells treated and non-treated with compound **3**, mock infected and infected cells were fixed and subjected to oligo-(dT) *in situ* hybridization to detect poly(A) RNA. Mock infected cells show an equal distribution of poly(A) RNA in the nucleus and the cytoplasm (Figure 8B). In contrast, cells infected with influenza virus alone show a dramatic accumulation of poly(A) RNA in the nucleus (Figure 8B). In influenza virus infected cells treated with **3**, there was a decrease in the number of cells that retained poly(A) RNA in the nucleus compared to the number of infected cells not treated with **3** (Figure 8B). A subpopulation of infected cells still presented mRNA export block in the presence of **3**; thus, it is possible that these cells are at different phases of the cell cycle, which is known to regulate mRNA export (184). Thus, **3** reverts the influenza virus-mediated widespread cytopathic effects and **3** partially antagonizes the mRNA export block in virus-infected cells.

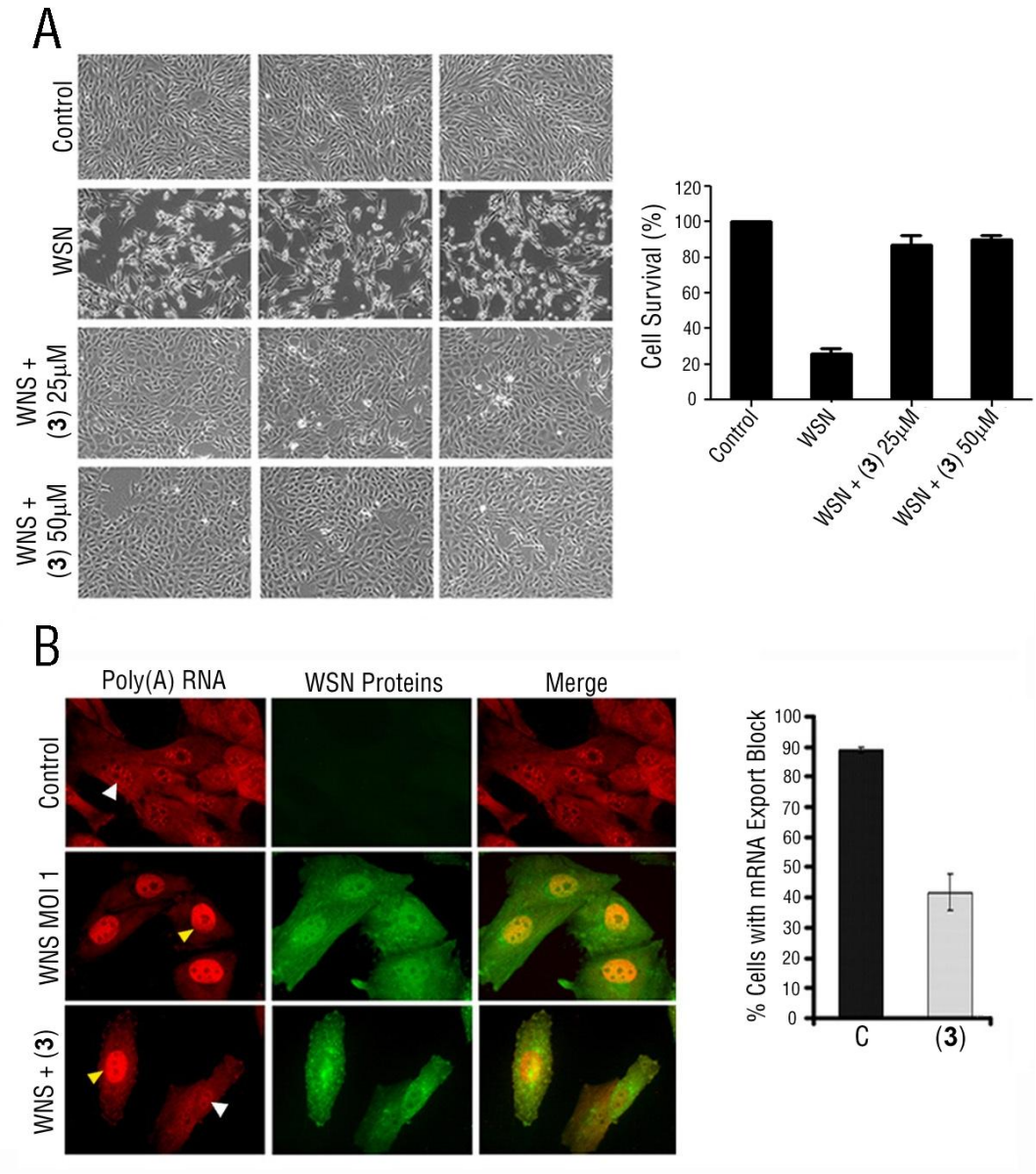


**Figure 8. Compound 3 reverts influenza virus-mediated cytotoxicity and mRNA export block.**

(A) MDCK cells were pretreated for 17 hours with DMSO or with the indicated concentrations of **3** and subsequently mock infected or infected with A/WSN/1933 virus at m.o.i. 0.001 for 48 hours. The indicated concentrations of compound were present during infection. Differential interference contrast (DIC) microscopy imaging was performed in a Zeiss Axiovert 200M. Cell survival was determined by counting live cells. Scale bar, 90 μm. (B) MDCK cells, mock infected or infected with A/WSN/1933 in the

presence or absence of 25 μM **3**, were fixed and subjected to oligo-dT *in situ* hybridization to detect poly(A) RNA distribution in the nucleus and cytoplasm. Influenza proteins were detected by immunofluorescence using antibodies specific for influenza proteins. Yellow arrowheads point to cells with mRNA export block, whereas white arrowheads point to cells that do not show blockage. Scale bar, 15 μm. Data from triplicate experiments were quantified and the percentage of infected cells retaining mRNA in the nucleus is shown. Data represent mean values ± s.d.

*Naphthalimide inhibits virus replication*

The effect of **3** on virus replication was then assessed using various strains of influenza virus: A/WSN/1933, A/Texas/1991 and the highly virulent A/Brevig/Mission/1/1918 strain that killed ~30 million people23 (Fig. 9A-C). Noncytotoxic concentrations of **3** reduced viral titers by 103 to 106 between 24 to 36 h after infection, depending on the influenza virus strain. The ratio of the concentration causing half-maximum cytotoxicity (CC50) to half-maximum inhibitory concentration (IC50) for **3** was 31 (Figs. 7A and 9A). Similar results were also observed in human A549 cells (Figure 10). As shown in Figure 3d, intracellular influenza virus proteins were also down-regulated in the presence of **3**. Thus, **3** decreased viral protein levels, contributing to the reduction of virus replication.

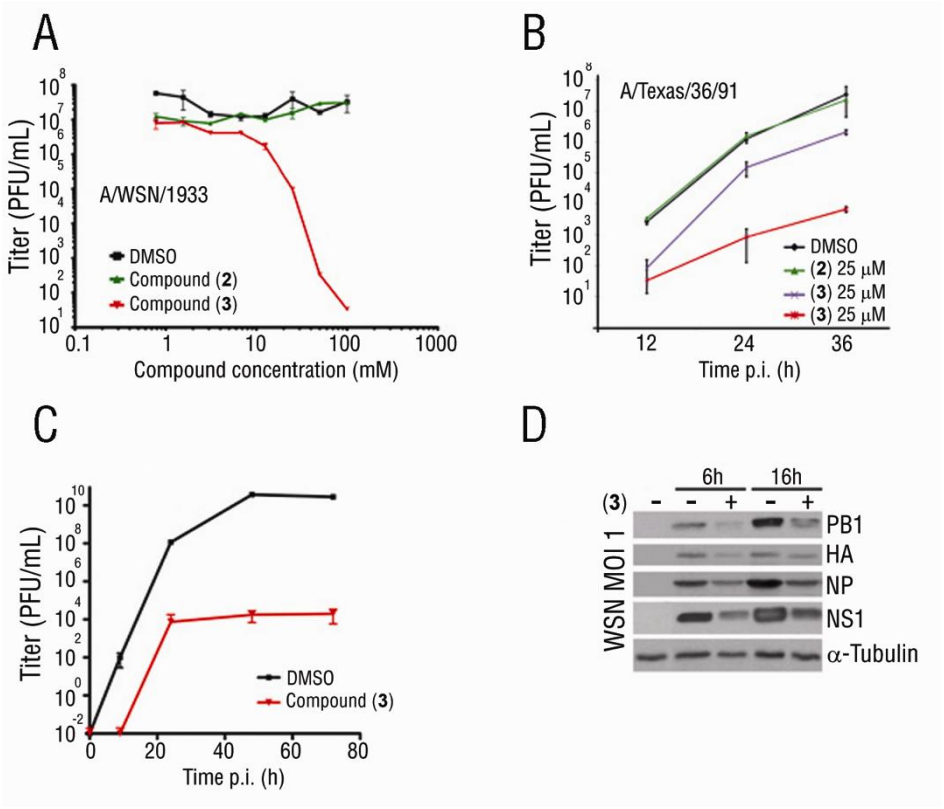


**Figure 9. Compound 3 inhibits virus replication and decreased viral protein levels.** (A-C) MDCK cells mock infected or infected at m.o.i. 0.001 with the influenza virus strains shown were left untreated or treated with compounds at the depicted concentrations, and the virus titers of culture supernatants were determined by plaque assay. Strain A/WSN/1933 is in (A), A/Texas/36/91 is in (B) and A/Brevig/Mission/1/1918 is in (C). (D) Intracellular viral protein concentrations were measured by immunoblot analysis with specific antibodies to the indicated proteins.

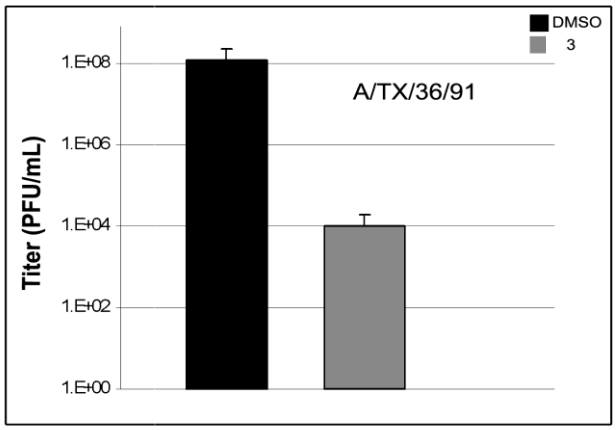


**Figure 10. Influenza virus replication is inhibited by 3 in human carcinomic alveolar basal epithelial cells.**
A549 cells were untreated or pre-treated with 30 μM of **3** overnight. Cells were then infected with A/Texas/36/1991 at m.o.i. 0.001 for 1 h at 22 $^0$C, in the absence of compound. Cells were shifted to 37 $^0$C.

*Antiviral activity of compound **3** is not mediated by IFN*

Type I interferon (IFN) response, represented by IFN-α and IFN-β, is a potent host defense mechanism against pathogens. IFNs have the ability to orchestrate a powerful antiviral innate immune response capable of restricting virus proliferation and stimulate an antiviral response in IFN-sensitive cells to prevent virus spread (185). Therefore, to test whether compound **3** was eliciting a type I IFN response which could lead to the reduction in virus replication as shown in Figure 9, the RNA expression levels of IFN-β and several IFN effector genes was measured by quantitative real-time PCR. Treatment of human A549 cells with compound **3** or DMSO alone for 36 hours did not elicit the expression of IFN-β or any of the IFN effector genes analyzed (IRF7, RIG-I and ISG-54; Figure 11). To demonstrate A549 cells are IFN competent, cells were infected

with Sendai virus (SeV, Cantell strain), a negative sense, single stranded RNA virus known to potently activate IFN antiviral response (186). After infection with SeV, RNA levels of IFN-β, IRF7, RIG-I and ISG-54 in A549 cells increased dramatically (Figure 11); demonstrating A549 cells are indeed capable of mounting a type I IFN response after virus infection. To rule out the possibility that compound **3** induced a type I IFN response only when cells were infected with influenza virus, compound **3** treated A549 cells were infected with virus strain A/WSN/1933 and the RNA expression of IFN-β and type I IFN effector genes was measured. A/WSN/1933 infected cells, whether in the presence or absence of compound **3**, were unable to induce a type I IFN response (Figure 11). As was previously shown by others, influenza virus blocks type I IFN production via its virulence factor NS1 protein (187) (Figure 11) . In sum, these results show that compound **3** did not induce IFN production or a type I IFN-mediated response.

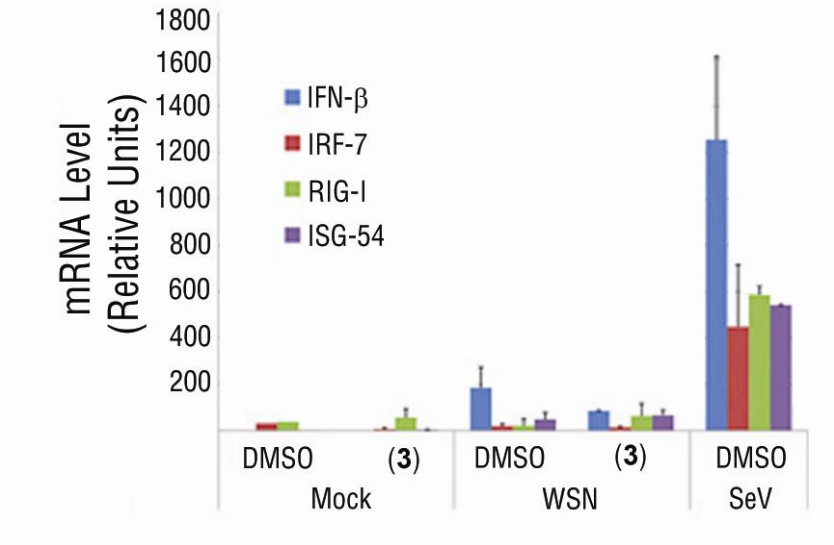


**Figure 11. Compound 3 does no induce a type I IFN response.**
Human A549 cells treated with DMSO or 25 μM **3** were mock infected or infected with A/WSN/1933 at m.o.i. 0.001, and after 36 h, RNA was isolated and the expression of IFN-responsive genes was quantified by real-time PCR.

To further show the antiviral activity of compound **3** is type I IFN-independent, compound **3** was tested for its ability to protect IFN-deficient cells from influenza virus-mediated cytotoxicity. We selected two different cell lines that are IFN deficient. First, Vero cells, derived from African green monkey kidney, fail to induce an interferon response when infected with virus (188). Secondly, *STAT1* knockout mouse embryonic fibroblasts are unresponsive to IFN due to the genetic deletion of the *STAT1* gene, an essential component of the type I and II IFN mediated signaling (189). First, no compound cytotoxicity was observed in Vero or *STAT1-/-* cell lines, as measured by cellular ATP levels (Figure 12A,B). Next, supernatants of influenza virus infected Vero cells treated with DMSO or compound **3** were subjected to hemaglutinin (HA) assay to

measure virus particle production. Treatment with **3** drastically reduced the amount of virus particles, as measured by hemagglutination units (HAU), whereas DMSO had no effect (Figure 12A). Moreover, *STAT1-/-* cell survival was determined, as measured by cellular ATP levels, after treatment with DMSO or compound **3** in the absence or presence of influenza virus. The results show compound **3** significantly protected *STAT1-/-* MEFs from viral-mediated cell death (Figure 12B).

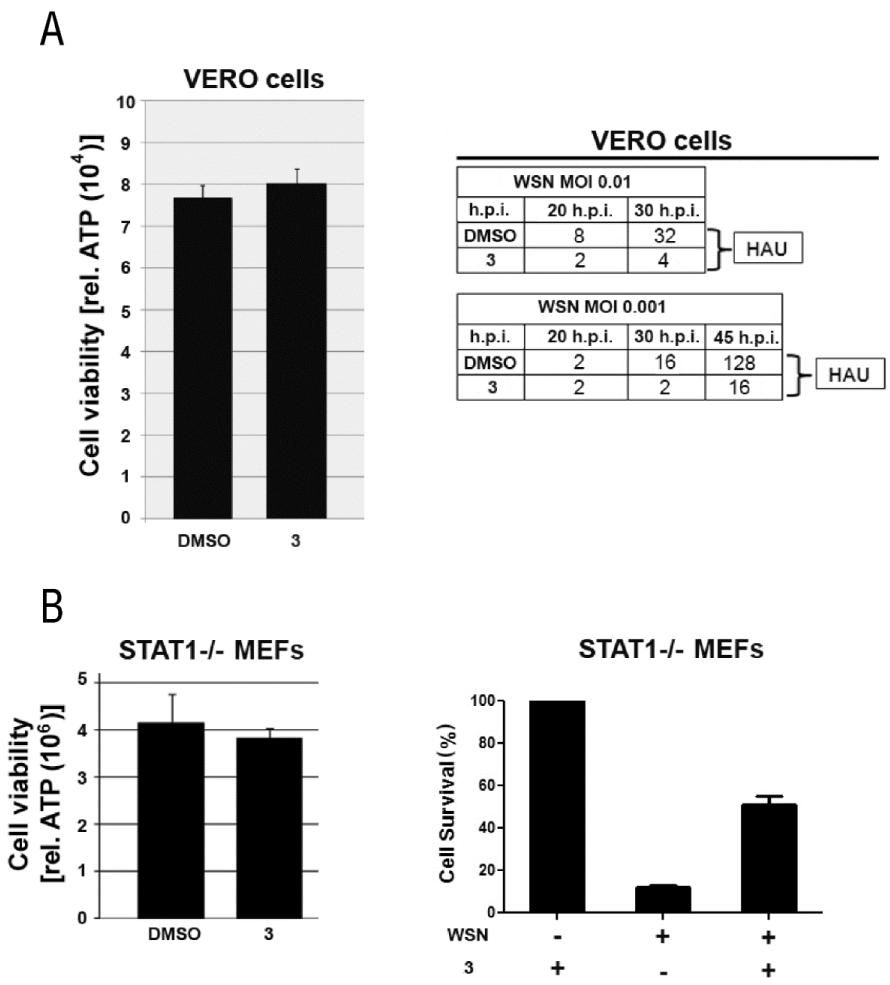


**Figure 12. Interferon response is not required for naphthalimide antiviral activity**. (A) Vero cells were untreated or treated with **3** (50μM) and ATP levels were measured. No cytotoxicity was observed at this concentration. Vero cells were then infected with A/WSN/1933 at an m.o.i. 0.01 or 0.001 for the indicated time points. Cells were treated with DMSO or **3** (50μM) during infection. Supernatants were subjected to hemaglutinin assays (HA) to measure viral titers. HAU, hemagglutination unit. Since Vero cells are interferon-deficient cells and were protected from virus replication by **3**, this compound does not act via interferon. (B) STAT1-/- cells were untreated or treated with **3** (40μM) and ATP levels were measured. No cytotoxicity was observed at this concentration. STAT1 -/- cells were then infected with A/WSN/1933 at an m.o.i. 0.01 for 72 h. Cells were untreated or treated with **3** (40μM) in the absence or presence of virus and cell survival was determined by measuring ATP levels. STAT1-/- cells were significantly protected from viral-mediated cell death in the presence of **3**.

Finally, the intracellular viral protein concentrations of virus infected Vero cells treated and untreated with compound **3** were measured as a function of time. Compound **3** treatment, and not DMSO, significantly decreased the protein levels of influenza virus proteins HA, NP and NS1 (Figure 13). Compound **3** antagonized the expression of large quantities of influenza virus proteins, which likely contributed to the reduction in virus replication. These observations indicate that compound **3** antiviral activity is independent of type I IFN response (Figures 11-13).

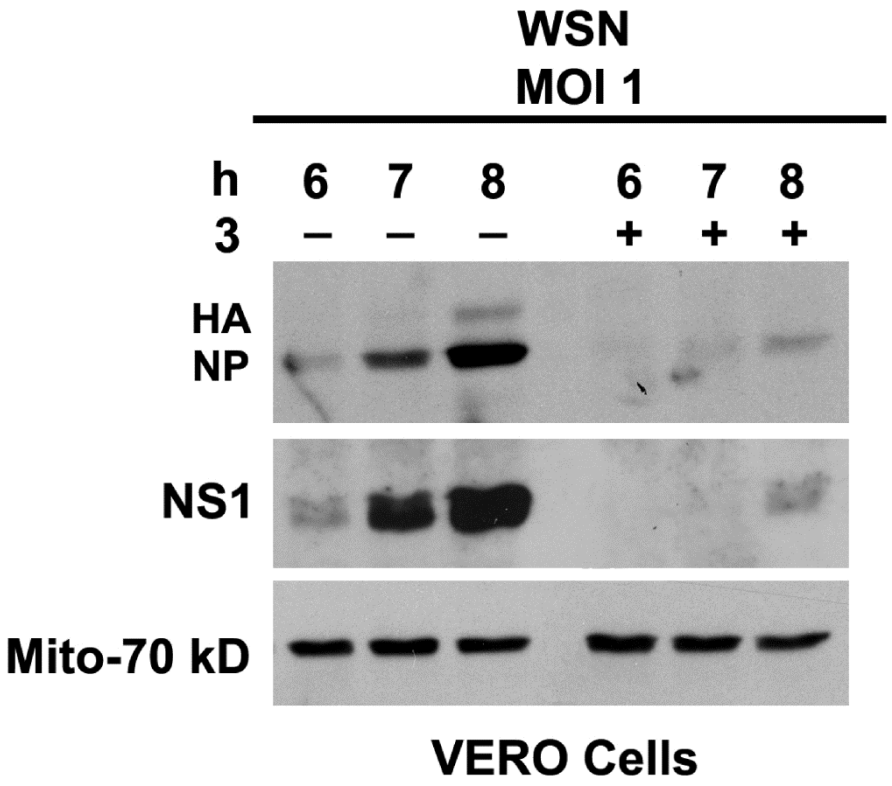


**Figure 13. Influenza virus protein levels are down-regulated by 3 in cells with impaired interferon response.**
Vero cells were pre-treated with **3** (50μM) for 2 h and then infected with A/WSN/1933, at m.o.i. 1 for 1 h in the absence of compound. One hour post-infection, **3** was added back and incubated for various time periods as depicted in the figure. Cell extracts were subjected to immunoblot analysis with antibodies against influenza virus proteins or with an antibody against a mitochondrial protein, used as loading control.

*Compound **3** protects against evolutionary diverse viruses*

To investigate whether **3** antagonized NS1directly or promoted host antiviral functions regulated by NS1 that could also affect the replication of other viruses, MDCK cells were infected with VSV, a negative sense, single stranded RNA virus, at a low m.o.i. in the absence or presence of compounds **2** or **3**. Treatment of infected cells with DMSO or compound **2** did not affect VSV replication (Figure 14). In contrast, compound **3**, in a dose dependent manner, inhibited VSV replication (Figure 14). These results show that **3** targets host cell functions that confer an antiviral state against evolutionarily diverse viruses.

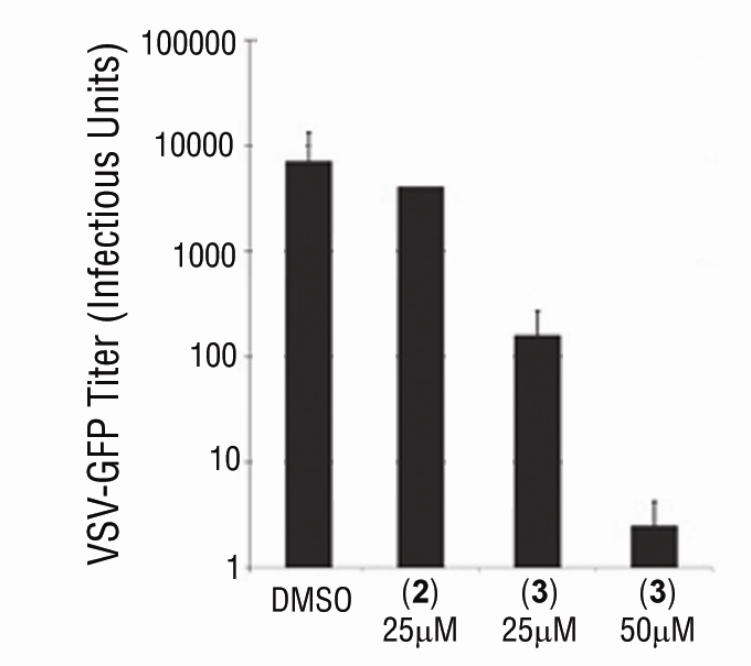


**Figure 14. Compound 3 protects against evolutionary diverse virus.**
MDCK cells mock infected or infected with VSV-GFP (m.o.i. = 0.001) were untreated or treated with the indicated compounds. At 24 h after infection, virus titers were determined in the supernatants.

**DISCUSSION**

Influenza A virus causes respiratory disease affecting all age groups (190). The emergence of resistant influenza virus strains to clinically-approved antiviral drugs, the lack of potential viral drug targets, and the recent pandemic outbreaks have raised concerns for the development of novel influenza therapies. Here, we took a chemical genetics approach to identify small molecule inhibitors of the influenza A virus NS1 protein. Our approach, in combination with SAR analysis, allowed the identification of numerous non-cytotoxic, stable synthetic compounds with anti-influenza activity.

Of particular interest to this study is compound **3**, a member of the naphthalimide family of compounds that significantly reverts the influenza virus-mediated mRNA export blockage (157). This reversal in mRNA export block by **3** likely results in the translocation of mRNAs that encode antiviral factors to the cytoplasm where they can help establish an antiviral state, limiting virus replication. In addition, compound **3** also blocks the replication of various influenza A virus strains. This is particularly important with respect to the high genetic diversity and rapid rate of mutation of influenza virus that often gives rise to novel infectious particles composed of segments from various subtypes to which no pre-existing immunity is present in the human population. Therapeutic modalities capable of targeting multiple virus strains could alleviate the need to constantly re-formulate anti-influenza vaccines every year and could represent an efficient measure for preventing or treating influenza infections. In the event of a pandemic, a previously mass-produced pan anti-influenza drug could effectively be utilized as a protective immunoprophylactic initially to provide a barrier against virus propagation while a specific vaccine is developed.

Our studies show in numerous experimental settings that the ability of compound **3** to inhibit influenza virus cytotoxicity is independent of IFN production or an IFN-mediated response, one of the first lines of host defense against virus infection (187). These results suggest that compound **3** may block the replication of influenza virus through a novel mechanism that does not require the IFN response pathway.

The ability of compound **3** to effectively block the replication of evolutionarily diverse viruses demonstrated that the antiviral activity of **3** is not to antagonize NS1 protein directly but instead it is modulating a host antiviral pathway(s) that establishes an antiviral state, suppressing the replication and propagation of these viruses. Understanding how **3** blocks virus replication could result in: 1) the identification of host cellular factors and/or pathways that are manipulated by viruses to effectively maintain high levels of replication, 2) provide information regarding key points of virus vulnerability that can be exploited for therapeutic intervention, and 3) reveal information about the regulation of these pathways by the host.

# CHAPTER FOUR
# Influenza virus activates the mTORC1 pathway

## INTRODUCTION

The mammalian target of rapamycin, mTOR, pathway is a regulator of cell growth, proliferation, and survival (19). mTOR is part of two distinct macromolecular complexes called mTORC1 and mTORC2. Each complex is composed of unique accessory proteins, which give each complex its identity. The accessory protein RAPTOR is only found associated with the mTORC1, whereas RICTOR associates with only with mTORC2 (191-193). Rapamycin, a potent antifungal natural product, has been a valuable experimental tool to dissect the host cellular pathways governed exclusively by mTORC1, since mTORC2 is rapamycin-insensitive (194). Two of the best characterized downstream mTORC1 effectors, which control protein synthesis, are the ribosomal protein p70-S6K (S6K) and the eukaryotic initiation factor 4E (eIF4E)-binding protein 1 (4E-BP1) (19).

The mTORC1 signaling pathway is tightly regulated by a number of environmental signals, such as growth factors and stress conditions, which activate or help to antagonize mTORC1 kinase activity. The PI3K/AKT pathway is a critical positive regulator of the mTORC1 pathway. Activation of AKT, via phosphorylation of Threonine 308 and Serine 473, leads to the indirect activation of mTORC1 by inactivation of the TSC1/TSC2 heterodimeric complex, an mTORC1 negative regulator, via AKT-mediated phosphorylation of the TSC2 subunit (195).

Host signaling pathways important for growth and survival have been exploited by a number of pathogens to establish a microenvironment suitable for virus replication and assembly. Many viruses activate AKT by stimulating PI3K (42-43). The direct binding of NS1 protein of influenza virus to PI3K results in activation of AKT (165-166, 196). This has been interpreted either as a means to inhibit apoptosis and prevent the cell from dying prematurely during infection or as a necessary step in promoting virus replication. A recent genome-wide siRNA screen implicated mTORC1 in influenza virus replication (15), suggesting that activation of that pathway might be one of the functions of elevated AKT1 signaling.

Our studies show that infection with influenza virus induces a robust induction of mTORC1 activity, as measured by phosphorylation of its downstream target S6K. Studies into the mechanism by which compound **3** exerts its antiviral activity revealed that **3** treatment, in the presence or absence of virus infection, inhibited the phosphorylation and activation of S6K, while bulk protein synthesis was unaffected by **3**.

## RESULTS

### *Compound **3** down-regulates the mTORC1 signaling pathway*

The results presented above show that compound **3** inhibits the replication of various influenza virus strains and VSV, which are evolutionary diverse virus. This suggests that **3** is likely targeting a host pathway(s) leading to the activation of an antiviral response which results in the inhibition of virus replication. To begin investigating host cellular pathway(s) targeted by **3**, host pathways were analyzed by

comparing the gene expression profiles of compound treated and untreated human A549 cells using gene set enrichment analysis (Figure 15). In cells treated with **3**, the mTORC1 pathway had one of the highest enrichment scores. The negative regulator of the mTORC1 pathway, REDD1 (35-37, 60) was up-regulated at the mRNA level several fold compared to DMSO treated samples (red oval, Figure 15).

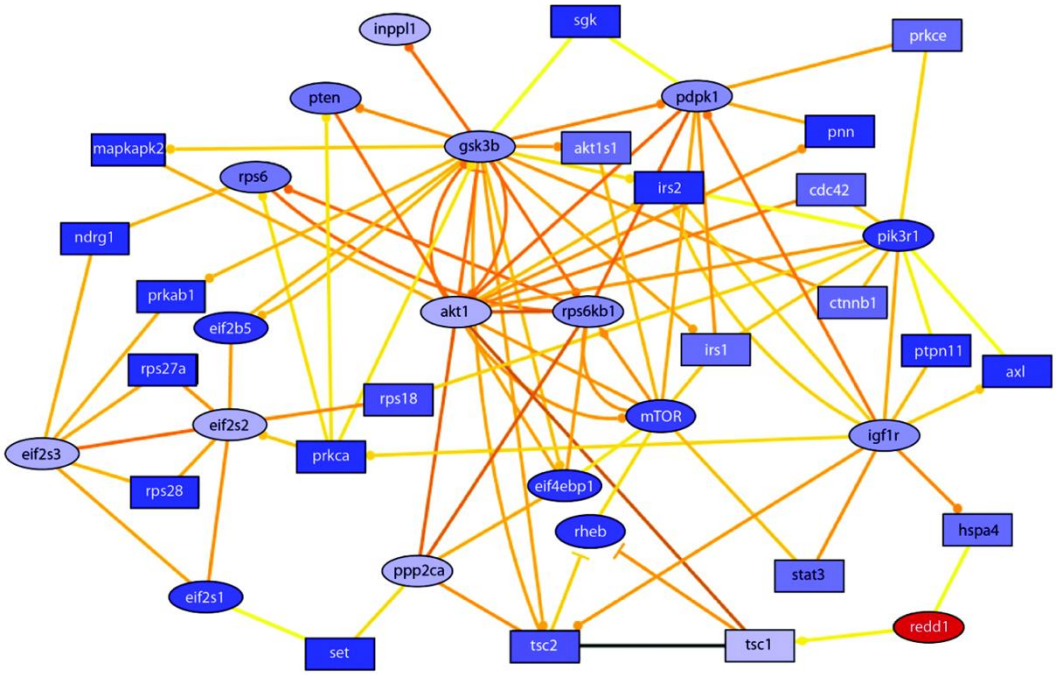


**Figure 15. The mTORC1 pathway is regulated by 3.**
A549 cells were treated with DMSO or with 30µM **3** for 3 h. RNA was isolated and processed for microarray analysis. The results of triplicate experiments were subjected to Gene Set Enrichment Analysis as described in Methods. Response networks after enrichment analysis of cells treated with **3** versus DMSO alone are shown: Node colors refer to fold changes - white denoting no change to dark blue indication down-regulation of a three-fold or more, and red depicts up-regulation. Oval shapes refer to enriched genes in the particular gene set, rectangles denote other genes that have been identified to function in the response network by NetworkExpress. Edge colors indicate edge scores after NetworkExpress analysis using average fold changes between connected nodes. Yellow edges indicate high edge score. Edge arrow shapes denote different types of interactions with arrows indicating metabolic reactions, circles identifying phosphorylation, and no arrow shape refers to protein-protein interactions. The diagram displays the MTORPATHWAY response network with 40 nodes and 92 edges calculated with parameters k= 3 and l= 5.

*Influenza virus induces mTORC1 activation*

Given the recent studies showing influenza virus activates the PI3K/AKT signaling pathway, which can regulate mTORC1, the potential effect influenza virus infection had on the mTORC1 signaling network was examined. One of the best characterized mTORC1 downstream effectors is the ribosomal protein p70-S6K (S6K). Activation of S6K, via phosphorylation by mTORC1 at Threonine 389 (Thr389), promotes protein synthesis (197). Therefore, S6K phosphorylation was used as readout for mTORC1 activity. Our results show that influenza virus greatly increased the phosphorylation levels of S6K at Thr389 four and seven hours post infection in A549 cells infected with influenza virus strain A/36/TX/1991 at a high m.o.i. (Figure 16A). Then, infected cells were treated with compound **3** and mTORC1 activity was measured. In contrast to non-treated influenza virus infected cells, compound **3** treatment greatly reduced S6K phosphorylation (Figure 16A). The total levels of S6K were assessed and no effect was observed under any experimental condition (Figure 16A); demonstrating that the effect of **3** occurred at the phosphorylation level and not at the total protein level. Inhibition of the PI3K/AKT signaling pathway could have also resulted in the decrease in mTORC1 activity. To determine if compound **3** had any effect on PI3K/AKT activity, AKT activation was monitored. The mTORC2 complex and the phosphoinositide-dependent kinase-1 (PDK1) have been previously shown to activate AKT by phosphorylating two major active sites, Serine 473 and Threonine 308, respectively (198-200). Previously, influenza virus was reported to activate AKT by stimulating mTORC2-dependent phosphorylation of Serine 473 (164-165). Therefore, to monitor the effect of **3** on AKT activation, A549 cells infected with influenza virus to induce AKT were treated

with compound **3** to assess Serine 473 phosphorylation. As reported, influenza virus robustly induced AKT Serine 473 phosphorylation seven hours post infection (Figure 16B). Treatment of virus infected cells with **3** or DMSO did not alter the phosphorylation of Serine 473 at early time point (Figure 16B). Similar to previous data shown in Figure 16A, compound **3** blocked influenza virus-induced S6K activation at 7 and 22 hours post infection (Figure 16B). At 22 hours after infection, **3** did not alter PDK1-dependent phosphorylation at AKT Threonine 308 but reduced phosphorylation at AKT Serine 473 (Figure 16B); however, this reduction is probably an indirect effect of **3** on the inhibition of viral replication rather than a direct effect of **3** on AKT. As a control for efficient virus infection, NS1 total protein levels were monitored. Similar to data shown in Figure 9D, compound **3** treatment significantly decreased the expression of the influenza NS1 protein (Figure 16B). Together, these observations indicate that compound **3** acts in parallel to or downstream of the PI3K/AKT pathway.

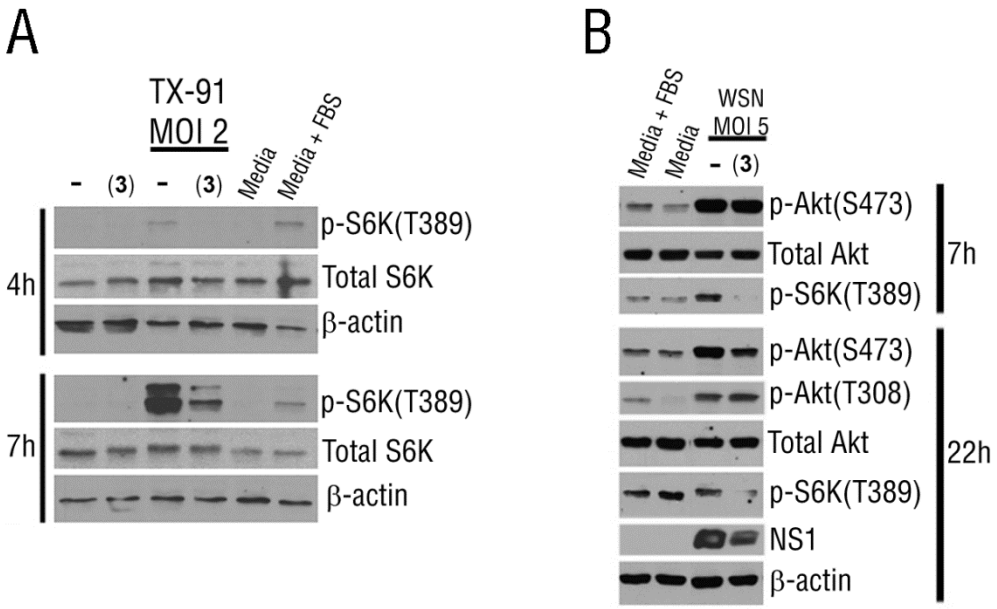


**Figure 16. Influenza virus activates the mTORC1 pathway.**
(A) A549 cells were untreated or treated with 30μM **3** for 18 hours before infection and during infection. Cell extracts were obtained at the depicted time points and subjected to immunoblot analysis with the indicated antibodies. (B) Phosphorylation of Akt or S6K was measured by immunoblot analysis in cell extracts of A549 cells infected with influenza virus in the presence or absence of **3**. Compound was added prior to and during infection as in (A).

To investigate whether **3** prevented S6K activation independently of influenza virus, the effect of **3** in H358 non-small cell lung cancer cells, which have chronically active S6K, was examined. Phosphorylation of S6K at Threonine 389 of H358 cells treated with compound **3** and inactive **2** was monitored. As Figure 17A shows, only **3** decreased S6K activation, whereas DMSO and **2** treatment had no effect on S6K. In two other cancer cell lines with chronically active AKT, H1993 (non-small cell lung cancer cells) and LnCAP (human prostate adenocarcinoma cells), **3** also reduced the activation of S6K (Figure 17B). This effect is at the phosphorylation level since total levels of S6K

remain unchanged in the presence or absence of **3** (Figure 17B). Moreover, mTORC2-mediated activation of AKT was monitored and no effect was observed on Serine 473 phosphorylation in compound **3** treated samples (Figure 17B). These data show that compound **3** inhibits the mTORC1 signaling pathway independent of AKT signaling.

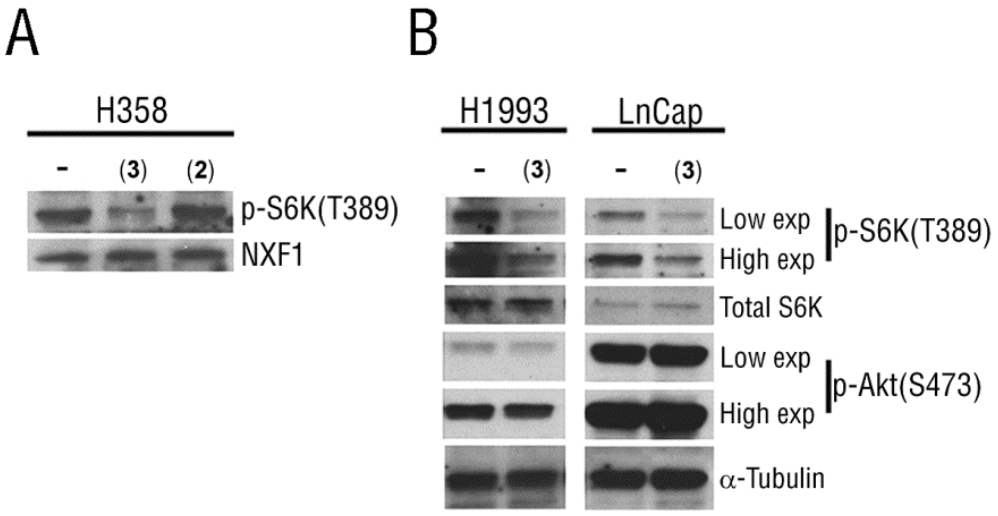


**Figure 17. Compound 3 inhibits the mTORC1 pathway independent of virus infection.**
(A) Human lung cancer H358 cells have chronically activated S6K signaling indicated by S6K p-Thr389, which is inhibited by **3** in the absence of virus, but not by **2**. (B) In two additional cancer cell lines with chronically activated S6K, **3** inhibited phosphorylation of S6K on Thr389, but did not inhibit AKT phosphorylation.

Based on the previous data showing that compound **3** inhibits the mTORC1 pathway and published work showing mTORC1 inhibition by rapamycin, in a concentration dependent manner, suppressed virus replication (15), viral protein expression after pharmacological inhibition of mTORC1 with rapamycin was examined. As shown in Figure 18, rapamycin treatment of influenza virus infected A549 cells reduced NS1 total protein levels, similar to the results obtained with compound **3** treatment of virus infected samples (Figure 9D and 16B). In total, inhibition of the mTORC1 pathway by rapamycin or compound **3** decreases viral protein production and hence reduces virus replication.

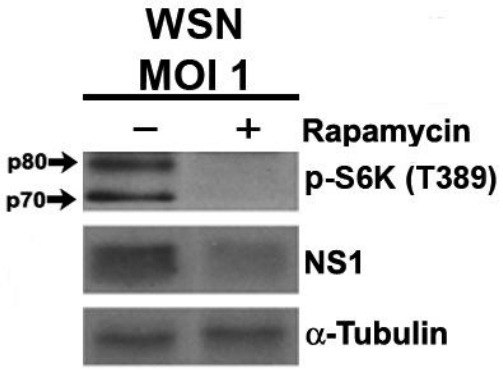


**Figure 18. Rapamycin treatment reduced the levels of influenza virus NS1 protein.** A549 cells were treated with 100 nM rapamycin for 18 hours and then infected with influenza virus A/WSN/1933 for 6 hours in the presence of rapamycin. Cell extracts were obtained and immunoblot analysis was performed with anti-NS1 antibodies.

mTORC1 is a master regulator of cell growth and proliferation (19). One of the key processes governed by mTORC1 is protein translation. The reduction in viral protein

expression and virus replication upon compound **3** treatment could have resulted from the inhibition of protein synthesis, which could be deleterious to the host. As shown in Figure 19, compound **3** did not affect bulk protein synthesis. Untreated and **3** treated MDCK cells were pulse labeled with $^{35}$S-Methionine for several time points and incorporation of labeled $^{35}$S-Methionine proteins was measured by scintillation counter. Compound **3** treatment did not alter global incorporation of $^{35}$S-Methionine into newly synthesized proteins at any of the time points assessed (Figure 19).

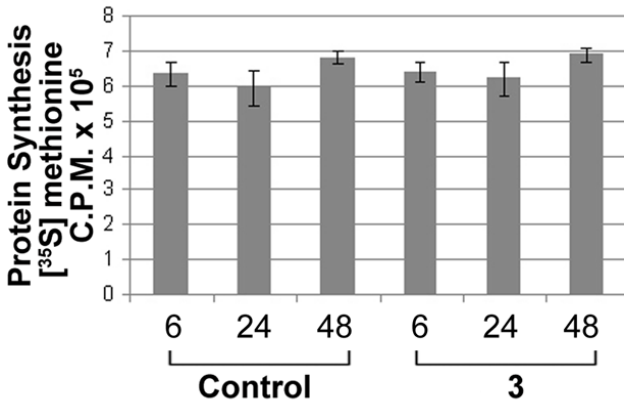


**Figure 19. Bulk protein synthesis is not inhibited by 3.**
Protein synthesis was measured by pulse labeling MDCK cells with $^{35}$S-methionine, untreated or treated with 50 μM of **3**. Samples were collected at the indicated time points and $^{35}$S-methionine labeled proteins were measured.

**DISCUSSION**

Our previous results indicated that compound **3** targeted a host signaling pathway(s) leading to the activation of antiviral response capable of inhibiting the replication of evolutionarily diverse viruses. Gene set enrichment analysis of compound treated samples indicated that the mTORC1 signaling pathway had one of the highest enrichment scores.

Recently, a genome-wide RNAi screen linked the mTORC1 signaling pathway and influenza virus replication (15). Suppression of mTORC1 activity resulted in the inhibition of influenza virus replication (15). The reason(s) for a reduction in virus replication after mTORC1 inhibition was not determined (15). In addition, a previous study also implicated influenza virus in the activation of the PI3K/AKT pathway, a known positive regulator of the mTORC1 pathway (165-166). This study failed to examine mTORC1 activation status. Herein, our work shows that influenza virus activates the mTORC1 pathway soon after infection. One of the cellular processes governed by mTORC1 is the translation of mRNAs (24). Modulation of this pathway by influenza virus could enhance the translation of viral transcripts and allow the virus to establish an environment that can support virus replication. In support of this idea, we observed that pharmacological inhibition of mTORC1 by rapamycin results in decreased viral protein expression. Influenza virus is not the only virus known to modulate the mTORC1 signaling network. The human herpesvirus 8 activates this pathway to control cell survival (44), adenovirus also requires activation of the mTORC1 pathway for virus replication in primary cells (45), and recently mTORC1 activity was shown to be elevated in VSV-infected cells (46). These findings underscore the crosstalk between

viruses and the mTOR pathway, a signaling network deregulated in a number of cancers. Furthermore, it demonstrates that understanding how viruses manipulate host cellular processes could reveal information about the complex regulation of these pathways by the host.

Our microarray analysis resulted in the identification of REDD1, a known inhibitor of mTORC1, to be up-regulated at the mRNA level by compound **3**. Treatment of virus-infected cells with **3** abolished mTORC1 activation and this effect was in parallel to or downstream of the PI3K/AKT pathway. Similar to the rapamycin effect on virus protein expression, compound **3**, at non-cytotoxic concentrations, also blocks the expression of several influenza virus proteins without negatively affecting bulk protein synthesis. By temporarily targeting host pathways without causing toxic effects, small molecules could play a major role as antiviral drugs given the increasing resistance to current anti-influenza therapeutics that specifically target a viral protein function(s).

Importantly, compound **3** blocked mTORC1 signaling in three independent lung cancer cells lines with chronically active AKT or S6K. mTORC1 control key cellular pathways that are deregulated in human cancers and disruption of positive and negative regulators of mTORC1 have been implicated in tumor development (38-39) In fact, rapamycin and rapalogues (rapamycin analogues) are currently being evaluated for the treatment of cancer (17) and some rapalogues have shown anti-tumor activity in patients with renal clear cell carcinoma and breast cancer (41).

# CHAPTER FIVE
# Antiviral activity of naphthalimide requires REDD1

## INTRODUCTION

Regulated in development and DNA damage response 1 (REDD1) protein was first identified in mammals as a direct transcriptional target of the hypoxia inducible factor-1α (HIF-1α) (47). This study showed that under normal conditions, REDD1 was detectable at low levels, but upon low oxygen conditions (hypoxia) the expression of REDD1 sharply increased ~5 fold (47). Subsequent studies in *Drosophila* and mammalian cells showed that REDD1 induction during hypoxia was followed by down-regulation of the mTORC1 pathway (35, 60) and genetic ablation of REDD1 abolished the hypoxia-induced inhibition of the mTORC1 pathway (35). Importantly, gain-of-function experiments showed REDD1 overexpression to be sufficient to downregulate mTORC1 activity in the presence of an intact TSC1/TSC2 complex (35), and ectopic expression of the *Drosophila* REDD1 orthologs (*scylla* and *charybdis*) resulted in organ size reduction in the adult fly (60). REDD1 has also been found to be induced during other types of environmental stress, such as energy depletion, DNA damage, glucocorticoid treatment, ER stress and oxidative stress (201).

In addition, REDD1 was shown to be induced in the liver of interferon-α (IFN-α) –treated chimpanzees (65). Its role as an interferon inducible gene was confirmed in an overexpression screen where REDD1 ectopic expression in a human liver carcinoma cell line, resulting in the reduction in HCV replication (67). As highlighted above, the mitochondria functions as an innate immune signaling platform during viral infection.

Surprisingly, REDD1 was reported to interact with several mitochondrial proteins by yeast two-hybrid assay (52) and was found to be localized to the mitochondria where it may regulate mitochondrial metabolism (50).

In cancer, REDD1 may play a role in tumor suppression. Several studies in mammalian cells indicate that REDD1 may function as a pro-apoptotic cellular factor (47, 52). In *Drosophila*, REDD orthologs have growth-suppressive properties (60). In addition, REDD1 transcripts levels are significantly decreased in 8 of 27 human primary breast carcinoma specimens (~30%) (61) and REDD1 has been shown to regulate the stability of the HIF-1$\alpha$ transcription factor, a cellular protein implicated in tumor development (56, 70).

In sum, these observations suggests that REDD1 is an important stress-response gene involved in 1) the regulation of mTORC1 activity, 2) the innate immune response to HCV, 3) as an antagonist of growth and proliferation, 4) and possibly of other cellular stress-response pathways.

Herein, we report the identification of REDD1 as a novel host defense factor. Our chemical screen identified a small molecule, compound **3**, which induces REDD1 at the transcriptional level in absence or presence of virus infection. The antiviral activity of **3** requires REDD1 as cells lacking *REDD1* become highly permissive to virus replication and fail to inhibit influenza virus pathogenesis. Furthermore, REDD1 expression is up-regulated shortly after virus infection, possibly as a host defense mechanism. However, at later time points influenza virus and VSV down-regulate REDD1 expression. Loss-of-function and gain-of-function experiments demonstrate that REDD1 is required to regulate viral protein expression and limit viral replication. The ability of compound **3** to

suppress virus replication via induction of REDD1 requires an intact TSC1/TSC2 complex. Finally, polysome profiling experiments show that influenza transcripts prematurely associate with polysome fractions in cells lacking *REDD1*. These studies demonstrate REDD1 is a novel host defense factor whose expression can establish an antiviral state in the host with the ability to inhibit the replication of evolutionary diverse viruses.

## RESULTS

*Compound **3** induces REDD1, an inhibitor of the mTORC1 pathway*

Gene enrichment analysis of human A549 cells treated with compound **3** showed that the mTORC1 pathway had one of the highest enrichment scores (Figure15). REDD1, a known inhibitor of the mTORC1 pathway, was shown to be up-regulated at the mRNA level. To confirm this result, the relative abundance of REDD1 transcripts was measured by quantitative Real-Time PCR (QPCR). In contrast to DMSO treated A549 cells, which failed to induce REDD1, compound **3** treatment induced REDD1 at the mRNA level as early as 30 minutes post-treatment and REDD1 continued to be up-regulated for the next 3 hours (Figure 20A). To demonstrate that **3** induced REDD1 at the transcription level, REDD1 transcript levels were measured after co-treatment of cells with the transcription inhibitor actinomycin D and compound **3**. Induction of REDD1 mRNA by **3** was abolished in the presence of actinomycin D (Figure 20A). In addition, REDD1 mRNA decayed over time in the absence or presence of **3** and actinomycin D (Figure 20A). Thus, these results suggest that induction of REDD1 mRNA by **3** occurs at the

transcriptional level. Next, total protein levels of REDD1 were measured after compound **3** treatment of A549 cells by immunoblot analysis. Similar to the results obtained at the mRNA level, REDD1 protein sharply increased approximately six- to eightfold in the presence of **3** alone or in the presence of both **3** and influenza virus infection (Figure 20B). Again, this induction of REDD1 protein by **3** was abolished in the presence of actinomycin D (Figure 20B). To show the induction of REDD1 is a specific effect of compound **3** and not a general effect of small molecules, the levels of REDD1 protein after treatment with the inactive naphthalimide were examined. Compound **2** failed to induce REDD1 protein alone or in the presence of both **2** and influenza virus infection (Figure 20B). Similar results were obtained with a renal carcinoma cell line treated with compound **3** (Figure 21). Based on these observations, we can conclude that the inhibition of influenza virus mediated activation of the mTORC1 pathway (Figure 16A,B) was mediated by compound **3**-mediated up-regulation of REDD1 protein (Figure 20).

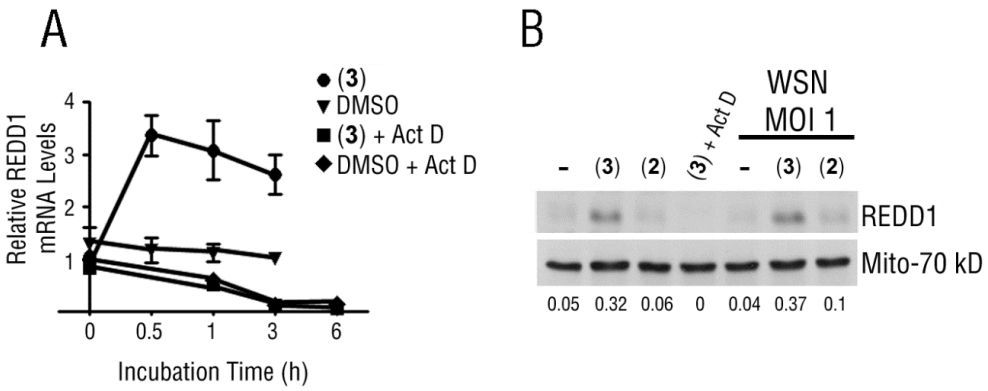


**Figure 20. Induction of REDD1 by 3 occurs at the transcriptional level.**
(A) A549 cells were untreated or treated with 30μM **3** for the indicated time periods, in the absence or presence of actinomycin D (0.5 μg/ml). REDD1 mRNA levels were quantified by real-time PCR. (B) A549 cells were untreated or treated with 30μM **3** (in the absence or presence of 0.5 μg/ml actinomycin D as indicated) for 18 h before infection and during infection. Cell extracts were obtained at 6 hours after infection and subjected to immunoblot analysis with the indicated antibodies. Densitometry analysis was performed to determine the ratio of REDD1 over loading control (Mito-70 kDa) using ImageJ.

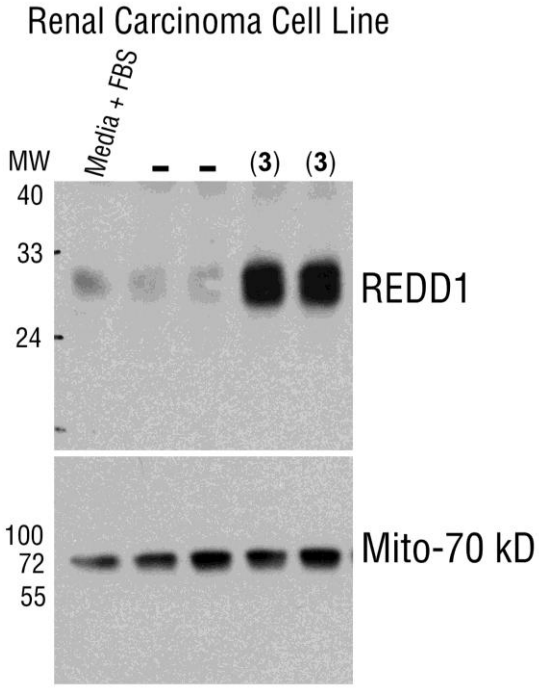


**Figure 21. REDD1 is induced by 3 in renal carcinoma cells.**
Renal carcinoma cells were untreated or treated with 20 μM 3 for 6 h. Cell extracts were analyzed by immunoblot analysis with antiREDD1 or anti-Mito-70kD antibodies

*Naphthalimide requires the mTORC1 inhibitor REDD1 for its antiviral activity*

To investigate if the antiviral activity of compound **3** required the presence of REDD1 gene, the antiviral effect of **3** in infected *REDD1+/+* or *REDD1-/-* mouse embryonic fibroblasts (MEFs) was tested. Wildtype MEFs were infected at an m.o.i. of 0.01 in the absence or presence of **3** and 72 hours post infection cell survival and virus titer were assessed. Wildtype cells succumbed to influenza virus infection after 72 hours post-infection. In contrast, compound **3** reversed this phenotype to nearly mock infected levels (Figure 22A). Replication of influenza virus was also suppressed ~300 fold in the

presence of **3** (Figure 22A). Cells were infected at 72 hours because, at this point, enough cell death had occurred so that protection by **3** could be determined. Infected *REDD1-/-* cells treated in the same conditions as *REDD1*+/+ cells were completely dead by 24 hours in the presence or absence of compound; therefore, *REDD1-/-*cells were infected with influenza virus at m.o.i. 0.001 for 48 hours, in the absence or presence of **3**. Even with this low m.o.i. and short infection time, **3** did not protect *REDD1-/-* cells from virus-mediated cell death or virus replication (Figure 22B). In addition, *REDD1-/-* cells infected at m.o.i. 0.001 for 48 hours produced approximately as many viral particles as *REDD1*+/+ cells infected at m.o.i. 0.01 for 72 hours (Figure 22A,B).

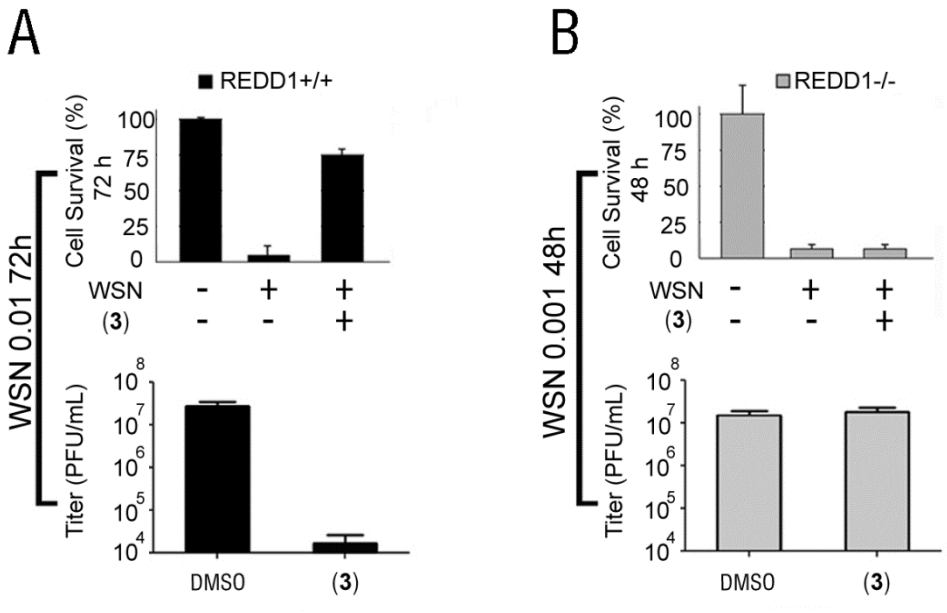


**Figure 22. Naphthalimide requires REDD1 for its antiviral activity**
(A) *REDD1*+/+ cells were untreated or treated with 3 and mock-infected or infected at m.o.i 0.01 with A/WSN/1933 for 72 hours. (B) *REDD1*–/– MEF cells, untreated or treated with 3, were infected with A/WSN/1933 at m.o.i. 0.001 for 48 hours. Cell survival was determined by Trypan blue exclusion assay and virus titers were measured by plaque assays.

When *REDD1-/-* cells were infected with influenza virus at m.o.i. 0.001, they produced ~200-fold more virus than *REDD1*+/+ cells infected in the same conditions (Figure 23). This effect was also observed in VSV-infected *REDD1*+/+ and *REDD1-/-* cells (described further below). To show that this phenotype was not due to compound **3** cytotoxic effects on these two cell lines, both *REDD1*+/+ and *REDD1-/-* cells were treated with DMSO or **3** alone and cell viability was assessed by cellular ATP levels. As shown in Figure 24, compound **3** did not cause cytotoxicity. Thus, *REDD1-/-* cells were more permissive to influenza virus replication than wild-type cells. As **3** did not inhibit

influenza virus-mediated cell death and virus replication in the absence of REDD1 (Figure 22B), REDD1 is required for the antiviral activity of **3**.

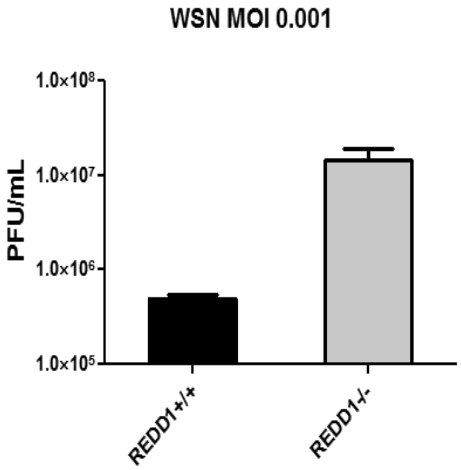


**Figure 23. *REDD1*-/- cells are permissive to influenza virus infection.**
*REDD1*+/+ and *REDD1*-/- cells were infected with A/WSN/1933 at m.o.i. 0.001 for 48 hours. Supernatants of infected cells were subjected to plaque assays to determine viral titers.

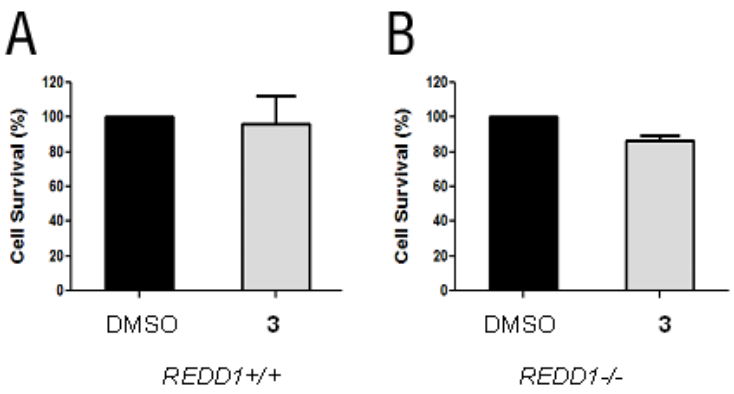


**Figure 24. Cell survival of *REDD1*+/+ and *REDD1*-/- cells treated with 3.** (A)*REDD1*+/+ and (B) *REDD1*-/- cells were treated with 10μM **3** for 72 hours and ATP levels were measured.

*REDD1 is a novel host defense factor*

These data indicate that REDD1 is an important host factor required for antiviral response, raising the possibility that viruses modulate REDD1 expression. To address this, A549 cells were infected with influenza virus and VSV at an m.o.i. of 2 and REDD1 expression was assessed over a time course of infection by immunoblot analysis. We observed that during early time points during influenza virus and VSV infection, REDD1 protein expression initially increased but was then down-regulated at later infection time points (Figure 25A,B), resulting in activation of S6K (Figure 16A). The initial up-regulation of REDD1 probably represented a host antiviral response, which was then inhibited by the virus, resulting in activation of the mTORC1 pathway.

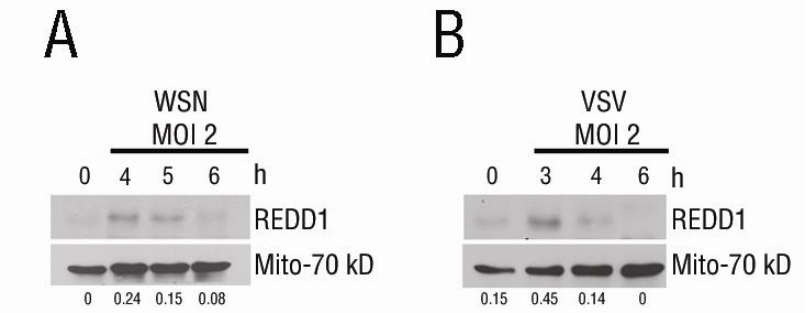


**Figure 25. Viral infection regulates REDD1 levels.**
Extracts from cells mock infected or infected with influenza virus (A) or VSV-GFP (B) were subjected to immunoblot analysis with depicted antibodies. Densitometry analysis was performed to determine the ratio of REDD1 over loading control (Mito-70 kDa) using ImageJ.

To show the importance of REDD1 in a general host-cell antiviral response, *REDD1*+/+ and *REDD1*-/- cells were infected with VSV-GFP at an m.o.i. of 2 and viral replication was assessed 24 hours post infection. Using fluorescent microscopy, VSV infection was visualized by monitoring GFP expression. As shown in Figure 26A and B, *REDD1*-/ - cells are also highly permissive to VSV replication compared to wildtype cells.

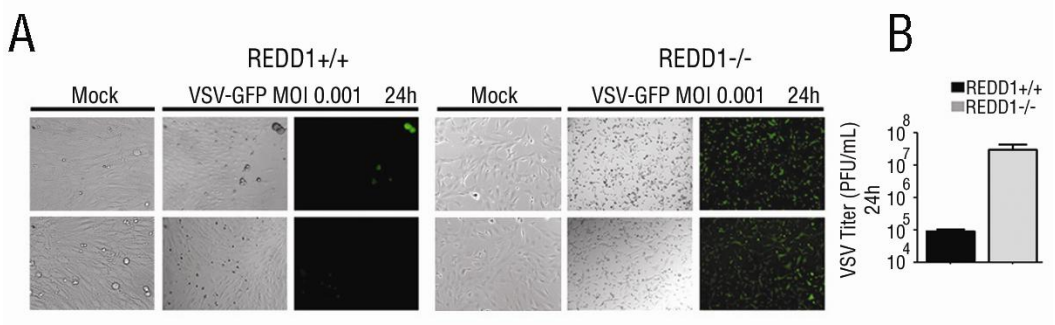


**Figure 26. *REDD1*-/- cells are permissive to VSV infection.**
(A) Wild-type or *REDD1−/−* MEF cells were infected with VSV-GFP at m.o.i. of 0.001 for 24 hours. DIC or fluorescent images of VSV-GFP are shown. Scale bar, 50 μm. (B) Supernatants of cells from (a) were subjected to plaque assays. Data represent mean values ± s.d.

*Naphthalimide antiviral activity requires REDD1 to inhibit VSV*

To examine whether the antiviral activity of **3** required REDD1 to protect against other evolutionary diverse virus, such as VSV, *REDD1+/+* and *REDD1-/-* cells were infected in the presence or absence of **3** with VSV at an m.o.i. of 0.001 and viral replication was assessed 24 hours post infection. Similar to the results obtained from influenza virus replication (Figure 22A), compound **3** treatment of *REDD1+/+*cells blocked VSV replication by ~100 fold (Figure 27A). In contrast, in *REDD1-/-* cells the antiviral activity of **3** was abolished (Figure 27B). Additionally, VSV replicated more efficiently in *REDD1-/-* cells as these cells produce ~200 fold more virus particles than its wildtype counterpart (Figure 32). Once again, this shows that REDD1 knockout cells are more permissive to virus replication than wild-type cells and that REDD1 is required for **3** antiviral activity (Figure 22 and 27).

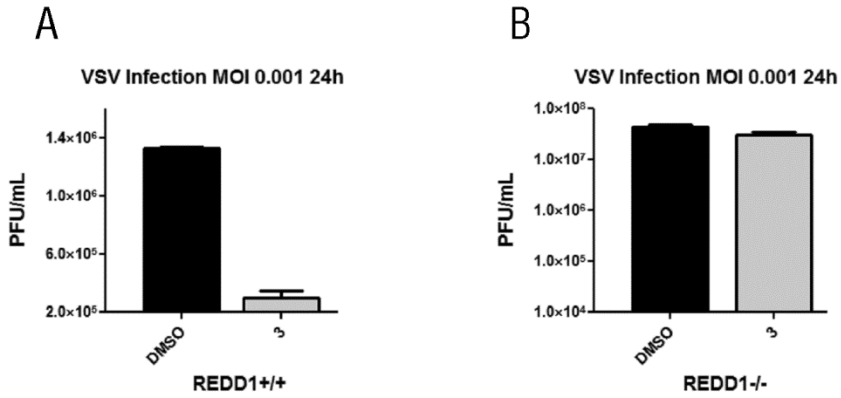


**Figure 27. REDD1 is required for naphthalimide antiviral activity.**
(A) *REDD1*+/+ or (B) *REDD1*-/- MEFs were untreated or pre-treated for 2 hours with **3** (10μM) and then infected with VSV at m.o.i. 0.001 for 1 h in the absence of compound. Then, **3** was added back and infection proceeded for 24 hours. Supernatants of infected cells were collected and subjected to plaque assays.

*Compound **3** antiviral activity is independent of autophagy*

As shown above, induction of REDD1 by compound **3**, followed by down-regulation of the mTORC1 signaling pathway, is an important host defense mechanism to mount an antiviral state and limit the replication of evolutionary diverse viruses. By limiting the activity of mTORC1, REDD1 may affect two biologically important mTORC1-regulated processes: autophagy and protein synthesis. Studies in mammalian cells have shown that mTORC1 negatively regulates autophagy, a process of cellular self eating (202). Moreover, pharmacological inhibition of mTORC1 induces autophagy (25). To examine whether compound **3** antiviral activity was mediated by autophagy, MEF cells lacking an essential autophagy related (ATG) gene, *ATG5*, required for autophagosome formation in mammals were used (203). *ATG5-/-* cells were infected with VSV at an m.o.i. of 0.001 in the absence or presence of **3** and viral replication 24 hours

post infection was assessed. In contrast to DMSO treated cells, treatment of *ATG5-/-* infected cells with compound **3** inhibited VSV replication (Figure 28).

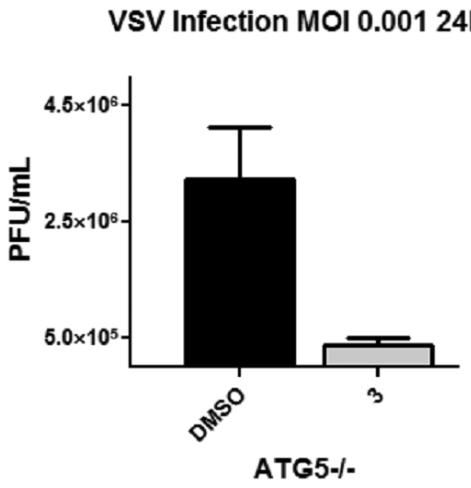


**Figure 28. REDD1 is required for naphthalimide antiviral activity independent of autophagy.**
*ATG5-/-* MEFs were untreated or pre-treated for 2 hours with **3** (10μM) and then infected with VSV at m.o.i. 0.001 for 1 hour in the absence of compound. Then, **3** was added back and infection proceeded for 24 hours. Supernatants of infected cells were collected and subjected to plaque assay.

To show that autophagy inhibition does not affect *REDD1-/-* viral permissiveness, we used the lysosomotropic agent chloroquine, a known inhibitor of autophagy, to assess viral protein synthesis over a time course of infection. Chloroquine raises the lysosomal pH which prevents proper lysosome-autophagosome fusion, thereby inhibiting autophagy (25).Chloroquine treated and untreated *REDD1-/-* cells were infected with influenza virus at an m.o.i. of 2 and PB1 and NS1 protein expression was

measured as a function of time. Treatment of cells with chloroquine did not affect the levels of PB1 and NS1 protein in *REDD1-/-* cells (Figure 29). Accumulation of the autophagy marker LC3-II was used to show that chloroquine blocked lysosome-autophagosome fusion (Figure 29). LC3 has been previously used as a specific marker to monitor autophagy. Induction of autophagy stimulates LC3-I lipidation with phosphatidylethanolamine, resulting in the formation of membrane associated LC3-II (204). Together, these results indicate that autophagy was not the mechanism involved in **3-**mediated inhibition of viral protein expression and replication. Thus, the requirement for activating mTORC1 for efficient virus replication is likely to be translation.

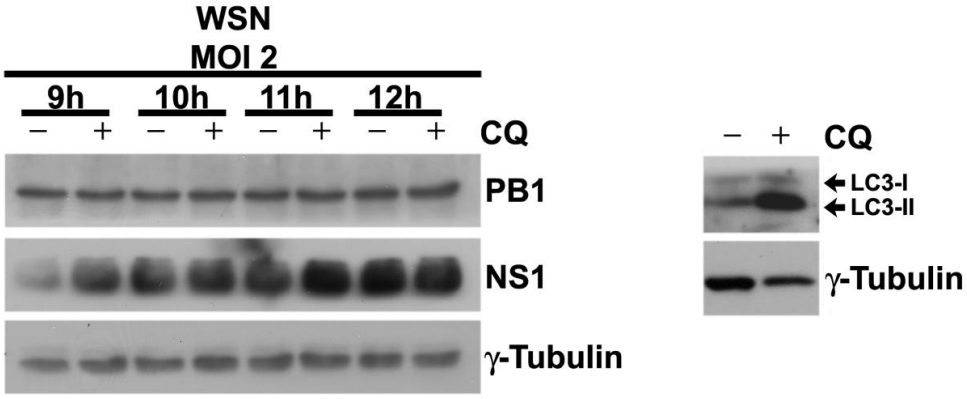


**Figure 29. *REDD1*-/- cells express the same amount of influenza viral proteins in the absence or presence of autophagy inhibitor.**
REDD1-/- cells were infected with influenza virus over time in the absence or presence of 50μM chloroquine, which was added 6 hours post-infection. Cells lysates were subjected to immunoblot analysis with the depicted antibodies. As positive control, LC3-II levels were monitored and were enhanced in the presence of chloroquine treatment. γ-tubulin was used as loading control.

Next, the other arm of the mTORC1 pathway, protein synthesis, was investigated. To determine whether the enhanced viral replication in *REDD1-/-* cells was due to a general increase in translation or an effect on specific viral proteins, the expression of several influenza virus and VSV proteins was measured as a function of time after infection of both REDD1 wildtype and knockout cells. Lysates from *REDD1+/+* and *REDD1-/-* cells infected with influenza virus and VSV at an m.o.i. of 2 were subjected to immunoblot analysis with antibodies against various virus proteins. *REDD1-/-*infected cells begin producing viral proteins PB1, NS1, HA, and NP at 6 hours post-infection. In contrast, REDD1 wildtype cells started producing viral proteins in much lower amounts 9 hours post-infection (Figure 30A and B). Thus, not only did *REDD1-/-* infected cells produced viral proteins earlier than its wildtype counterpart, but also express higher levels of every influenza virus protein analyzed in this study (Figure 30).

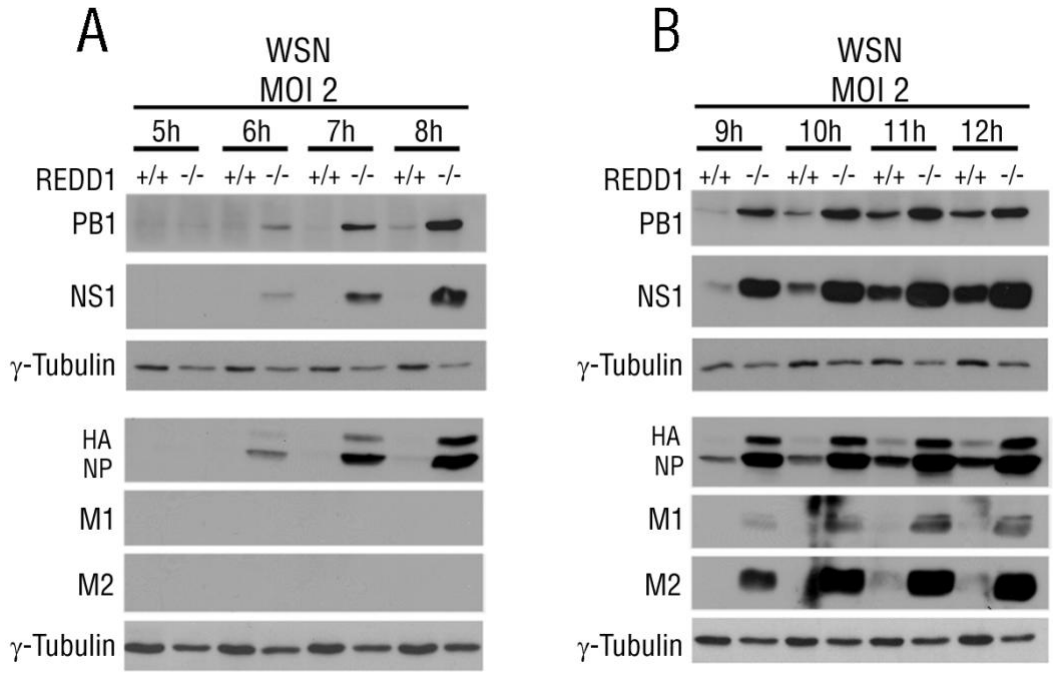


**Figure 30. *REDD1*-/- MEFs express high levels of viral proteins.**
(A) *REDD1*+/+ and *REDD1–/–*cells were infected with influenza virus WSN at m.o.i. 2 for 1 hour at 22 °C and then shifted to 37 °C. Viral protein levels were monitored over time by immunoblot analysis with the depicted antibodies. (B) Viral protein levels were monitored as in (A).

In addition to assessing viral protein expression in wildtype and *REDD1-/-* cells, total levels of several viral RNAs (vRNAs) were examined at 3 and 6 hours post-infection by real-time RT-PCR. No significant difference in NS, PB1, and NP vRNA levels was detected when comparing wildtype and REDD1 knockout cells at the earliest time point (Figure 31). At 6 hours post-infection, however, the levels of these vRNAs was enhanced several hundred fold in the *REDD1-/-* infected cells (Figure 31).

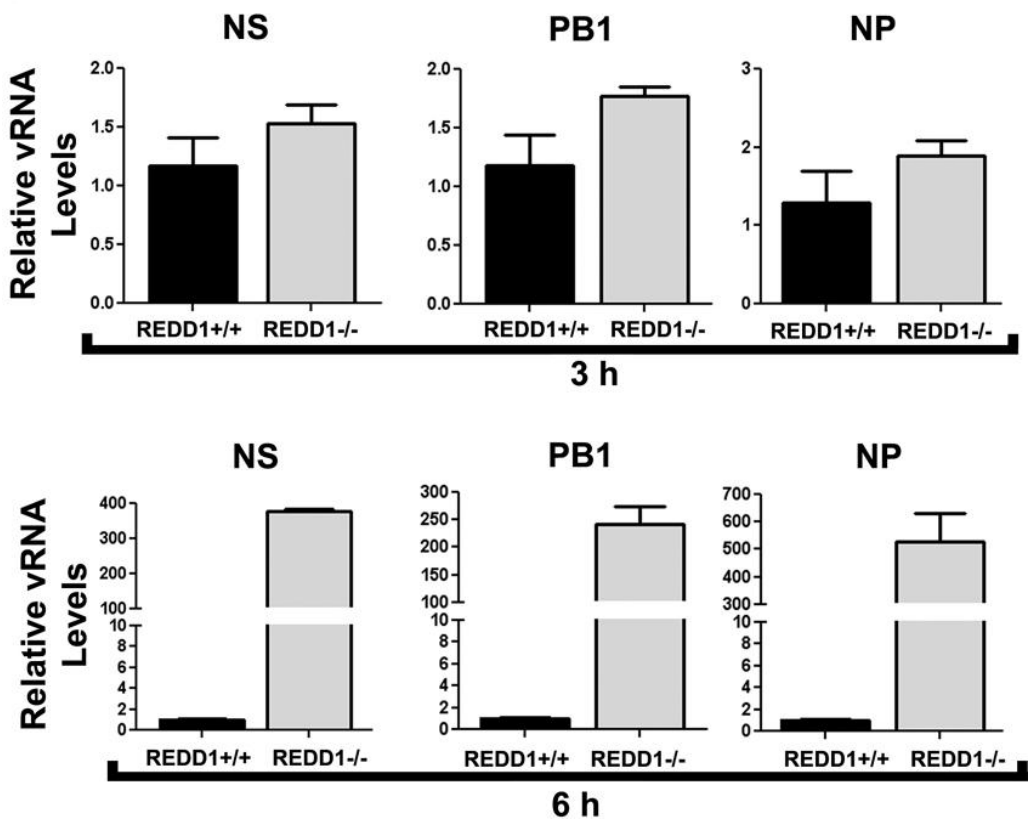


**Figure 31. *REDD1*-/- cells express higher levels of vRNAs than REDD1+/+ cells.** *REDD1*+/+ and *REDD1*-/- cells were infected with WSN at m.o.i. 2 for 1 hour at 22 °C and then shifted to 37 °C. Viral RNA (vRNA) levels were monitored by quantitative real time PCR at 3 and 6 hours. Briefly, total RNA was isolated at 3 and 6 hours post-infection using Rneasy Mini Kit (Qiagen, Valencia, CA), following manufacture's protocol. RT was carried out using First Strand cDNA Synthesis using the SuperScript II RT kit (Invitrogen) and specific primers. Real time PCR was performed using gene-specific primers and normalized to *HPRT1* and *RPS11*.

The expression of several VSV proteins was also measured as a function of time after infection of both REDD1 wildtype and knockout cells. As Figure 32 shows, *REDD1-/-* cells begin expressing viral proteins G, N/P, and M five hours post-infection. In contrast, REDD1 wildtype cells produced viral proteins seven hours post-infection, two hours later than REDD1 knockout cells (Figure 32). Similar to our previous studies of influenza virus infected cells (Figure 30), *REDD1-/-* cells express higher levels of VSV virus proteins than *REDD1+/+* cells (Figure 32).

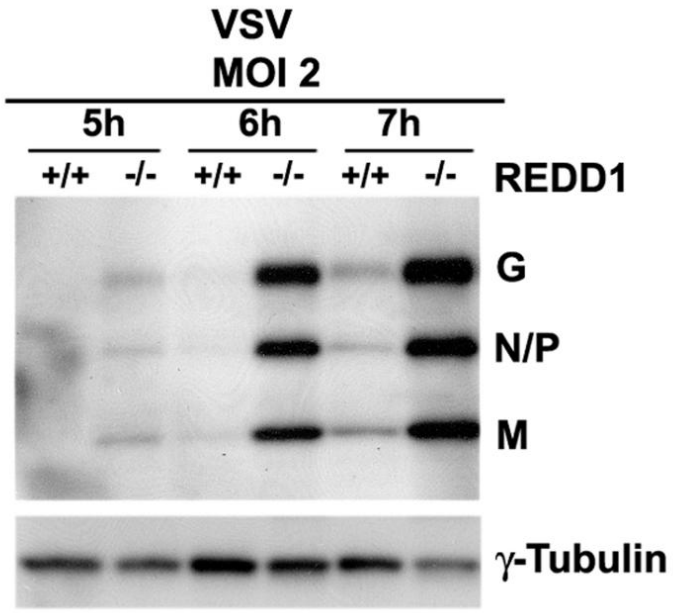


**Figure 32. REDD1-/- cells express higher levels of VSV proteins than REDD1+/+ cells.**
*REDD1+/+* and *REDD1-/-* cells were infected with VSV at m.o.i. 2 for 5, 6, or 7 hours. Cell extracts were subjected to immunoblot analysis with antibodies against VSV proteins.

To determine whether the increase in viral protein expression in *REDD1-/-* cells was due to the activity of mTORC1 in translation, we took advantage of the selective small molecule inhibitor of mTORC1, rapamycin. Rapamycin-treated and untreated REDD1 wildtype and REDD1 knockout cells were infected with influenza virus at an m.o.i. of 1 and virus protein expression was assessed at several time points after infection. Rapamycin treatment, and not DMSO, decreased the levels of influenza virus NS1 protein in *REDD1+/+* and *REDD1-/-* cells infected samples (Figure 33). In addition, PB1 protein levels were also down-regulated by rapamycin treatment of virus infected *REDD1-/-* cells (Figure 34). These data indicated that induction of high viral protein levels in *REDD1-/-* cells occurs via activation of the mTORC1 pathway.

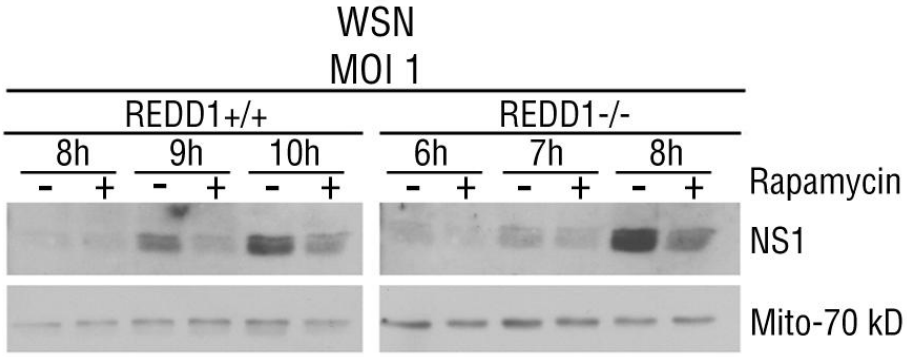


**Figure 33. Rapamycin down-regulates NS1 protein expression in *REDD1*-/- MEFs.** WSN-infected *REDD1*+/+ and *REDD1–/–* cells were treated with 100 nM rapamycin. Rapamycin was added 1 hour after infection. NS1 levels were monitored over time by immunoblot analysis.

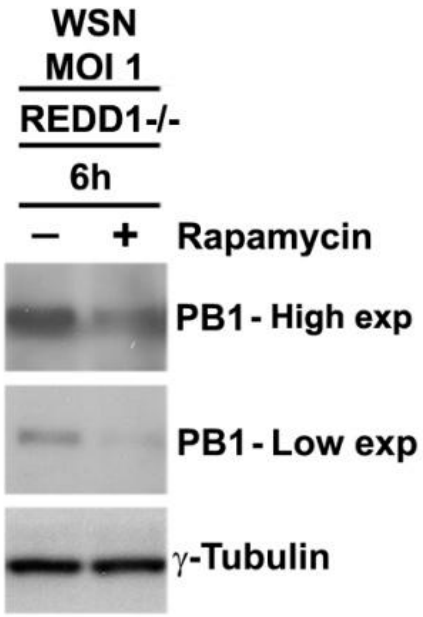


**Figure 34. Rapamycin down-regulates PB1protein levels in *REDD1*-/- MEFs.** WSN-infected *REDD1*-/- cells were treated with 100nM Rapamycin for 6 hours. Rapamycin was added one hour post-infection.

*REDD1 overexpression down-regulates viral protein expression*

Loss-of-function experiments showed REDD1 to be an important host factor required to suppress virus-mediated pathogenesis. To investigate the effects of ectopic expression of REDD1 on influenza virus and VSV protein production, a human osteosarcoma cell line (U2OS) was obtained which conditionally over-expresses REDD1 upon tetracycline treatment. Tetracycline-treated and untreated U2OS cells were infected with influenza virus and VSV at an m.o.i. of 1 and viral protein levels were monitored. Tetracycline treatment robustly induced REDD1 protein levels (Figure 35). In cells conditionally expressing large amounts of REDD1, the levels of influenza virus NS1

protein and VSV M protein were reduced (Figure 35). This gain-of-function experiment further fortifies the role REDD1 plays as a host defense factor.

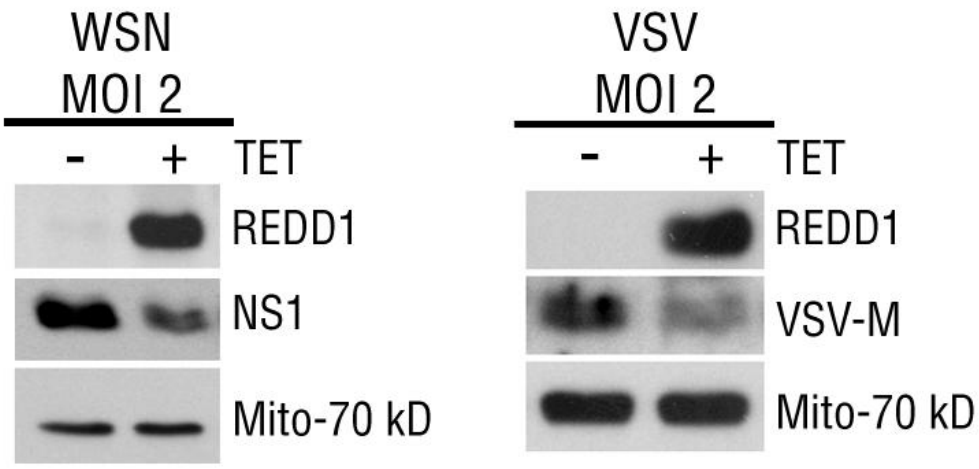


**Figure 35. REDD1 conditional overexpression reduces viral protein expression.** U2OS cells, untreated or treated with tetracycline to induce *REDD1* overexpression, were infected with both influenza virus and VSV. NS1 or VSV-M protein levels were monitored by immunoblot analysis.

*An intact TSC1/TSC2 complex is required for **3** antiviral activity*

The PI3K/AKT pathway is an activator of the mTORC1 complex under insulin and growth factor stimulation (194). mTORC1 signaling is regulated by the GTP binding protein Rheb. GTP-bound Rheb directly associates and activates mTORC1 (30). Rheb in turn is regulated by the heterodimeric complex formed by TSC1/TSC2, which acts as GTPase activating protein (GAP) on Rheb (29, 205). Activation of AKT leads to the

phosphorylation and inactivation of the TSC1/TSC2 complex, leading to down-regulation of mTORC1 activity (206). Recent data has shown that REDD1 relieves the AKT-mediated inactivation of the TSC1/TSC2 complex resulting in the inhibition of mTORC1 activity (35, 59). Inhibition of mTORC1 by REDD1 requires an intact TSC1/TSC2 complex as genetic deletion or depletion of TSC2 by RNAi blocks REDD1-mediated inhibition of mTORC1 (35). To determine whether the effect of REDD1 on mTORC1 is dependent on the TSC1/TSC2 complex or whether REDD1 blocks mTORC1 activation through an alternative mechanism, compound **3**-treated and untreated TSC2 wild-type and TSC2 knockout MEFs were infected at an m.o.i. of 2 and influenza virus protein levels were assessed at different time points. In influenza infected TSC2 wildtype cells compound **3** treatment led to the reduction in the levels of viral proteins, NS1 and PB1, compared to vehicle-treated infected cells at 5 and 6 hours post infection (Figure 36A and B). In contrast, compound treatment of virus infected *TSC2-/-* cells did not affect the expression levels of these two viral proteins (Figure 36A and B). Altogether, these findings show that the antiviral activity of **3** occurs by repressing the activity of mTORC1 in a TSC1/TSC2–dependent manner.

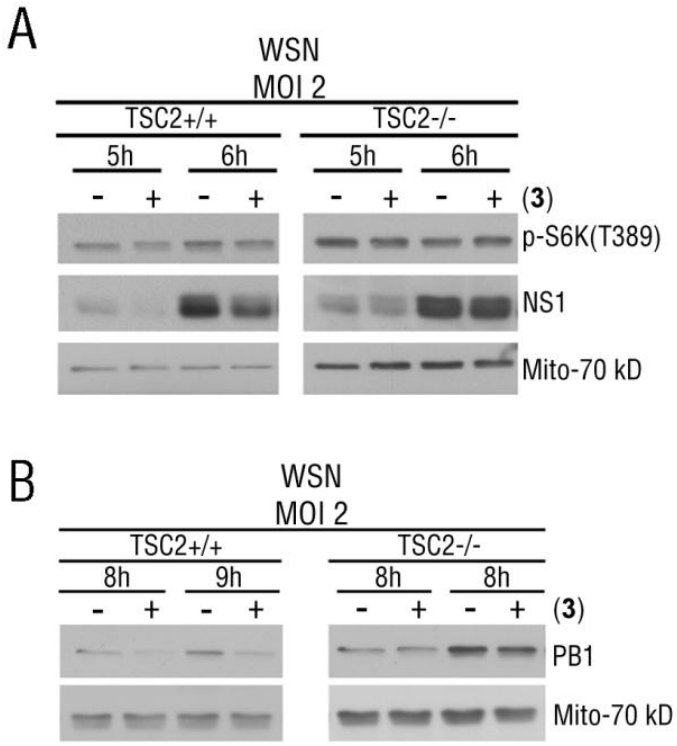


**Figure 36. Antiviral activity of 3 occurs in a TSC1-TSC2 dependent manner**
*TSC2*+/+ and *TSC2*–/– cells were pretreated with 10 μM **3**. Cells were then infected with influenza virus WSN at m.o.i. 2 for 1 hour at 22 °C and then shifted to 37 °C in the absence of compound. After 1 hour of infection, **3** was added back. Cell extracts were obtained at 5 and 6 hours after infection in (A) and 8 and 9 hours after infection in (B), then subjected to immunoblot analysis with the indicated antibodies.

Our data thus far suggest that compound **3** blocks mTORC1 activity via induction of *REDD1* in a TSC1/TSC2 complex-dependent manner (Figure 20, 21 and 36). It is also possible that **3** directly interfere with S6K phosphorylation. As shown previously, inhibition of mTORC1 activity occurs via induction of REDD1 by compound **3**. To determine if **3** acts directly on S6K phosphorylation, REDD1 knockout cells were infected with influenza virus at an m.o.i of 2 and virus-mediated S6K activation was assessed. Our results show that influenza virus induced S6K phosphorylation in *REDD1-/-* cells (Figure 37). Similar results were obtained with A549 virus infected cells (Figure 16). To show whether activation of S6K is virus-mediated, we also analyzed un-infected samples in parallel in which no S6K phosphorylation was observed (Figure 37). Treatment of virus infected *REDD1-/-*cells with compound **3** did not affect S6K phosphorylation (Figure 37). Moreover, activation of AKT was observed under virus infection only, and **3** did not reduce AKT phosphorylation at Threonine 308, similar to our results in A549 cells (Figure 37 and 16, respectively). These results thus show that compound **3** does not affect S6K or AKT phosphorylation directly and further supports our findings related to the activation of the mTORC1 pathway by influenza virus.

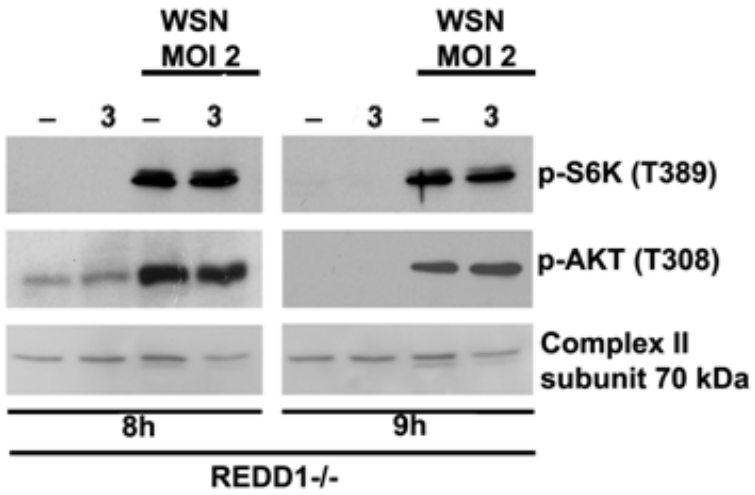


**Figure 37. Activation of AKT and S6K is not down-regulated by naphthalimide in WSN-infected *REDD1*-/- cells.**
*REDD1*-/- cells were untreated or treated with **3** and mock infected or infected with influenza virus at m.o.i. 2. Cell extracts were obtained at 8 and 9 hours post-infection and subjected to immunoblot analysis with the depicted antibodies.

Next, to investigate if the TSC1/TSC2 complex was required for the antiviral effect of REDD1, TSC2 wild-type and TSC2 knockout MEFs were infected with influenza virus at an m.o.i. of 2 and viral protein levels were measured as a function of time. As shown in Figure 38, *TSC2*-/- cells not only express higher levels of influenza virus NS1, NP, HA, and PB1 proteins but also them earlier than its wildtype counterpart. This result demonstrates that the antiviral activity of REDD1 requires an intact TSC1/TSC2 complex to down-regulate the mTORC1 signaling pathway and consequently limits virus protein synthesis and replication.

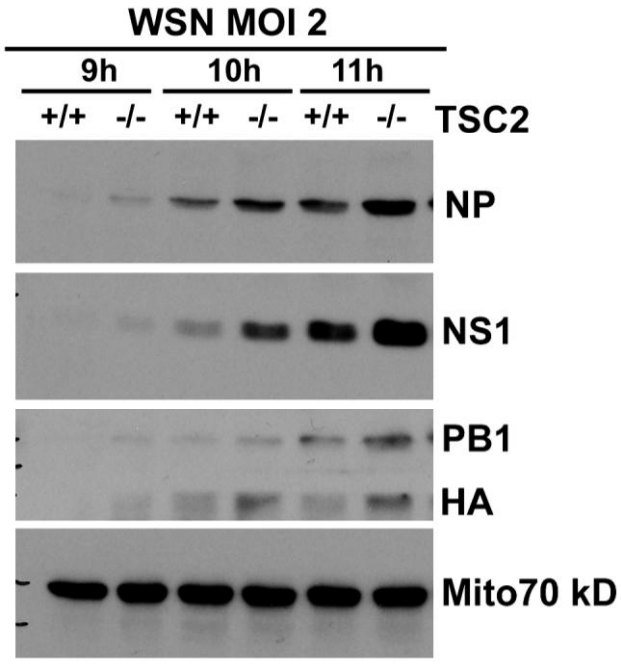


**Figure 38. *TSC2*-/- cells express higher levels of influenza virus proteins than *TSC2*+/+ cells.**
*TSC2* +/+ and TSC2-/- cells were infected with influenza virus at m.o.i. 2 for 9, 10 and 11 hours. Cell extracts were subjected to immunoblot analysis with antibodies against influenza virus proteins.

*Influenza virus transcripts prematurely associate with polysome fractions in REDD1-/- cells*

Our results show that REDD1 knockout MEFs produce higher levels of influenza virus RNA and protein compared to wildtype cells (Figure 30 and 31). To investigate if this increase in virus protein production in infected *REDD1-/- MEFs* is due to an increase in viral mRNA translation, polysome-bound RNA from *REDD1+/+* and *REDD1-/-* cells infected with influenza virus at an m.o.i. of 2 for 9 hours was isolated via sucrose

gradient fractionation (Figure 39). Viral mRNA association to monosomes and polysome fractions was measured by semi-quantitative PCR. Cell lysates were collected and loaded on a 10% to 50% sucrose gradient to separate RNA associated to monosomes (top, light fractions 4-9 ) and RNA associated to polysomes (bottom, heavy fractions 10-19) by ultracentrifugation (Figure 39). β-actin mRNA, a highly translated host transcript, was used as a control for proper RNA fractionation. As expected, β-actin mRNA from wildtype and REDD1 knockout MEFs primarily associates with heavy polysome fractions (fractions 10-19; Figure 40A, B). Next, viral mRNA association to polysome fractions was measured. In influenza infected *REDD1-/-* cells viral NS1, M, PA and PB1 mRNAs prematurely associate with polysome fractions 10-19 compared to wildtype infected cells (Figure 40A, B). The transcript encoding the influenza virus IFN antagonist, NS1 mRNA, was detected in the polysome fractions of REDD1 knockout cells at cycle 24 compared to cycle 33 in wildtype cells (Figure 40A, B). PB1 and PA mRNA, components of the heterotrimeric RNA-dependent-RNA polymerase complex, were detected in the polysome fractions of infected *REDD1-/-* cells at cycle 22. In contrast, in wildtype infected MEFs PB1 and PA mRNAs were detected at cycles 28 and 27, respectively (Figure 40A, B). Lastly, viral M transcript in wildtype cells first appeared at cycle 29 compared to cycle 26 in *REDD1-/-*infected cells (Figure 40A, B). These data collectively shows influenza virus mRNAs are prematurely loaded onto the polysomes of REDD1 knockout cells, likely resulting in higher viral protein production as seen in Figure 30.

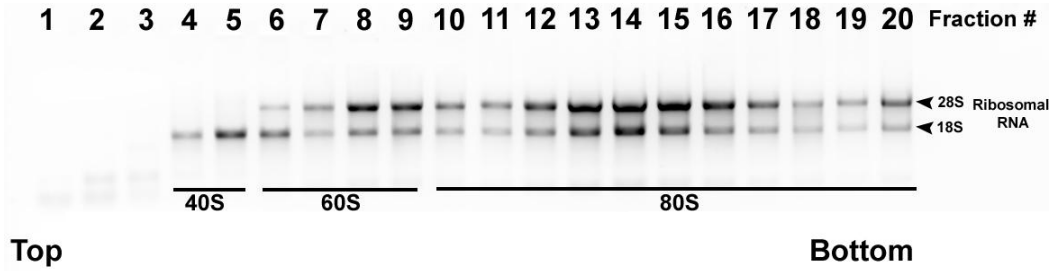


**Figure 39. Isolation of polysome-bound RNA by sucrose gradient fractionation.** Lysate from MEF cells was loaded on top of a sucrose gradient and ultracentrifuged for 2 hours at 4° C. The gradient was separated to 20 fractions (0.6mL/fraction) and RNA was isolated usin TriZol, following manufactures instructions. Polysome sedimentation profile was analyzed using a 1.5% agarose gel. Fractions 4-5 contain the 40S ribosomal subunit, as visualized by a strong 18S rRNA band. Fractions 6-9 contain the 28S rRNA band. Fractions 10-20 show equal amounts of 28S and 18S rRNA, indicating intact polysomes.

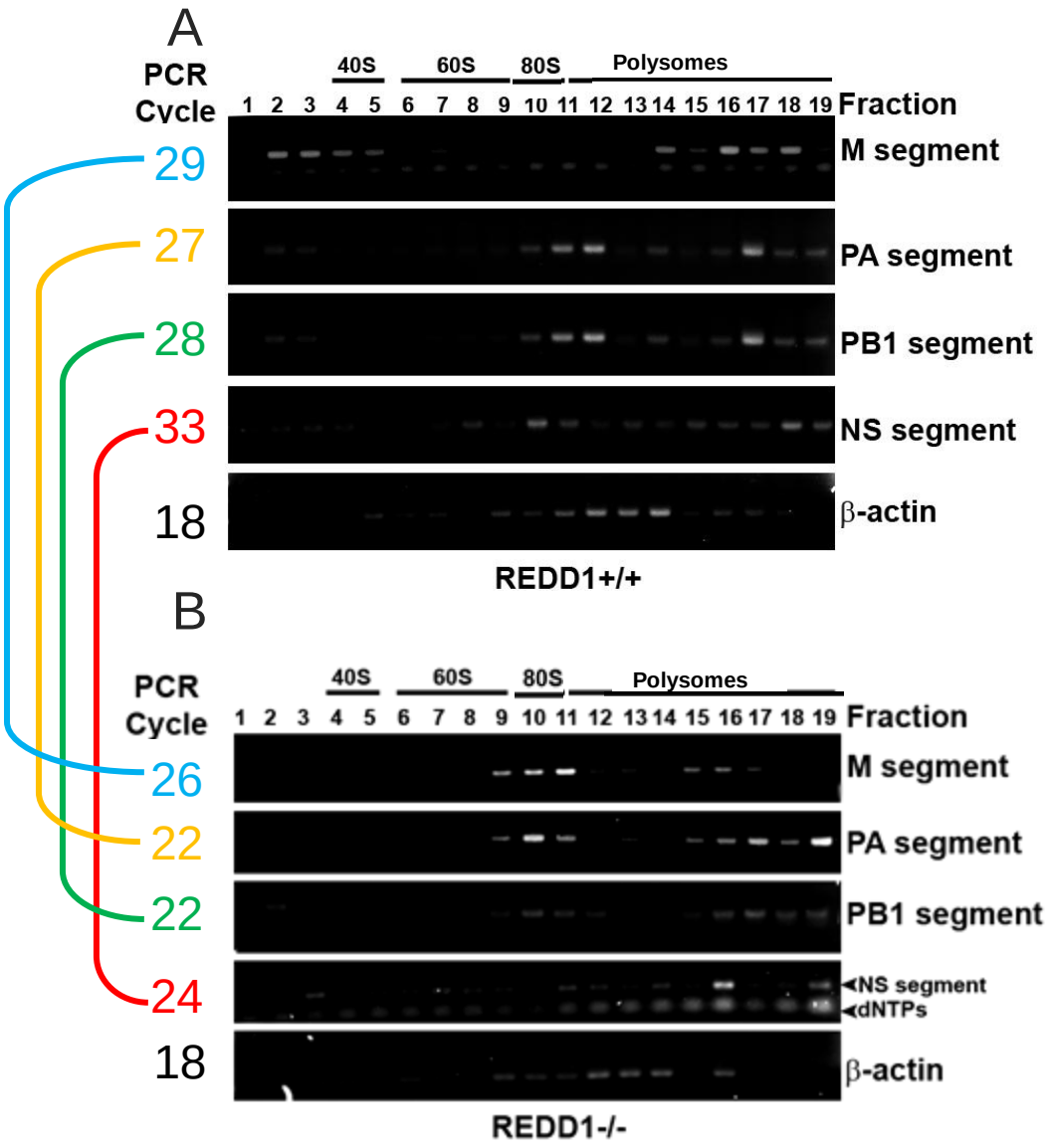


**Figure 40. Influenza virus transcripts prematurely associate with polysome fractions in *REDD1*-/- MEFs.**
REDD1 wildtype and REDD1 knockout MEFs were infected with influenza virus at m.o.i. 2 for 9 hours. After infection, RNA was isolated from each fraction and used for RT-PCR of host β-actin and viral mRNA transcripts.

*Compound **4** is a more potent inhibitor of the H1N1/1918 flu strain*

Initial SAR studies permitted the identification of small molecules that upon modification increased or loss their ability to inhibit influenza virus replication (Figure 6). Modifications to **3** led to the identification of compound **4**. To examine the effect of compound **4** on virus-mediated cytotoxicity, **4**-treated and untreated MDCK cells were infected with influenza virus at an m.o.i of 0.001 for 48 hours. Treatment of virus infected MDCK cells with compound **4** largely prevented the cytopathic effects observed in untreated MDCK infected cells (Figure 41A). To determine whether **4** induced REDD1 protein expression, induction of REDD1 after treatment of cells with **4** in the presence or absence of infection was examined. Our results show that REDD1 is induced after **4** treatment in virus-infected and uninfected samples (Figure 41B). Lastly, the replication of the highly pathogenic H1N1/1918 influenza virus strain after treatment with **4** was assessed. As Figure 41C shows, compound **4**, more potently than **3,** inhibited the replication of the 1918 strain. Altogether, these findings reveal REDD1 as a novel host antiviral factor and show that the antiviral activity of **3** requires REDD1.

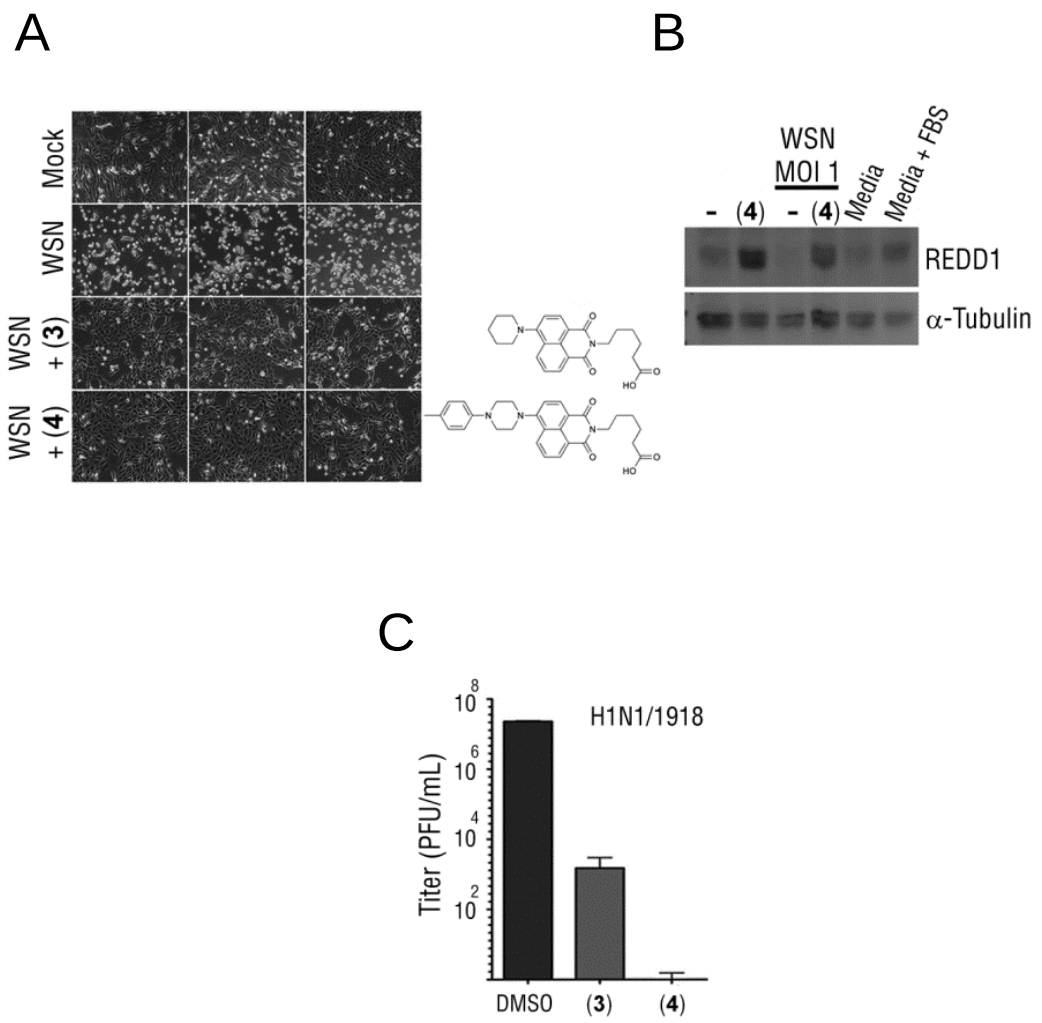


**Figure 41. Analog of the naphthalimide 3 more effectively inhibits the highly pathogenic H1N1/1918 influenza virus.**
(A) MDCK cells were pre-treated for 17 hours with DMSO or with 25μM **3** or **4** and subsequently mock infected or infected with A/WSN/1933 at m.o.i. 0.001 for 48 hours. Compounds were present during infection. DIC imaging was performed. (B) Cells were untreated or treated with 25μM of **4** and mock infected or infected with A/WSN/1933 at m.o.i.1 for 6 hours. Cell extracts were subjected to immunoblot analysis with the depicted antibodies. (C) H1N1/1918 virus replication in MDCK cells, in the absence or presence of **3** or **4,** was measured by plaque assays

**DISCUSSION**

REDD1 is an important stress-response gene as various cellular stress conditions induce its expression resulting in the modulation of the mTORC1 pathway and likely other signaling networks. In this study we show that REDD1 is a cellular factor induced by **3** and is required for it's the antiviral activity. Genetic deletion of *REDD1* results in permissiveness to virus infection in compound-treated or untreated murine cells, demonstrating that REDD1 is an important cellular antiviral factor. Providing further support for REDD1 as a host defense factor, our results indicate that soon after influenza virus and VSV infection, REDD1 expression is up-regulated but was quickly down-regulated a few hours following infection. This initial up-regulation of REDD1 likely represents a host antiviral response that is then down-regulated by both viruses, resulting in the full activation of the mTORC1 pathway.

Our results indicate that compound **3** blocks virus replication independently of the autophagy pathway. This is important as autophagy has been previously implicated in antiviral response by targeting viral components for lysosomal degradation (207). After excluding autophagy, we turned our attention to protein translation, a process governed by mTORC1. Influenza and VSV infected cells that lack *REDD1* expressed higher levels of all the viral proteins examined compared to its wildtype counterpart, suggesting that REDD1 negatively regulates the expression of viral proteins and suppresses virus-mediated pathogenesis. The elevated expression levels of virus proteins in *REDD1* deficient cells were sensitive to pharmacological inhibition of mTORC1 indicating the increased expression of viral proteins in *REDD1* deficient cells occurs via activation of the mTORC1 pathway. Further providing support for REDD1 as a cellular antiviral

factor, ectopic expression of REDD1 results in the down-regulation of influenza virus and VSV proteins. Others have also shown that REDD1 ectopic expression in Huh-7 cell line before infection with HCV resulted in reduction of HCV replication (67). Our work show that temporarily inducing host cellular factors and/or signaling pathways using small molecules could represent a novel therapeutic strategy to establish an antiviral state against pathogen invasion.

Genetic experiments demonstrate that the antiviral activity of **3** requires the TSC1/TSC2 complex and TSC2 deficient cells are highly permissive to influenza virus infection. Although it is possible that REDD1 may be acting on other cellular processes, our results indicate that REDD1 suppresses viral protein expression and virus pathogenesis by down-regulating mTORC1 activity. Examination of viral mRNA association to polysome fractions revealed that influenza virus mRNAs prematurely associate with polysome fractions in REDD1 deficient cells. Further experimental evidence is required to determine whether the increased association of viral transcripts with polysome fractions is simply due to the higher levels of viral RNAs in *REDD1-/-* cells and/or because viral transcripts contain specific sequences and/or associated proteins that allow them to specifically associate with translation initiation factors or preferentially gain access to the translational apparatus in the absence of REDD1.

SAR studies of **3** lead to the identification of **4**, an inhibitor of influenza virus-mediated pathogenesis and potent inhibitor of the highly pathogenic 1918 Spanish influenza virus. Similar to **3**, compound **4** also induced the REDD1 expression.

In sum, our work suggests that by inducing a stress response cellular factor or pathway without harming the host can provide cellular resistance against pathogen

invasion while minimizing damage to surrounding cells/tissues. In addition, induction of REDD1 or pharmacological inhibition of the mTORC1 pathway represents a potential therapeutic strategy for the treatment of influenza virus infection.

# Chapter Six
# Influenza infection animal studies

## INTRODUCTION

In response to virus infection, mammalian cells engage a variety of evolutionary conserved signaling pathways to limit the replication and spread of the virus. Recognition of viral determinants (PAMPs) triggers the production of proinflammatory cytokines and the activation of the type I IFN response pathway (72). Viral PAMPs are sensed by two distinct pattern recognition receptors (PRR): the Toll-like receptors (TLR) and the RIG-I-like receptors (RLRs) (72). After receptor-mediated endocytosis, the virus genomic material is released into the cytoplasm. TLR7, a resident of the endosomal compartment, detects influenza virus single stranded RNA genome following virus-mediated endosomal acidification (114-115, 122). In the cytoplasm, the RNA helicase RIG-I, a member of the RLR family, detects influenza virus single stranded RNA genome upon release into the cytosol (78-82). After ligand binding, both PRRs signal to downstream targets to elicit a type I IFN response mediated by IRF3 or IRF7-dependent expression of IFN-$\alpha/\beta$ (99-103), and induce the production of proinflammatory and immunoregulatory cytokines such as TNF-$\alpha$, IL-6, and IL-12 in an NF-$\kappa$B dependent manner (72, 109).

In mammals, influenza virus infects the upper and lower respiratory tracts, causing a wide variety of respiratory signs and symptoms. Epithelial cells lining the airway of the respiratory tract are the first line of defense against influenza virus infection (208). Failure to control the infection results in the release of virions that can be sensed

and taken up by specialized cells in the lungs (209). Dendritic cells and macrophages, specialized cells of the immune system, fill the respiratory epithelium constantly surveying their environment (209).

Two subsets of macrophages found in the lung include alveolar macrophages and $CD11b^+$ $CD11c^-$ macrophages (208). In response to influenza virus infection, the number of macrophages and production of the proinflammatory cytokine IL-6 increases, macrophages mature and stimulate naïve T-cells via antigen presentation (210-211). Infection studies with a recombinant virus expressing genes from the 1918 Spanish influenza pandemic show a robust recruitment of alveolar macrophages into the lungs of infected mice (212). Infiltration of macrophages into the lungs of infected mice provided antiviral immunity as depletion of this immune cell type before infection resulted in increased mortality after virus infection (212). In pigs, macrophages were also shown to be necessary for controlling influenza infection (213).

In addition, two major subtypes of respiratory DCs are found in the lungs, $CD11b^+$ $CD11c^+$ $CD103^-$ and $CD11b^+$ $CD11c^+$ $CD103^+$ subsets (208). The $CD11b^+$ $CD11c^+$ $CD103^+$ respiratory DC subtype, which is important during influenza virus infection, has been shown to be a major producer of type I IFN, IL-1, IL-6, IL-10 and IL-12 (214-215). Similar to the extensive recruitment of macrophages to the site of infection, large number of DCs infiltrate influenza virus infected lungs early after infection (216). In response to respiratory influenza infection, DCs process viral determinants to generate peptide antigens for presentation by MHC molecules located at the cell surface to trigger the activation and proliferation of naïve $CD4^+$ and $CD8^+$ T-cells into effector cells (217-218). DCs acquire influenza virus antigens by either phagocytosis of infected/dying

respiratory epithelial cells or through direct infection (219). The $CD11b^+$ $CD11c^+$ DC subtype population takes up viral antigens and produces IL-6/12 resulting in activation of T-helper type I ($T_H1$) $CD4^+$ T cells to provide protection against virus infection via IFN-γ (220). $CD4^+$ T cells are important for the establishment of memory $CD8^+$ T-cells (221). Activation of naïve $CD8^+$ cells into cytotoxic T lymphocytes cells, which infiltrate the lungs of influenza virus infected mice, also results in the production of IFN-γ (222). Expression of IFN-γ interferes with virus replication, stimulates specific immune effectors, and promotes recruitment of effector T cells into the site of infection (223-224). Cytotoxic T-lymphocytes are important for efficient influenza virus clearance (225). In sum, a balanced innate and adaptive immune response is necessary to recognize, limit, and clear invading pathogens while maintaining the integrity of surrounding tissues and minimizing damage to local surfaces.

Our *in vitro* studies revealed that REDD1 is an important host defense. In line with our previous results, genetic deletion of *REDD1* in mice results in increased susceptibility to influenza virus infection. To identify the pathways involved in influenza virus-mediated early fatality of *REDD1-/-* mice, we screened immunological parameters including: immune cell number, expression of surface molecules and cytokine production, which mediate innate and adaptive immunity. These parameters were evaluated in *REDD1+/+* and *REDD1-/-* mice infected with influenza virus. While no significant differences in the total numbers of $CD4^+$ and $CD8^+$ T-lymphocytes between *REDD1+/+* and *REDD1-/-* infected mice, we observed significantly higher DC and macrophage infiltration in the lungs of influenza virus infected *REDD1-/-* mice. In addition, the subpopulation of DCs $CD11b^+$ $CD11c^+$ in the lungs of infected *REDD1-/-*

mice express significantly lower levels of the pattern recognition receptor TLR7, which is key to induce specific and early cytokine production. Furthermore, both $CD11b^+$ $CD11c^+$ DCs and $CD11b^+$ $CD11c^-$ macrophages in the lungs of infected *REDD1-/-* mice express significantly lower levels of the antigen presenting MHC class II molecules as compared to REDD1+/+ mice. Thus, the particular defects in TLR7 signaling and MHC presentation led to specific alterations of cytokine production. In fact, preliminary results show that while IFN-β production is similar in both *REDD1*+/+ and -/- mice, but *REDD1-/-* infected mice produce lower levels of IFNγ and the proinflammatory cytokine IL-6. In sum, the combination of abnormal high infiltration of macrophages in the lung of REDD1-/- infected mice causing an out of control inflammatory response with poor cytokine production due to impaired TLR7 signaling and antigen presentation are likely key contributors to the susceptibility of these mice to viral infection.

## RESULTS

### *REDD1-/- mice are susceptible to influenza virus infection*

Our *in vitro* cell culture infection studies demonstrate that REDD1 is a novel host defense factor which limits virus protein production and replication at least in part by down-regulating mTORC1 activity, a host signaling pathway activated and required for influenza virus replication. To demonstrate that REDD1 is an important host factor required for antiviral response *in vivo*, animal infection studies were conducted. Wildtype and *REDD1-/-* mice were intranasally infected with influenza virus A/WSN/1933 strain with a $5X10^6$ virus dose per animal. Body weight and survival were

measured daily. Decrease in body weight of more than 25% was considered experimental end point and mice were humanely euthanized. As shown in Figure 42, 60% of *REDD1-/-* mice succumbed to infection as early as 3 and 4 days after virus inoculation, 20% survived until day 6, and only one was able to able to clear the infection. In marked contrast, 75% of *REDD1+/+* mice survived until 6 and 7 days post-infection (Figure 42). These results indicate that *REDD1-/-* mice are more sensitive to influenza virus infection and provide conclusive evidence that REDD1 is a critical cellular factor required for antiviral response.

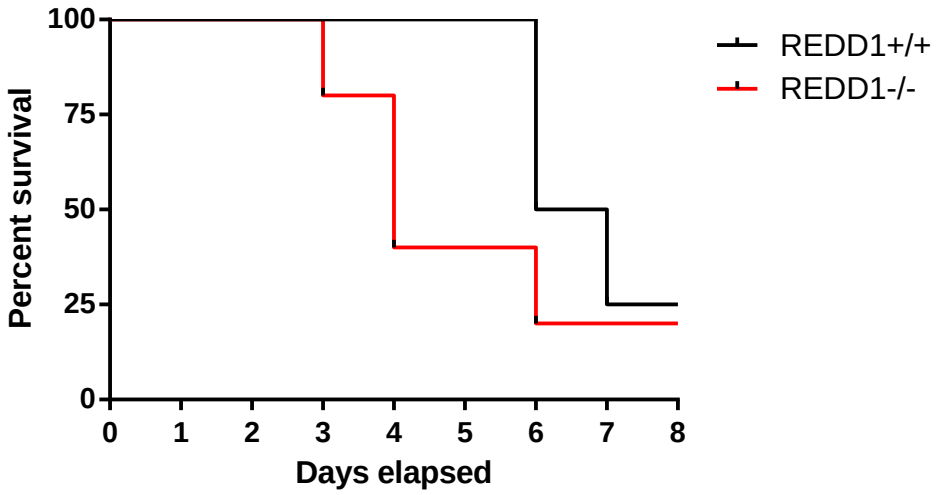


**Figure 42. REDD1 deficient mice are susceptible to influenza virus infection.** REDD1 wildtype (n=4) and knockout mice (n=5) were intranasally infected with A/WSN/1933 influenza strains at an m.o.i. of $5X10^6$ pfu per animal diluted in 50μL PBS. Body weight and survival were measured daily. Decrease in body weight of more than 25% was considered experimental end point and mice were humanely killed.

The increased susceptibility to influenza virus observed in *REDD1-/-* mice led us to investigate the immunological response of *REDD1*+/+ and *REDD1-/-* mice to influenza virus infection. The host immune system, comprised of the innate and adaptive immune response, is essential to recognize and limit the replication of the virus early during infection while promoting the infiltration of immune cells to the site of infection to ensure clearance of the pathogen in an effort to minimize damage to the surrounding tissues. To determine the underlying cause for the *REDD1-/-* increased sensitivity to virus infection, we screened immunological parameters in *REDD1*+/+ and *REDD1-/-* infected mice: immune cell number, expression of surface molecules and cytokine production, which mediate innate and adaptive immunity. Age-matched *REDD1*+/+ and *REDD1-/-* mice were anesthetized and intranasally infected with influenza virus A/WSN/1933 strain at a $5X10^5$ virus dose per animal. To examine the early immunological response to influenza virus infection, infected and non-infected mice were humanly killed 48 hours post-infection. Once sacrificed, broncoalveolar lavage (BAL) fluid, lung and spleen tissues were collected for further analysis.

Dendritic cells are constantly surveying their microenvironment for self and non-self antigens (209). DCs load antigens onto major histocompatibility complex (MHC) class I and II molecules found on the surface of the cell (226). Through direct cell-to-cell contact, DCs potently stimulate the activation and proliferation of naïve $CD8^+$ and $CD4^+$ T-cells into effector T-lymphocytes initiating immune response (226). Following respiratory influenza infection, DCs load viral peptide antigens onto MHC molecules and induce the activation of $CD3^+$ $CD4^+$ T-helper type I ($T_H1$) T-cells and $CD3^+$ $CD8^+$ cytotoxic T cells (220). $T_H1$ cells provide protection against influenza virus infection by

producing the proinflammatory cytokine IFN-γ (220). T-helper type I cells are also important for establishing memory $CD8^+$ T-cells (221). Activation of naïve $CD3^+$ $CD8^+$ cells into cytotoxic T lymphocytes cells by DCs also results in the production of IFN-γ (222). Expression of this proinflammatory cytokine not only interferes with virus replication, it also stimulates specific immune effectors, and promotes recruitment of effector T cells into the site of infection (223-224). Cytotoxic T-lymphocytes are important for efficient influenza virus clearance (225). Given the critical role these cells play during viral infection, we measured the percent of $CD4^+$ and $CD8^+$ T-lymphocytes in the lungs of non-infected and infected *REDD1*+/+ and *REDD1*-/- mice by flow cytometry. As Figure 43 shows, no significant difference was observed in the percent of $CD8^+$ and $CD4^+$ T-lymphocyte in the lungs of *REDD1*+/+ and *REDD1*-/- before or after influenza infection. We did observe a slight increase in $CD4^+$ T-lymphocytes at 48 h after infection in both genotypes (Figure 43). Under infection conditions, the number of $CD8^+$ and $CD4^+$ T-lymphocytes increases after several days of infection. In addition, we also measured the percent of $CD11b^+$ immune cells (DCs and macrophages) in the lungs of infected *REDD1*+/+ and *REDD1*-/- mice. Our data show a significant increase in the number of DCs and macrophages infiltrating the lungs of *REDD1*-/- infected mice compared to its wildtype counterpart (Figure 44).

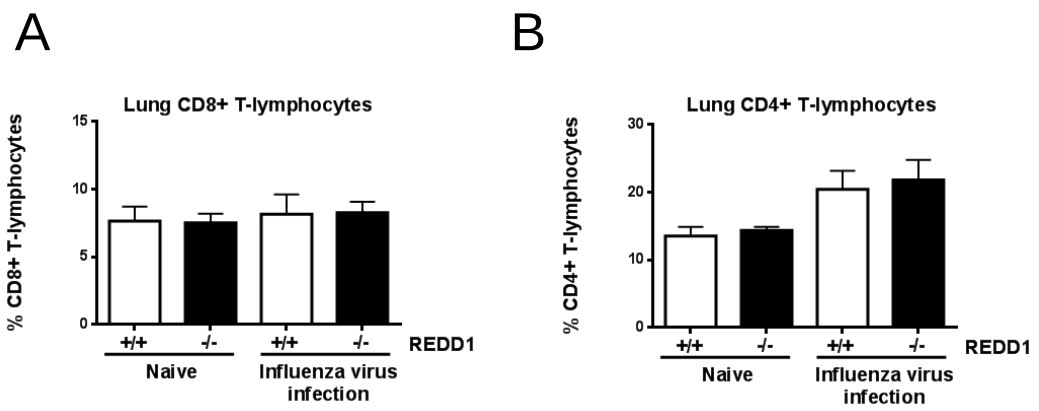


**Figure 43. Similar levels of effector T-cells in the lungs of *REDD1*+/+ and *REDD1*-/- non-infected and infected mice.**
(A) Lung tissue from *REDD1*+/+ and *REDD1*-/- infected mice was isolated 48 hours post-infection. Tissue was dissociated and single cell suspension was obtained. The percent of $CD8^+$ T-lymphocytes in the lungs of non-infected and infected *REDD1*+/+ and *REDD1*-/- mice was measured by flow cytometry. (B) Samples were treated as in (A) but the percent of $CD4^+$ T-lymphocytes was measured.

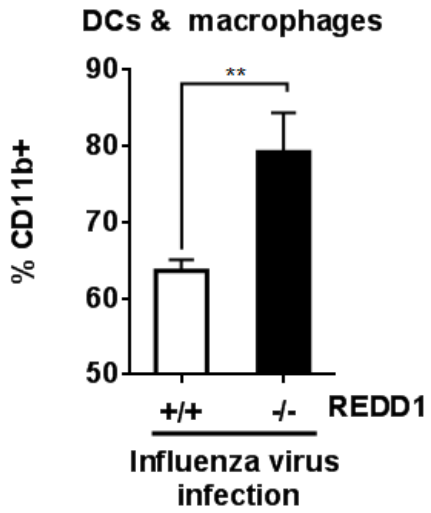


**Figure 44. Increased DC and macrophage infiltration in the lungs of *REDD1-/-* virus infected mice.**
(A) Lung tissue from *REDD1*+/+ and *REDD1-/-* infected mice was isolated 48 hours post-infection. The percent of $CD11b^+$ immune cells in the lungs of infected *REDD1*+/+ and *REDD1*-/- mice was measured by flow cytometry.

Dendritic cells and macrophages are constantly surveying their microenvironment for non-self antigens (209). These sentinel cells acquire influenza virus antigens by phagocytosis dead or dying respiratory epithelial cells or through direct infection (219). Influenza antigens are proteolytically processed into peptides that are loaded onto major histocompatibility complex (MHC) class II molecules found on the surface of DCs and macrophages; a process known as antigen presentation (226). In the absence of infection, DCs present antigens inefficiently. However, uptake of antigens induces DC maturation and become efficient antigen presenting cells (APC) capable of triggering the activation and proliferation of naïve $CD4^+$ and $CD8^+$ T-lymphocytes into effector T-cells initiating an adaptive immune response (217-218). Based on their

important role during virus infection, we measured the expression of MHC class II molecules on the surface of DCs and macrophages isolated from the lungs of *REDD1*+/+ and *REDD1*-/- non-infected and influenza infected mice. In *REDD1*+/+ mice, infection with influenza virus significantly increased the expression of MHC class II molecules in DCs and macrophages (Figure 45A, B). In great contrast, no up-regulation in the expression of MHC class II surface molecules was observed in influenza infected *REDD1*-/- DCs and macrophages (Figure 45A, B). Compared to wildtype influenza infected DCs and macrophages, the expression levels of MHC class II molecules in *REDD1*-/- mice was significantly down-regulated (Figure 45A, B). These results suggest that *REDD1*-/- DCs and macrophages are impaired in their ability to function as antigen presenting cells. Reduction in MHC class II molecules would likely result in decreased antigen loading, antigen presentation, and effector T-cell activation hindering the ability to control the virus infection. Moreover, a compensatory mechanism could be at place where decreased MHC class II expression and antigen presentation could result in increased recruitment of $CD11b^{+}$ cells to the lungs of *REDD1*-/- mice in an effort to compensate for the loss of effector T-cell activation via antigen presentation.

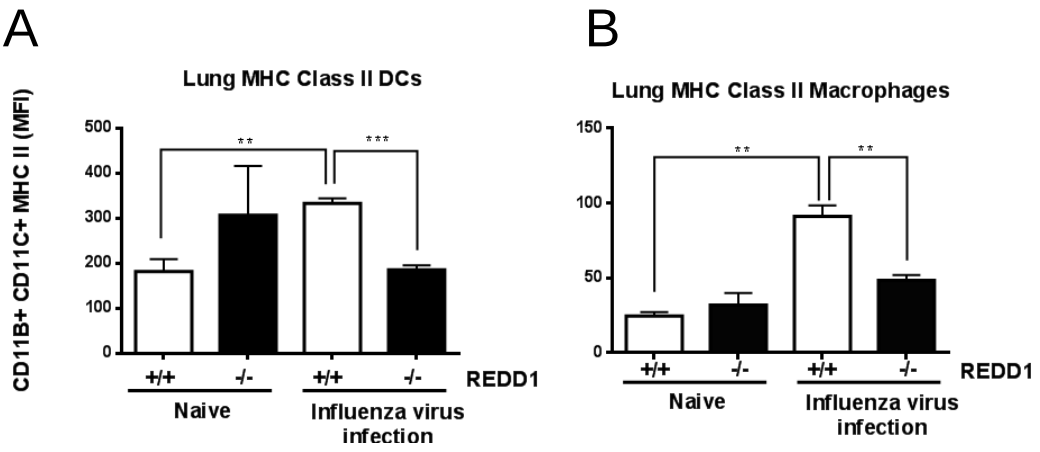


**Figure 45. Lower MHC class II expression in lung DCs and macrophages of *REDD1-/-* influenza infected mice.**
(A) Lung tissue from *REDD1*+/+ and *REDD1-/-* infected mice was isolated 48 hours post-infection. Tissue was dissociated and single cell suspension was obtained. The expression of surface MHC class II molecules in DCs ($CD11b^+$ $CD11c^+$) was assessed by flow cytometry. (B) Lung tissue was treated as in (A) and the expression of surface MHC class II molecules in macrophages ($CD11b^+$ $CD11c^-$) was assessed by flow cytometry.

The respiratory epithelium represents the first line of defense against influenza virus infection (208). Virus particles released from dying or dead airway epithelial cells are taken up by DCs and macrophages, sentinel cells in the lungs that are constantly surveying their microenvironment (209). These specialized cells have the ability to control the replication of influenza virus early during infection and also play a critical role in connecting the innate and adaptive immune response after infection (216). The single stranded RNA genome of influenza virus triggers an innate and adaptive immune response in a TLR7-depdendent manner following uptake by DCs to neutralize and clear the virus infection (114-115, 122). TLR7 activation results in the recruitment of various immune signaling molecules leading to the production of IFN $\alpha/\beta$ (99-103), and

proinflammatory cytokine IL-6 (72, 109). To begin to understand mechanistically the reasons for decreased MHC class II expression and increased recruitment of $CD11b^{+}$ cells in *REDD1-/-* mice, the expression levels of the influenza virus sensor, TLR7, in non-infected and influenza infected *REDD1+/+* and *REDD1-/-* DCs were measured by flow cytometry. In the absence of infection, detectable levels of basal TLR7 were observed in *REDD1+/+* and *REDD1-/-* DC (Figure 46). In virus infected *REDD1+/+* the expression levels of TLR7 in DCs increased ~three-fold 48 hours post-infection (Figure 46). Contrary to the virus-induced up-regulation observed in *REDD1+/+* DCs, the expression of TLR7 was significantly down-regulated in *REDD1-/-* DCs (Figure 46). In fact, the expression of TLR7 did not increase above baseline in *REDD1-/-* mice. These results indicate that *REDD1-/-* mice is deficient in TLR7 signaling, which could likely result in down-regulation of MHC class II expression and reduced antigen presentation. Failure to activate an innate immune response and induce T-cell activation may affect the ability of *REDD1-/-* mice to limit and clear influenza virus infection.

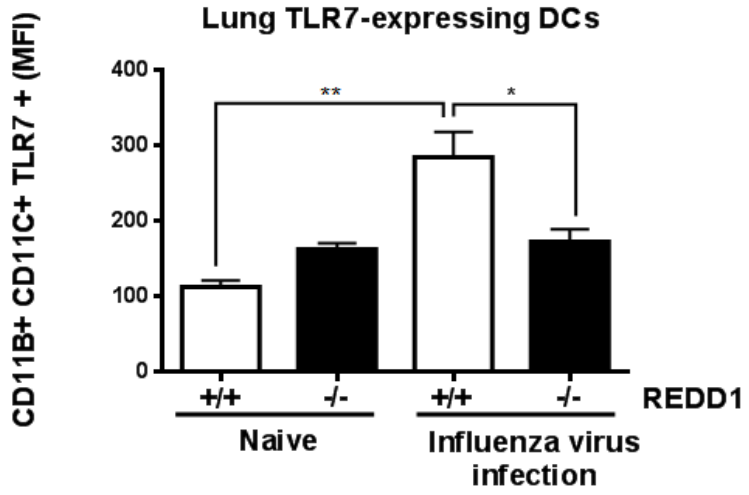


**Figure 46. Virus infected *REDD1-/-* DC express significantly less TLR7 than *REDD1+/+* DCs.**
Lung tissue from *REDD1+/+* and *REDD1-/-* infected mice was isolated 48 hours post-infection. Tissue was dissociated and single cell suspension was obtained. The expression of the TLR7 receptor in lung dendritic cells subtype $CD11b^{+}CD11c^{+}$ was assessed by flow cytometry.

Influenza virus PAMPs triggers the production of proinflammatory cytokines and the activation of the type I IFN response pathway in a TLR7-dependent manner (72, 114-115, 122). Ligand binding promotes TLR7 activation and recruitment of immune signaling molecules leading to the expression of type I IFN genes (IFN-α/β) in an IRF7-dependent manner (99-103) and production of proinflammatory and immunoregulatory cytokines (TNF-α and IL-6) mediated by NF-κB (72, 109). IFN induction by APCs have numerous biological activities that range from induction of host factors required for inhibiting virus replication to activation of immune cells to block virus spread (216, 227-229). In addition, secretion of TNF-α, IL-6 and IL-1 by APCs results in immune cell activation, induction of fever, promotes tissue regeneration, and initiates the adaptive

immune response (214, 216, 228). Our previous results indicate that *REDD1-/-* mice express significantly less TLR7, the influenza virus host sensor (114-115). Decreased TLR7 expression could result in reduced downstream signaling leading to low IFN and cytokine production. To determine if *REDD1-/-* mice are impaired in their ability to induce these immune effector molecules involved in the antiviral defense, we examined IFN-β and IL-6 production following virus infection in *REDD1+/+* and *REDD1-/-* mice. In the absence of virus infection, our preliminary results show that IFN-β was undetectable in the BAL of both genotypes, as measured by ELISA (Figure 47A). Two days after infection, however, we detected similar IFN-β levels in *REDD1+/+* and *REDD1-/-* mice (Figure 47A). Although these data is preliminary, no IFN defect was observed in *REDD1-/-* mice. These data is supported by our results showing that primary and SV40 large T antigen transformed *REDD1-/-* MEFs induce type I IFN genes to the same extent as *REDD1+/+* cells (Chapter 7). We also measured cytokine production in *REDD1+/+* and *REDD1-/-* mice 48 hours post virus infection. Our results, although preliminary, show that *REDD1+/+* mice produce more IL-6 than *REDD1-/-* infected mice (Figure 47B). In addition, we have preliminary evidence that IFNγ levels are reduced in infected *REDD1-/-* mice (0.6 pg/ml) as compared to *REDD1 +/+* mice (6.56 pg/ml) after 5 days of infection. A larger number of mice is necessary for these experiments, which will be performed again in the near future. However, these data suggest that REDD1 may be required for proper induction of the proinflammatory cytokine IL-6 and IFNγ, and not of type I IFN, upon influenza virus infection.

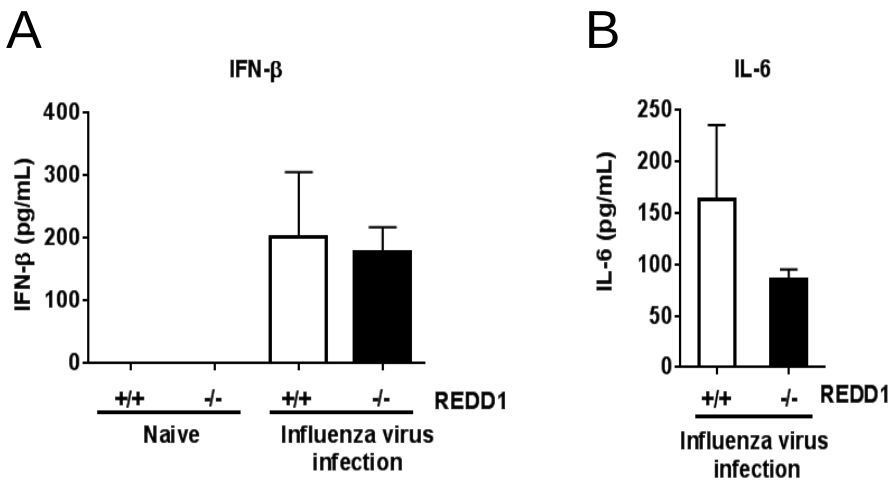


**Figure 47. REDD1 is required for proinflammatory cytokine production and not for type I IFN response.**
BAL was collected from the lungs of *REDD1*+/+ and *REDD1*-/- influenza virus infected mice. IFN-β and IL-6 levels were measured by ELISA.

**DISCUSSION**

Our previous *in vitro* data shows that REDD1 is an important host defense factor required to suppress influenza virus pathogenesis. Now, we present *in vivo* data further supporting the requirement for REDD1 as a host defense factor during influenza virus infection. *REDD1* deficient mice are more sensitive to influenza virus infection compared to its wildtype counterpart conclusively showing that REDD1 is a critical cellular factor required for antiviral response.

To begin to understand why *REDD1-/-* mice are more susceptible to virus infection, a complete immunological screen was performed in virus infected *REDD1+/+* and *REDD1-/-* mice to examine the early immune response (48 hours) to influenza infection. Defects in activation and proliferation of naïve $CD8^+$ and $CD4^+$ T-cells can have profound negative effects as these cells provide protection against influenza virus infection by producing proinflammatory cytokines, inducing the activation and recruitment of effector T cells, and promoting virus clearance (220, 222-225). No significant difference in the percent of $CD8^+$ and $CD4^+$ T-lymphocytes in the lungs of virus infected and non-infected *REDD1+/+* and *REDD1-/-* mice was observed. It is important to point out that our data reflects the mouse immunological response against influenza virus at an early time point after infection. It is conceivable that differences in the percent of $CD8^+$ and $CD4^+$ T-cells could be observed at later stages of infection. This remains to be explored.

At early stages of infection, influenza virus targets the respiratory epithelium, the host's first line of defense (208). Failure to control the infection results in virus particles released that are subsequently up taken up by DCs and macrophages, specialized antigen

presenting cells (APC) (209). Immature APCs express few MHC class II molecules on the surface (226). However, soon after TLR7-dependent pathogen sensing, APCs up-regulate MHC class II expression and efficiently load processed antigens onto these surface molecules for antigen presentation and activation of T-lymphocytes, thereby initiating an adaptive immune response (217-218, 226). We found that early during infection, a significant increase in the number of DCs and macrophages infiltrated the lungs of *REDD1*-/- mice compared to wildtype infected mice. While an increase in number was observed, these $CD11b^+$ cells were deficient in their antigen presenting properties as less MHC class II surface molecules were detected on *REDD1*-/- APCs. The excessive recruitment of $CD11b^+$ cells to the lungs of *REDD1*-/- mice could be a compensatory mechanism to alleviate the reduced antigen presentation observed in *REDD1*-/- DCs and macrophages in an effort to establish an innate immune response and activate effector T-lymphocytes to clear the virus infection. The substantial increase in DC and macrophage infiltration in the lungs of *REDD1*-/- infected mice could also have detrimental effects that instead of helping clear the infection may cause tissue damage.

Influenza virus is sensed by APCs via the endosomal-bound TLR7 receptor, which triggers an immune response to neutralize and clear the virus infection (114-115, 122). Our analysis of TLR7 expression after influenza infection shows that *REDD1*-/- DCs express significantly less of the pattern recognition receptor than wildtype infected mice. Decreased TLR7 expression after virus infection would likely result in deficient innate immune response signaling and reduced type I IFN and/or of proinflammatory/immunoregulatory cytokine production that could negatively impact the host's ability to mount an innate and adaptive immune response to limit virus

proliferation. In line with this idea, our data suggest REDD1 is an important cellular factor for the production of the NF-κB-induced proinflammatory cytokine IL-6. A previous report supports these observations. Yoshida and colleagues recently reported that REDD1 is necessary and sufficient for NF-κB-reporter activation (230). Individuals with chronic obstructive pulmonary disease (COPD), caused by cigarette smoke exposure (CSE), had increased expression of REDD1 at the RNA and protein levels. CSE results in increase oxidative stress and subsequent lung inflammation through the NF-κB signaling pathway (231-232). Previous reports have shown that oxidative stress induces REDD1 expression (201). CSE-mediated induction of oxidative stress is required for REDD1 expression as the antioxidant *N-acetyl-$_L$-cysteine* (NAC) efficiently blocks REDD1 protein expression. In addition, REDD1 is shown to be necessary and sufficient to activate the expression of an NF-κB luciferase reporter gene (230). Importantly, overexpression of REDD1 in the lungs of mice, achieved by adenovirus infection, increases oxidative stress and significantly enhances lung macrophage infiltration and lung injury (230). In the absence of REDD1, mTORC1 activity is elevated in the lungs of mice and provides protection against CSE-mediated lung injury. Overall, these data provide a link between lung inflammation as a consequence of oxidative stress generated by CSE and the expression of REDD1 under these environmental stress conditions. It has been previously shown that under oxidative stress conditions NF-κB drives the expression of proinflammatory cytokines (IL-1, IL-6, and TNF-α) (233) and regulates macrophage recruitment via induction of the macrophage inflammatory protein-2α cytokine (234).

Together, these findings underscore the tight balance and timing of REDD1 expression. While expressing proper levels of REDD1 in the lungs may function as an antiviral strategy against influenza virus infection, high levels of REDD1 may cause complications due to oxidative stress, immune cell infiltration and subsequent inflammation that can lead to lung damage. On the contrary, absence of REDD1 can result in excessive virus replication, impaired innate and adaptive immune responses, and also result in lung damage. Therefore, it is important to understand the spatiotemporal control of REDD1 expression that is beneficial to the host and how excessive or impaired expression can lead to tissue injury.

# CHAPTER SEVEN
# Impaired type I IFN response in passage immortalized *REDD1-/-* MEFs

## INTRODUCTION

Viruses trigger a diverse array of immune responses to limit virus replication and facilitate clearance. Host senses pathogens via conserved molecular determinants, known as pathogen-associated molecular patterns (PAMPs). Viral PAMPs include single and double stranded RNA (ssRNA/dsRNA, respectively), and viral glycoproteins. Host PAMP sensors, known as patter recognition receptors (PRRs), represents the first line of defense against pathogens that can induce the activation of a type I interferon (IFN) response, a critical signaling pathway with potent antiviral and antiproliferative effects (71, 187). Intracellular viral PAMPs are recognized by the cytosolic RNA helicases RIG-I like receptors (RLRs) which include RIG-I, MDA5, and LGP2 (72). All these cytosolic sensors share a central RNA helicase domain with RNA binding ability and a C-terminus repressor domain (73-75). Only RIG-I and MDA5 contain two tandem CARD domains at the N-terminus involved in signaling and found in proapoptotic signaling proteins (73-75).

Binding to viral or synthetic RNA through the helicase domain of RIG-I and MDA5 leads to their signaling activation. Uncapped 5'-triphosphorylated RNAs (5'-ppp RNA), generated during virus replication, are RIG-I substrates that promote its activation and downstream signaling (77). *In vivo*, RIG-I is responsible for recognizing viruses in the following genera: Rhabdovirus, Orthomyxovirus, and Flavivirus (78-82). *RIG-I-/-* mice are susceptible to infection to the viruses above mentioned when compared to

infected wildtype mice (78). On the other hand, detection of high-molecular-weight synthetic dsRNA poly(I:C) (HMW poly(I:C)) by MDA5 results in its activation and downstream signaling (78, 87-88). MDA5 is essential for Picornavirus detection as mice lacking MDA5 are sensitive to encephalomyocarditis virus infection (78, 87).

Virus or synthetic RNA activation of RLRs results in CARD domain exposure and CARD domain-mediated association with MAVS (also known as IPS-1, Cardif, and VISA), a signaling adaptor molecule found in the mitochondrial membrane (92-95). The mitochondria is a signaling platform to recruit and activate an innate immune response upon RLR-mediated detection of viral or synthetic RNA. RLRs associate with MAVS and recruits various innate immune signaling molecules, forming the MAVS signalosome (96). MAVS signalosome is required to activate IKKε and TBK1 (96). Phosphorylation of the antiviral response transcription factors, IRF3 and IRF7, by IKKε and TBK1 results in their activation (97-98). Following virus infection-induced phosphorylation, IRF3 forms a homodimer or IRF3-IRF7 heterodimerize and translocates to the nuclei of infected cells where they induce the expression of a battery of genes including type I IFN genes (i.e. IFN-α/β) as well as IFN-inducible genes (such as RIG-I and MDA5) (99-103). IFN-α/β are then secreted from infected cells to signal to neighboring non-infected cells by binding to the type I IFN receptors resulting in the amplification of the IFN response mediated by activation of the JAK/STAT signaling pathway (74, 105-108). This complex signaling cascade activated by the recognition of viral PAPMs allows cells to establish an antiviral state to limit and facilitate virus clearance.

A number of reports suggest that the type I IFN response pathway is modulated by the mTORC1 signaling network. Synthetic DNA or virus induced IFN production is

blocked in plasmatocytoid dendritic cells (pDC) upon inhibition of the mTORC1 pathway (129). Also, the translation of the antiviral transcription factor IRF7 has been show to be regulated by the mTORC1 pathway as deletion of the mTORC1 substrate 4E-BP1 and 2 results in the translation of IRF7 and increased IFN-α/β production (130). Finally, decreased type I IFN production and increased susceptibility to virus infection is observed in MEFs and mice lacking the mTORC1 downstream target S6K (131). In sum, these observations indicate that the mTORC1 pathway is a critical regulator of the innate immune system.

Our interest in this cellular signaling network was ignited by our influenza virus animal infection studies and by the following reports linking REDD1 to the innate immune response pathway: *REDD1* was shown to be induced by IFN-α in the livers of chimpanzees; the ability of REDD1 to function as an interferon inducible gene and inhibit the replication of influenza virus, VSV, and HCV; its localization to the mitochondria (a signaling platform for innate immune signaling) and the identification of mitochondrial proteins as potential REDD1 interacting partners; its role in NF-κB-reporter activation; and reports indicating that mTORC1 regulates the cellular innate immune response.

Our studies reveal a potential new connection between REDD1 and the IFN response pathway in transformed cells. We observed impaired type I IFN induction in passage immortalized *REDD1*-/- MEFs when exposed to dsRNA. Our data suggest that this defect in type I IFN induction is due to the absence of the dsRNA sensor MDA5 and significant reduction in the induction of RIG-I, resulting in limited IRF3 nuclear translocation. Paradoxically, SV40 large T antigen transformed or primary *REDD1-/-*

MEFs respond to dsRNA and induce a type I IFN response to the same level as *REDD1*+/+ cells. These studies suggest that REDD1 knockout MEFs may require ablation of the IFN signaling pathway to become immortalized by serial passaging, a previously uncharacterized link that may be important in cancer development.

## RESULTS

### *Impaired type I IFN response in passage immortalized REDD1-/- MEFs*

Taking advantage of the passage immortalized REDD1 wildtype and knockout MEFs reported in this study, we began investigating whether REDD1 is involved in type I IFN response induced by virus infection. During infection of host cells, RNA viruses generate RNA products (viral PAMPs) in the process of RNA-dependent RNA synthesis, which are recognized by the host leading to the activation of immune response. However, viruses have evolved strategies to antagonize the host innate immune response to proliferate at the expense of the host (187). Therefore, we took a minimalistic approach and took advantage of synthetic analogs of viral dsRNA, HMW poly(I:C) (heavy molecular weight polyriboinosinic:polyribocytidylic acid) and 5'-ppp dsRNA (5'-triphosphate double stranded RNA), which robustly activate the type I IFN response pathway by driving the expression of IFN-α/β and many IFN responsive genes, such as MDA5 and RIG-I (74, 77, 87-88). Passage immortalized wildtype and REDD1 knockout MEFs were transfected with HMW poly(I:C) via a liposome-delivery system to stimulate a type I IFN response. After 6 and 12 hours of transfection, the relative abundance of IFN-β mRNA was measured by quantitative Real Time PCR (Q-PCR). Minimal IFN-β

mRNA was detected in control, lipofectamine-treated passage immortalized *REDD1*+/+ and *REDD1-/-* cells (Figure 48). In REDD1 wildtype cells, HMW poly(I:C) robustly induced the expression of IFN-β mRNA 6 hours after transfection and this response was substantially amplified by 12 hours post-transfection (h.p.t.; Figure 48). In marked contrast, IFN-β mRNA levels were undetectable at 6 hours after HMW poly(I:C) transfection in passage immortalized REDD1 knockout cells and only minimal amounts IFN-β mRNA were detected at 12h.p.t. (approximately a 100-fold difference between *REDD1*+/+ and *REDD1-/-* IFN-β mRNA induction 6h.p.t.; Figure 48).

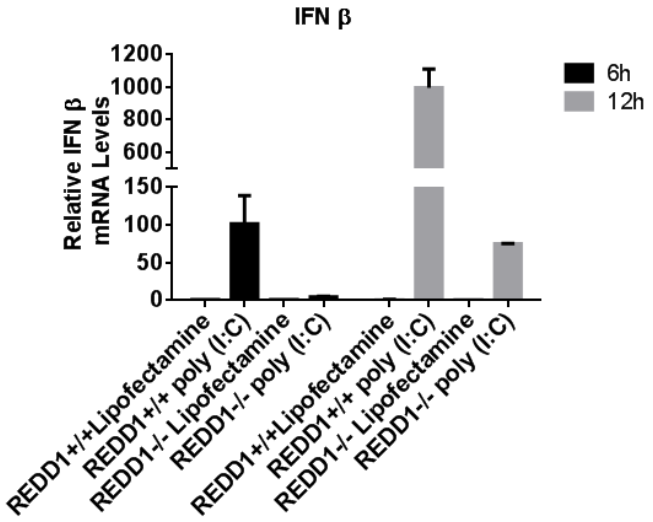


**Figure 48. Impaired IFN-β induction in passage immortalized *REDD1-/-* cells.** REDD1 wildtype and knockout passage immortalized clone #1 MEFs were transfected with HMW poly(I:C) (0.5μg/mL) for 6 and 12 hours. Total RNA was extracted 6 and 12 hours post transfection and real time PCR was performed.

Next, the relative abundance of IFN responsive genes IRF3, MDA5 and RIG-I was measured after HMW poly(I:C) transfection. No difference in IRF3 mRNA levels was observed between passage immortalized REDD1 wildtype and REDD1 knockout MEFs (Figure 49A). We then measured the expression of MDA5 and RIG-I. In contrast to wildtype cells, both MDA5 and RIG-I mRNA levels were decreased in passage immortalized *REDD1-/-* cells 6 hours after HMW poly(I:C) transfection (Figure 49B and C). Contrary to MDA5 mRNA levels which remained downregulated in *REDD1-/-*cells 12h.p.t., RIG-I mRNA was induced to the same extent in both wildtype and REDD1 knockout cells exposed to dsRNA for 12 hours (Figure 49B and C). The minimal increase in MDA5 and the recovery in RIG-I expression in passage immortalized *REDD1-/-* cells 12 h.p.t. is likely a result of secondary effect(s) associated with the modest induction of IFN-β mRNA observed in Figure 48 after 12 hours of HMW poly(I:C) transfection. These data indicate that passage immortalized *REDD1-/-* MEFs are impaired in their ability to induce a type I IFN response when challenged with the synthetic dsRNA HMW poly(I:C).

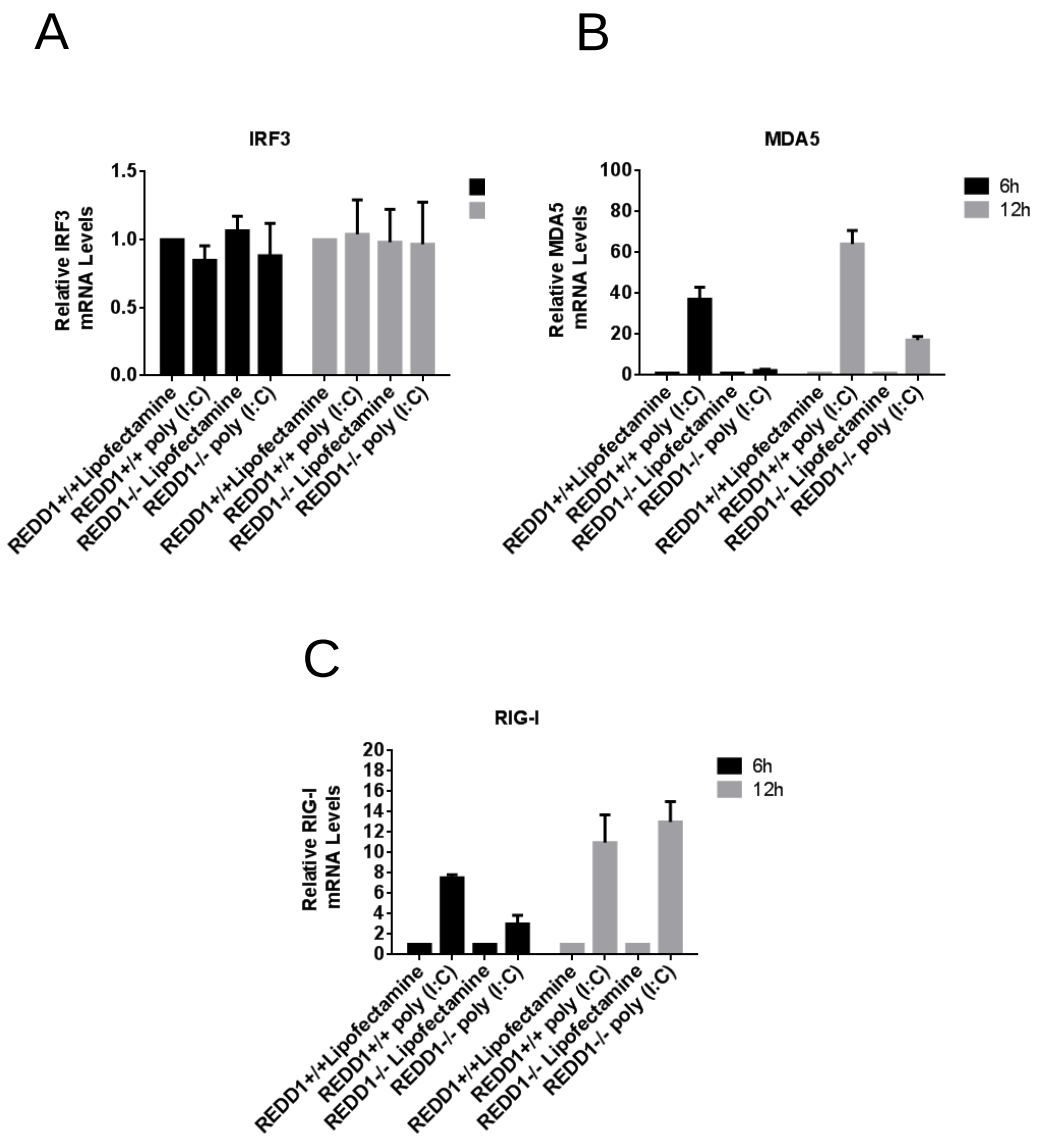


**Figure 49. MDA5 and RIG-I mRNA levels are decreased in passage immortalized *REDD1-/-* cells exposed to dsRNA.**
(A-C) REDD1 wildtype and knockout passage immortalized clone #1 MEFs were transfected with HMW poly(I:C) (0.5μg/mL) for 6 and 12 hours. Total RNA was extracted 6 and 12h post transfection and real time PCR was performed using (A) IRF3, (B) MDA5, and (C) RIG-I specific primers.

A possible explanation to the results above is that through its repressive activity on the mTORC1 signaling pathway, REDD1 could facilitate a type I IFN response when exposed to synthetic dsRNA. Therefore, to mimic REDD1 activity on mTORC1 in *REDD1-/-* cells, passage immortalized cells were co-treated with HMW poly(I:C) and the translation inhibitor cyclohexamide (CHX) or inhibitors of the mTORC1 pathway rapamycin and Torin. After co-treatment with HMW poly(I:C) with these inhibitors, the relative abundance of IFN-β mRNA was measured by QPCR. As shown in Figure 50, HMW poly(I:C) transfection in the presence or absence of CHX or mTORC1 inhibitors robustly induced IFN-β mRNA in passage immortalized *REDD1+/+* MEFs. Ongoing protein synthesis has been previously shown to be dispensable for IFN-β mRNA synthesis (235). Rapamycin, Torin, or CHX treatment of HMW poly(I:C) transfected passage immortalized *REDD1-/-* cells failed to rescue IFN-β mRNA expression (Figure 50). These results show that inhibition of mTORC1 activity or inhibition of an mTORC1-regulated cellular mechanism (i.e. protein synthesis) in passage immortalized wildtype MEFs has no effect on IFN-β mRNA expression when challenged with a dsRNA analog. In addition, the IFN response phenotype in passage immortalized *REDD1-/-* cells is not a result of the loss of inhibition on mTORC1 activity as inhibitors of the pathway are unable to rescue IFN-β mRNA expression.

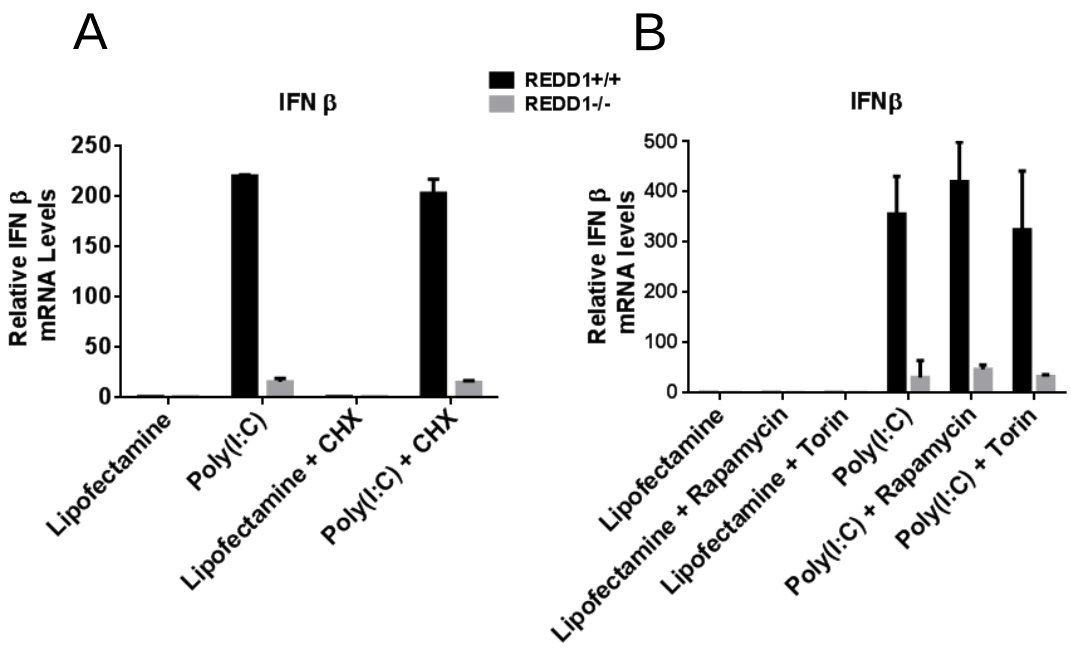


**Figure 50. Inhibition of protein synthesis and mTORC1 activity does not rescue IFN-β induction in passage immortalized *REDD1-/-* cells.**
(A)REDD1 wildtype and knockout passage immortalized clone #1 MEFs were treated with cyclohexamide (CHX) (100μg/mL) transfected with HMWh poly(I:C) (0.5μg/mL) for 6 hours. Total RNA was extracted 6h post transfection and real time PCR was performed. (B) Cells were treated as in (A) with the exception that cells were also treated with rapamycin (250nM) or Torin (250nM).

RIG-I-like receptors recognize viral PAMPs and signal to downstream effectors leading to the phosphorylation, dimerization, and translocation of IRF3 from the cytoplasm to the nucleus where it activates the transcription of type I IFN genes (74). Detection of IRF3 nuclear translocation by immunoflouresnces can allow us to map the location at which passage immortalized *REDD1-/-* cells fail to induce an IFN response when challenged with HMW poly(I:C). Decreased nuclear IRF3 would map the defect upstream of IRF3 translocation (i.e. from initial dsRNA sensing to dimerization of

phosphorylated IRF3) and similar levels of nuclear IRF3 in passage immortalized *REDD1*+/+ and *REDD1*-/- cells would map the defect downstream of IRF3 translocation (i.e. transcription of type I IFN genes). Therefore, mock transfected and HMW poly(I:C)-transfected passage immortalized cells were subjected to immunoflouresnces analysis 6h.p.t. Mock-transfected passage immortalized wildtype and REDD1 knockout cells have no detectable basal levels of nuclear IRF3 (Figure 51). However, HMW poly(I:C) transfection robustly induced IRF3 translocation in passage immortalized wildtype cells (as observed by the increase in nuclear FITC stain; Figure 51). In contrast, passage immortalized *REDD1*-/- cells treated with HMW poly(I:C) show approximately 70% reduction in IRF3 nuclear translocation (Figure 51). These results indicate that the IFN response defect in passage immortalized *REDD1*-/- cells maps upstream of IRF3 nuclear translocation and provides a narrow set of genes that can be interrogated to begin to dissect the link between REDD1 and the IFN response pathway.

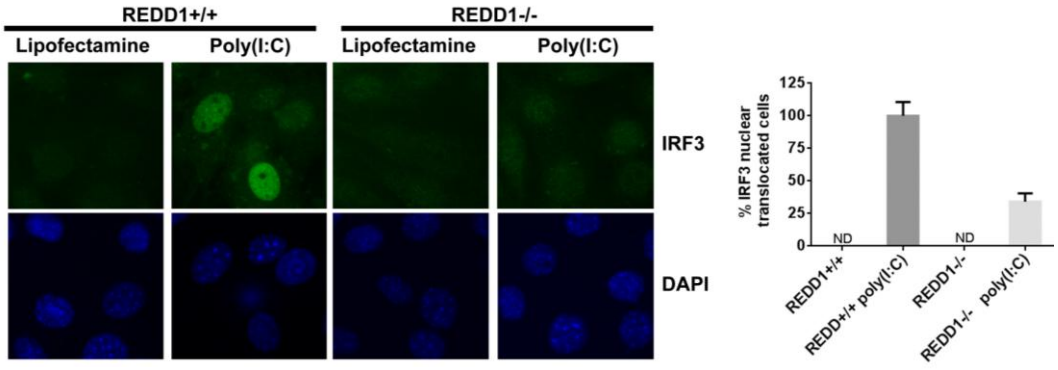


**Figure 51. Reduced IRF3 nuclear translocation in passage immortalized *REDD1-/-* MEFs.**
REDD1 wildtype and knockout passage immortalized clone #1 MEFs were transfected with HMW poly(I:C) (1μg/mL) for 6 hours. After transfection, cells were subjected to immunofluorescence analysis using total IRF3 antibodies (FITC). Nuclei is DAPI stained. Data from triplicate experiments were quantified and the percentage of IRF3 nuclear translocation is shown.

Our previous results indicate passage immortalized *REDD1-/-* MEFs are impaired in their ability to induce a type I IFN response due to a defect upstream of IRF3 nuclear translocation (Figure 51). To understand how loss of REDD1 leads to impaired IFN response, we began by interrogating the genes that sense dsRNA in the cytoplasm and trigger IRF3 nuclear translocation to drive an IFN response. MDA5 and RIG-I are cytoplasmic dsRNA sensors that signal to downstream targets to induce a type I IFN response (76, 87). Our data from Figure 49B and C show that MDA5 and RIG-I mRNA expression levels are down-regulated in passage immortalized *REDD1-/-* cells compared to wildtype cells at the initial phase of the IFN response triggered by HMW poly(I:C). This led us to examine basal and dsRNA-mediated induction of MDA5, RIG-I, and IRF3 at the protein level in passage immortalized *REDD1+/+* and *REDD1-/-* cells by

immunoblot analysis. As a control for IFN response induction by HMW poly(I:C), we assessed IRF3 phosphorylation by immunoblot analysis. Phosphorylation of IRF3 at Serine 396 (S396) has been previously shown to play an essential role in IRF3 activation and dimerization (236). One hour following HMW poly(I:C) transfection, no phospho-IRF3 was detected in *REDD1*+/+ or *REDD1*-/- cells (Figure 52A). However, HMW poly(I:C) greatly increased S396 phosphorylation of IRF3 six hours post-transfection in passage immortalized wildtype cells. In contrast, no detectable phospho-IRF3 was detected in passage immortalized *REDD1*-/- cells at this time point (Figure 52A). Total levels of IRF3 were assessed and no significant differences were detected between cell types and/or treatments (Figure 52A); showing that absence of IRF3 phosphorylation in *REDD1*-/- cells is not due to decrease in IRF3 total protein levels. These results confirm our previous IRF3 translocation studies in which less active, nuclear IRF3 was detected in passage immortalized *REDD1*-/- MEFs (Figure 51). Next, MDA5 and RIG-I protein levels were examined in both cell types. Passage immortalized *REDD1*+/+ cells express basal levels of MDA5 protein and transfection of HMW poly(I:C) robustly increase its levels starting at 6 hours and continue increasing through 9, 12, and 24h.p.t. (Figure 52 and 53). In contrast, passage immortalized *REDD1*-/- cells have no detectable basal levels of MDA5 protein and transfection of HMW poly(I:C) fails to induce MDA5 expression (Figure 52 and 53). Subsequently, the expression of RIG-I expression in both passage immortalized cell lines was assessed. In our experimental conditions, no basal RIG-I levels were detected in either cell type (Figure 53). However, HMW poly(I:C) transfection induced RIG-I expression 12 and 24h.p.t. in *REDD1*+/+ cells (Figure 53). On the other hand, minimal, but detectable amounts of the RIG-I protein were observed

in *REDD1-/-* cells transfected with HMW poly(I:C) for 12 and 24 hours (Figure 53). To determine the effect that pharmacological inhibition of the mTORC1 signaling pathway has on HMW poly(I:C)-mediated activation of IRF3 or MDA5 expression, we treated HMW poly(I:C) transfected cells with rapamycin or Torin. Both mTORC1 inhibitors had no effect on IRF3 phosphorylation or MDA5 induction in *REDD1*+/+ cells (Figure 52). Co-treatment of *REDD1-/-* cells with HMW poly(I:C) and mTORC1 inhibitors did not rescue IRF3 phosphorylation or MDA5 expression (Figure 52). These results confirm our previous observations showing that passage immortalized *REDD1-/-* cells are impaired in their ability to drive a type I IFN response (Figures 48-51). The minimal RIG-I expression detected in *REDD1-/-*cells after dsRNA transfection is likely a result of the slight induction of IFN β mRNA observed in Figure 48. Moreover, pharmacological inhibition of mTORC1 does not block dsRNA-mediated activation of the type I IFN response pathway in *REDD1*+/+ cells and fails to rescue the impaired IFN response in *REDD1-/-* cells. In sum, these data suggest that REDD1 through an unknown mechanism may be required for the expression of both RNA sensors as genetic ablation of *REDD1* results in the absence of MDA5 and diminished RIG-I expression, leading to a deficient type I IFN response to dsRNA.

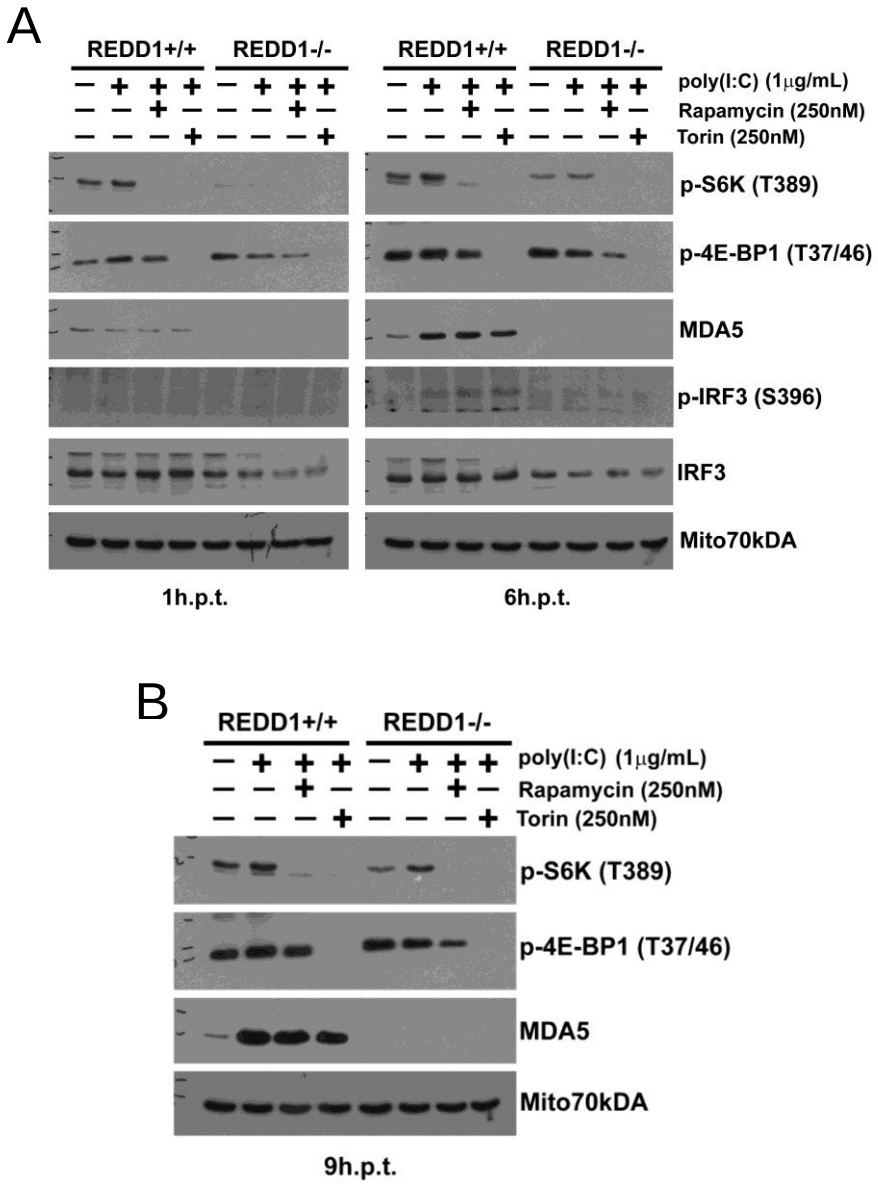


**Figure 52. Deficient synthetic dsRNA sensing and type I IFN response in passage immortalized *REDD1-/-* MEFs.**
(A) REDD1 wildtype and knockout passage immortalized clone #1 MEFs were co-treated with rapamycin (250nM) or Torin (250nM) and transfected with HMW poly(I:C) (1μg/mL). Cell extracts were obtained after the indicated time points post-transfection and subjected to immunoblot analysis with the indicated antibodies. (B) Cells were treated as in (A) with the exception that cell extracts were obtained 9h.p.t.

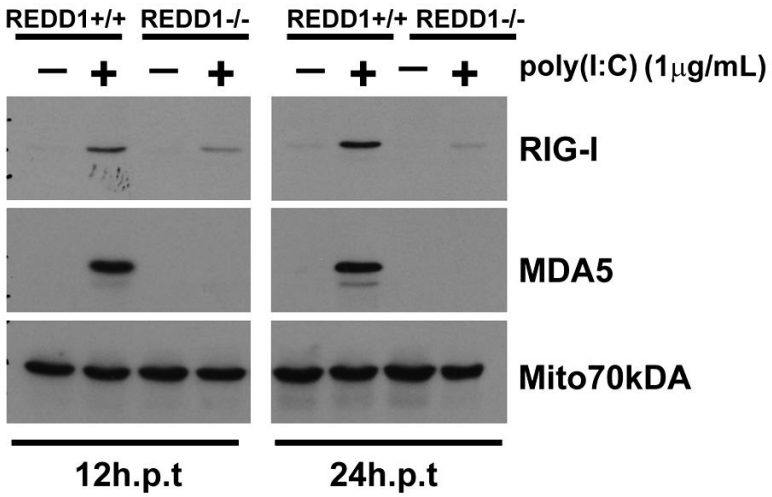


**Figure 53. REDD1 regulates the expression of MDA5 and RIG-I in passage immortalized *REDD1-/-* MEFs exposed to dsRNA.**
REDD1 wildtype and knockout passage immortalized clone #1 MEFs were transfected with HMW poly(I:C) (1μg/mL) for 12 and 24 hours. Cell extracts were obtained 12 and 24h.p.t. and subjected to immunoblot analysis with the indicated antibodies.

Activation of RLRs is dependent on the structure of the RNA. MDA5 specifically recognizes HMW poly(I:C) while RIG-I selectively recognizes 5'-ppp dsRNA (77, 87). Our data suggest that passage immortalized *REDD1-/-* MEFs are unable to drive an IFN response when exposed to HMW poly(I:C) in part due to the absence of the sensor MDA5 (Figure 52 and 53). To determine if a RIG-I specific ligand could induce an IFN response, passage immortalized *REDD1+/+* and *REDD1-/-* cells were transfected with 5'ppp dsRNA and the expression of MDA5 and RIG-I was used as a surrogate for IFN activation. Similar to our results using the MDA5-specific ligand HMW poly(I:C), *REDD1-/-* cells were unable to activate an IFN response as measured by the inability of these cells to induce the expression of the IFN-responsive genes MDA5

and RIG-I (Figure 54). Thus, REDD1, through an unknown mechanism, regulates the expression of both MDA5 and RIG-I, and highlights the importance of this gene in the dsRNA-mediated activation of the IFN response pathway.

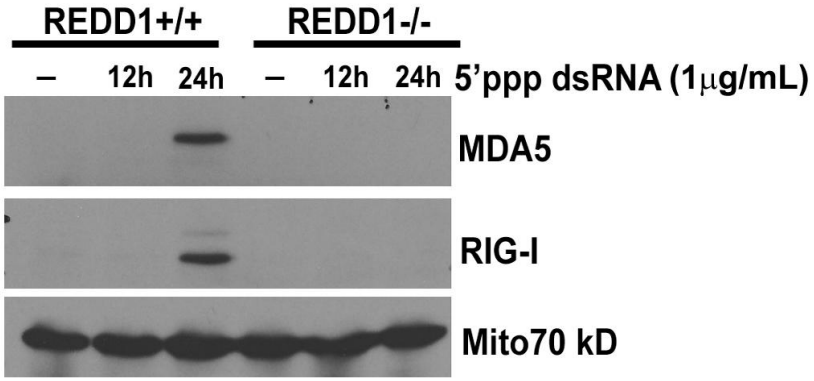


**Figure 54. Impaired MDA5 and RIG-I expression in passage immortalized *REDD1-/-* MEFs treated with the RIG-I ligand 5'-ppp dsRNA.**
REDD1 wildtype and knockout passage immortalized clone #1 MEFs were transfected with 5'-triphosphate dsRNA (1μg/mL) for 12 and 24 hours. Cell extracts were obtained 12 and 24 hours post-transfection and subjected to immunoblot analysis with the indicated antibodies.

As our study indicates that passage immortalized mammalian cells lacking REDD1 are not only highly susceptible to virus infection but are also unable to activate an intracellular immune response when exposed to synthetic IFN agonists HMW poly(I:C) or 5'-ppp dsRNA. During the process of cellular immortalization by serial passaging of mouse embryonic fibroblast, a number of genetic events may take place that

allows some cells to gain proliferative/growth advantage over the rest. Interferons have potent antiviral and antiproliferative activity and inactivation of this pathway could provide cells with such a proliferative/growth advantage. Therefore, to determine if the phenotype observed in passage immortalized *REDD1-/-* cells is a result of a random genetic event or whether the phenotype is in fact a result of the loss of REDD1, the IFN signaling pathway was assessed in a separate passage immortalized clone, referred here as passage immortalized clone#2. The relative abundance of IFN-β and MDA5 mRNA was measured by Q-PCR following treatment with HMW poly(I:C). Similar to the results obtained with passage immortalized clone#1, wildtype cells robustly express IFN β and MDA5 mRNA 6 hours after dsRNA transfection. In contrast, IFN-β and MDA5 mRNAs were minimally detected in passage immortalized *REDD1-/-* clone#2 cells (Figure 55).

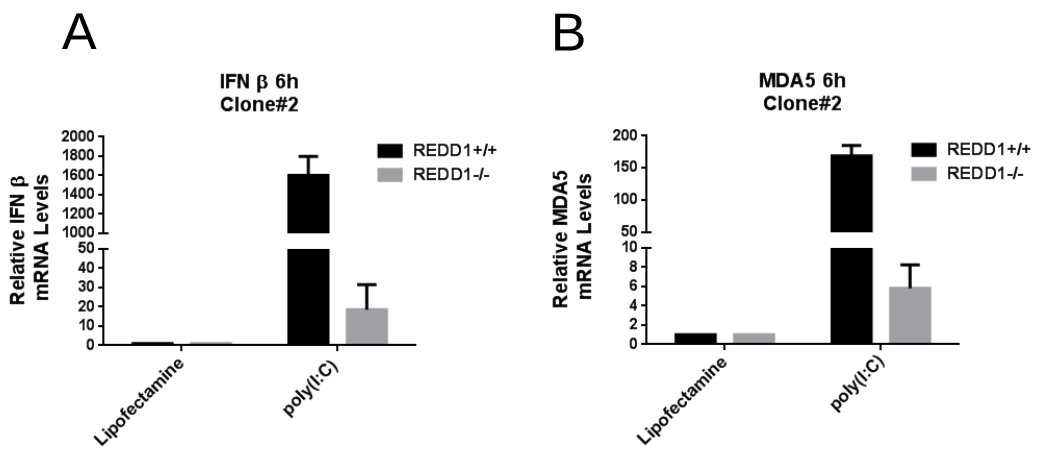


**Figure 55. Impaired IFN-β and MDA5 induction in passage immortalized *REDD1-/-* clone#2 treated with synthetic dsRNA.**
(A-B) REDD1 wildtype and knockout passage immortalized clone #2 MEFs were transfected with HMW poly(I:C) (0.5μg/mL) for 6h. Total RNA was extracted 6 h post transfection and real time PCR were performed as previously described using (A) IFN-β and (B) MDA5 specific primers.

Our characterization of passage immortalized *REDD1+/+* and *REDD1-/-* clone#2 MEFs continued by assessing MDA5 and RIG-I protein expression following HMW poly(I:C) transfection. As shown in figure 56, dsRNA transfection robustly stimulates MDA5 and RIG-I expression in *REDD1+/+* clones#1 and 2. On the contrary, passage immortalized *REDD1-/-* clones#1 and 2 transfected with HMW poly(I:C) have no detectable MDA5 protein levels and minimal RIG-I expression is detected (Figure 56A and B). To determine if 5'-ppp dsRNA, a RIG-I specific ligand, can activate an IFN response in passage immortalized *REDD1-/-* clone#2 MEFs, MDA5 and RIG-I expression was examined following 5'-ppp dsRNA transfection. Similar to our previous results (Figure 54), we observed *REDD1-/-* clone#2 cells are unable to induce MDA5

expression and only minimal RIG-I amounts were detected in response to dsRNA (Figure 57). Altogether, our data from two passage immortalized *REDD1-/-* clones show a significant reduction in the expression of the RNA sensors MDA5 and RIG-I in response to two types of dsRNA which results in the inability of the cell to respond to exogenous RNA leading to impaired activation of the type I IFN response pathway. This newly discovered link between REDD1 and innate immunity may be important during cancer development as interferons are antiproliferative cytokines.

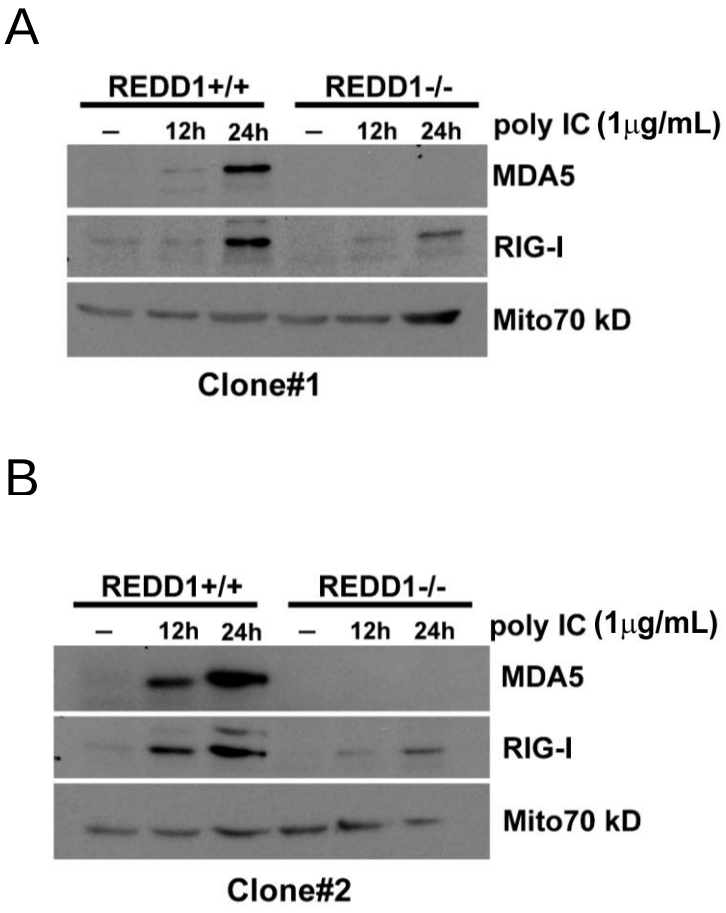


**Figure 56. MDA5 and RIG-I induction is impaired in passage immortalized *REDD1-/-* clones#1 and 2 transfected with poly(I:C).**
(A-B) Passage immortalized clones #1 and #2 MEFs were transfected with HMW poly(I:C) (1μg/mL) for 12 and 24 hours. Cell extracts were obtained 12 and 24 hours post-transfection and subjected to immunoblot analysis with the indicated antibodies.

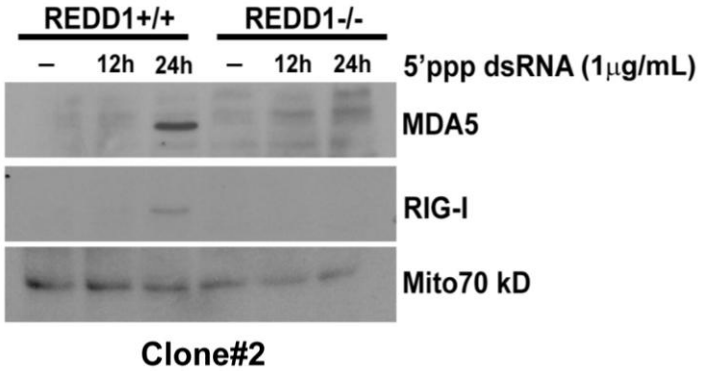


**Figure 57. Impaired MDA5 and RIG-I expression in passage immortalized *REDD1-/-* clone#2 MEFs treated with 5'-ppp dsRNA.**
REDD1 wildtype and knockout passage immortalized clone #2 MEFs were transfected with 5'-triphosphate dsRNA (1μg/mL) for 12 and 24 hours. Cell extracts were obtained 12 and 24 hours post-transfection and subjected to immunoblot analysis with the indicated antibodies.

Our data from passage immortalized MEFs demonstrate that REDD1 loss results in sensitivity to virus infection and impaired IFN response. To further investigate if the phenotype observed in passage immortalized *REDD1-/-* clones is recapitulated in other REDD1 knockout cells immortalized through an alternative method, mouse embryonic fibroblasts transformed by transfection with the SV40 large T antigen were analyzed. In addition, primary *REDD1+/+* and *REDD1-/-* were also examined. First, the relative levels of IFN β mRNA were measured in large T antigen-transformed MEFs treated with HMW poly(I:C). Surprisingly and contrary to the results obtained with passage immortalized MEFs, the levels of IFN β mRNA were slightly, but not significantly decreased in large T antigen transformed *REDD1-/-* MEF compared to *REDD1+/+* cells (Figure 58A). Next, MDA5 and RIG-I protein levels were measured in large T antigen

transformed *REDD1*+/+ and *REDD1*-/- MEFs before and following HMW poly(I:C) transfection. In passage immortalized *REDD1*-/- cells no basal levels of MDA5 or RIG-I were detected, whereas large T antigen transformed *REDD1*-/- cells expressed both RNA sensors in low amounts (Figure 58B). The small, but detectable amounts of MDA5 and RIG-I protein were sufficient to sense and activate an IFN response following HMW poly(I:C) transfection in large T antigen transformed *REDD1*+/+ and *REDD1*-/- cells as the levels of these two RLRs robustly increased 24h.p.t (Figure 58B). In contrast, passage immortalized *REDD1*-/- are unable to responds to dsRNA as no MDA5 and minimal amounts of RIG-I were detected (Figure 58B). These data suggests that cellular immortalization of *REDD1*-/- cells by serial passage, and not driven by the SV40 large T antigen, may require the loss of the IFN response pathway.

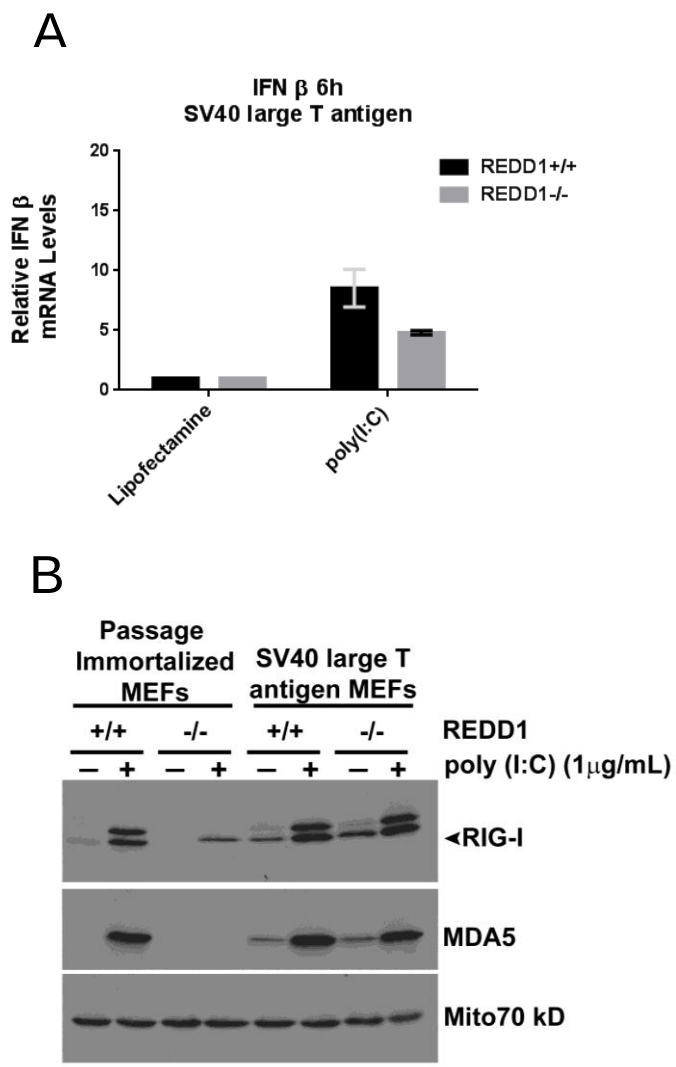


**Figure 58. SV40 large T antigen transformed *REDD1-/-*cells induce MDA5 and RIG-I expression following HMW poly(I:C) transfection.**
(A) SV40 large T antigen immortalized REDD1 wildtype and knockout MEFs were transfected with HMW poly(I:C) (0.5μg/mL) for 6 hours. Total RNA was extracted and Q-PCR was performed. (B) MEFs of two genotypes (either passage immortalized clone#1 or transformed with the SV40 large T antigen) were transfected with HMW poly(I:C) (1μg/mL) for 24 hours. Cell extracts were obtained 24 hours post-transfection and subjected to immunoblot analysis with the indicated antibodies.

Passage immortalized *REDD1-/-* MEFs are highly susceptible to virus infection compared to wildtype cells (Chapter Five). Infection of mammalian cells by viruses triggers a type I IFN response to promote virus inhibition, clearance, and apoptosis of infected cells (66). To examine if the viral permissiveness in passage immortalized *REDD1-/-* cells is a result of the ablation of the IFN response pathway (Figures 48-57), large T antigen transformed *REDD1+/+*and *REDD1-/-* cells were infected with influenza virus WSN strain at an m.o.i. 1 and viral protein expression was assessed as a function of time. Large T antigen transformed *REDD1-/-*infected cells begin producing viral protein NP at 8 hours post-infection whereas HA, M1/M2, and PB1 expression is detected at 10 hours. In contrast, *REDD1+/+* cells begin to express influenza virus NP and M1/M2 proteins at 10 hours post-infection, while no detectable levels of HA or PB1 proteins are observed at this time point (Figure 59). Not only is virus protein production detected earlier, large T antigen transformed *REDD1-/-* infected cells express higher levels of every influenza virus protein analyzed (Figure 59). These data confirms that genetic deletion of REDD1, independently of the cellular immortalization method used, results in virus permissiveness regardless of the IFN response phenotype.

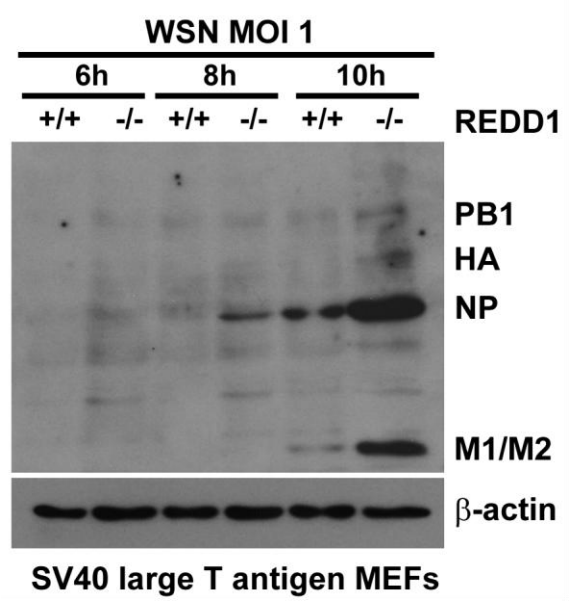


**Figure 59. Large T antigen transformed *REDD1-/-* cells express higher levels of influenza virus proteins.**
REDD1 wildtype and knockout MEFs transformed with the SV40 large T antigen were infected with influenza virus at m.o.i. 1 for 6, 8, and 10 hours. Cell extracts were subjected to immunoblot analysis with antibodies against influenza virus proteins. β-actin was used as a loading control.

Next, the type I IFN response in mouse primary *REDD1+/+* and *REDD1-/-* MEFs after HMW poly(I:C) transfection was measured by Q-PCR and immunoblot analysis. Primary MEFs transfected with dsRNA show no significant difference in the relative amounts of IFN-β mRNA, similar to the results obtained from large T antigen transformed cells (Figure 60). To confirm IFN-β induction results in the expression of IFN responsive genes, the expression levels of MDA5 was measured following transfection of the IFN agonists HMW poly(I:C) and 5'-ppp dsRNA. Treatment of primary *REDD1+/+* and *REDD1-/-* cells with poly(I:C) results in up-regulation of

MDA5 protein levels 12 h.p.t (Figure 60B). Similar results were obtained when primary MEFs were exposed to the IFN agonist 5'-ppp dsRNA, MDA5 up-regulated (Figure 61). These results indicate that primary *REDD1+/+* and *REDD1-/-* MEFs are competent in their ability to sense and activate a type I IFN response when challenged with synthetic dsRNA.

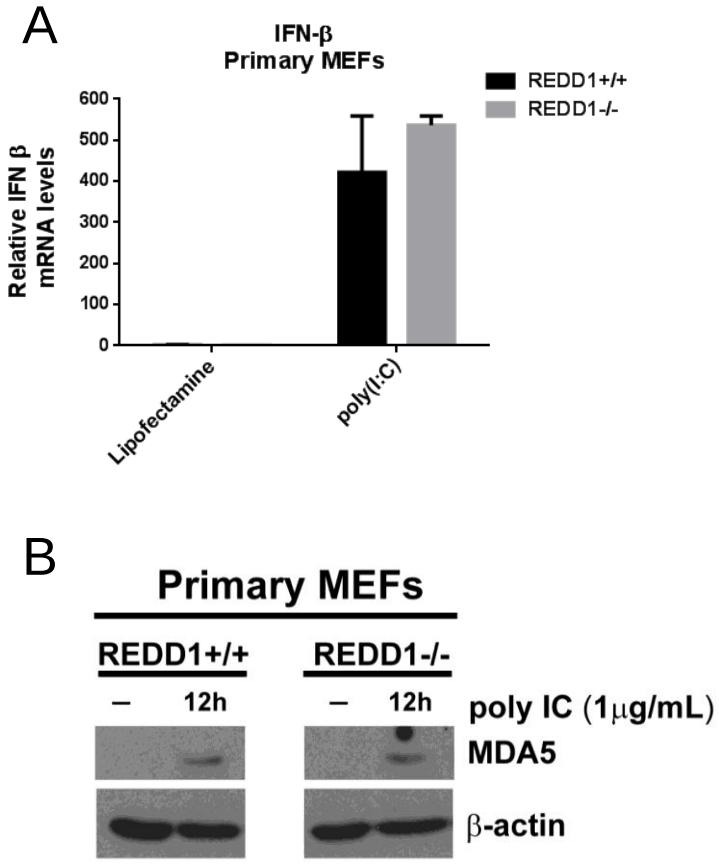


**Figure 60. HMW poly(I:C)-mediated activation of type I IFN and induction of MDA5 in primary *REDD1-/-* MEFs.**
(A) Mouse primary REDD1 wildtype and knockout MEFs were transfected with HMW poly(I:C) (1μg/mL) for 6 hours. Total RNA was extracted and Q-PCR was performed. (B) *REDD1+/+* and *REDD1-/-* primary MEFs were transfected with HMW poly(I:C) (1μg/mL) for 12 hours. Cell extracts were obtained 12 hours post-transfection and subjected to immunoblot analysis with the indicated antibodies.

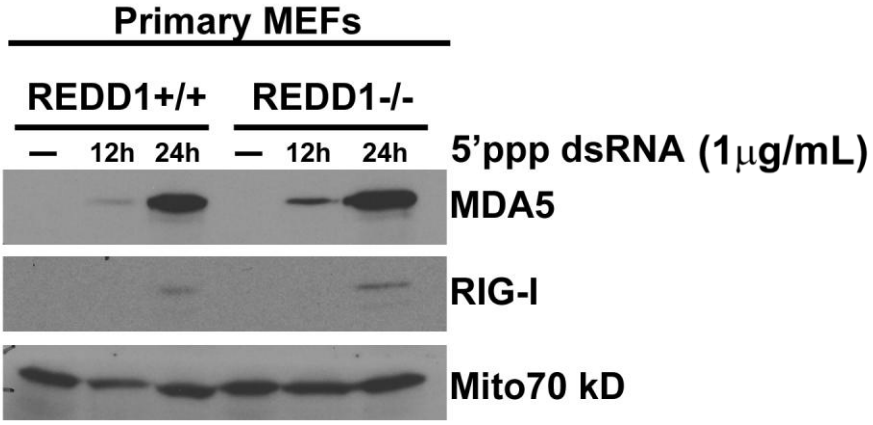


**Figure 61. 5'-ppp dsRNA-mediated induction of MDA5 and RIG-I expression in primary *REDD1-/-* MEFs**
REDD1+/+ and REDD1-/- primary MEFs were transfected with 5'-ppp dsRNA (1μg/mL) for 12 and 24 hours. Cell extracts were obtained 12 and 24 hours post-transfection and subjected to immunoblot analysis with the indicated antibodies.

To confirm our previous influenza infection results showing passage immortalized and large T antigen transformed *REDD1-/-* MEFs express higher levels of viral proteins compared to their wildtype counterparts, mouse primary *REDD1+/+* and *REDD1-/-* cells were infected with influenza virus strain A/WSN/1933 at m.o.i. 2 and virus protein expression was assessed 8 hours post-infection by immunoblot analysis. In contrast to primary wildtype influenza infected cells, higher levels of virus M1/M2, NP, and HA proteins were detected in primary *REDD1-/-* MEFs (Figure 62), further confirming that ablation REDD1results in virus permissiveness.

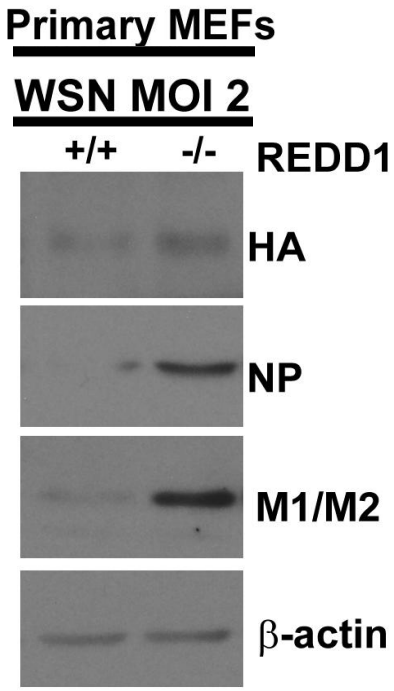


**Figure 62. *REDD1*-/- primary MEFs express higher levels of influenza virus proteins than *REDD1*+/+ cells.**
*REDD1* +/+ and *REDD1-/-* primary MEFs were infected with influenza virus at m.o.i. 2 for 8 hours. Cell extracts were subjected to immunoblot analysis with antibodies against influenza virus proteins.

Finally, to determine if the susceptibility to influenza virus infection observed in *REDD1-/-* mice (Chapter 6) is also due to a defect in the expression of MDA5 and/or RIG-I, mouse liver tissue from *REDD1+/+* and *REDD1-/-* mice was isolated to assess the protein levels of both RNA sensors. Genetic deletion of REDD1 gene in mice has no effect on the basal expression levels of RIG-I and MDA5 (Figure 63). Collectively, our work shows that immortalizated *REDD1-/-* cells by serial passaging fails to activate a

type I IFN response. This study may have revealed a new link between REDD1 and the IFN response pathway that may be important in cellular immortalization and cancer.

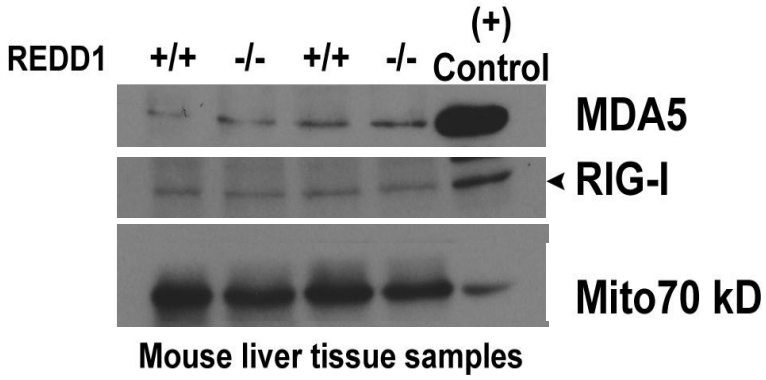


**Figure 63. Similar basal MDA5 and RIG-I protein levels detected in *REDD1*+/+ and *REDD1*-/- mouse liver tissue samples.**
*REDD1* +/+ and *REDD1-/-* mouse liver tissue was homogenized with RIPA extraction buffer overnight. Protein extracts were subjected to immunoblot analysis with antibodies depicted.

**DISCUSSION**

Virus infection of mammalian cells results in the activation of evolutionary conserved signaling pathways to limit virus proliferation. Cytoplasmic or membrane bound PRRs recognize viral PAMPs and trigger the production of proinflammatory cytokines and the activation of the type I IFN response pathway (72). Based on 1) our influenza virus animal infection studies, 2) reports indicating mTORC1 regulates the innate immune response, and 3) previous reports linking REDD1 to the innate immune response, we assessed the innate immune signaling pathway in passage immortalized, SV40 large T antigen transformed, and primary *REDD1+/+* and *REDD1-/-* cells.

The process of cellular immortalization by serial passaging requires a number of genetic events such as disruptions to growth control mechanisms that provides a clonal advantage. Our work identified the type I IFN response pathway, a signaling network with potent antiviral and antiproliferative effects (66), as a cellular pathway potentially involved in providing a proliferative/growth advantage to passage immortalized *REDD1-/-* cells.

The immune system has the capacity to recognize not only between self and non-self but it is capable of detecting subtle differences between self and transformed self, a cellular process known as cancer immunoediting (237). Although originally recognized for its potent antiviral activity, type I interferons have emerged as immunoregulatory molecules modulating and connecting both innate and adaptive arms of the immune system and as important cytokines involved in cancer immunoediting (237). Mice treated with a blocking antibody specific for type I IFN receptor IFNAR1 failed to initiate an antitumor immune response and reject chemically-induced sarcomas, and *IFNAR1-/-*

mice exposed to chemical carcinogens were more susceptible to tumor formation (238). Importantly, several naturally occurring human tumors have acquired mutations that render them IFN-insensitive and cannot induce an antitumor response (237). Recognition of transformed cells by the innate and adaptive immune systems results in the elimination of these cells at least in part by natural killer (NK) cells and T-lymphocytes, the activation of which is mediated by type I IFNs. These immune cells interact with specific ligands expressed by transformed cells leading to their elimination (237). IFN-α and IFN-β are approved by the US Food and Drug Administration (FDA) for the treatment of several cancers including leukaemias, lymphomas, and melanomas (237), thus further work is required to delineate the molecular and cellular effects of IFNs on cancer immunosurveillance.

Of importance to our studies, a growing body of evidence suggests type I IFNs may have the potential to block the transformation of normal cells into tumor cells. Type I IFNs (IFN-α and β) were shown to induce tumor suppressor p53 expression at the mRNA and protein levels (239). In a p53-dependent manner, IFN-β suppressed oncogene-induced cell transformation. The enhanced p53 expression mediated by IFN-β treatment results in increased sensitization to chemotherapeutic agent- or X-ray irradiation-induced apoptosis (239). Interestingly, VSV infection elevated p53 activation leading to the induction of pro-apoptotic genes resulting in increased apoptosis and decreased virus replication as p53 deficient cells and mice expressed higher virus titers, failed to undergo apoptosis, and were highly susceptible to VSV infection (239). In sum, this suggests that the antitumor properties of type I IFNs may also involve p53 induction

and show that p53 activation is an important host antiviral defense mechanism that contributes to limit virus replication (239).

Additional studies have suggested the IFN stimulated gene RNaseL functions as a tumor suppressor in human prostate cancer cells (240). RNaseL germline mutations have been linked to the hereditary prostate cancer 1 (HPC1) locus, increasing the risk of developing prostate cancer (240). This report further shows type I IFNs may play a role in inhibiting cellular transformation.

Our results suggest that passage immortalization of *REDD1*-/- MEFs requires the loss of the type I IFN response pathway. Among the genetic mutations that can disrupt growth control mechanisms and provide a clonal advantage is inactivation of the tumor suppressor p53. As other have reported, p53 enhances IFN signaling and antiviral protection upon virus infection (241). Inactivation of p53 is likely not the reason for impaired type I IFN in passage immortalized *REDD1-/-* MEFs because cells transformed with the SV40 large T antigen, an oncogenic virus product known to bind and abrogate p53 responses (242), are IFN-competent. It is important to determine the cause(s) for the impaired IFN response in the absence of REDD1 that results in cellular immortalization. Currently, we are examining the transcriptional landscape between passage immortalized and primary *REDD1*-/- MEFs by RNA-sequencing to determine what transcriptional perturbations took place during the process of cellular transformation. Knowledge obtained from this analysis and others could reveal a previously uncharacterized relationship between REDD1 and cancer development as growing body of evidence suggests that REDD1 may function as a tumor suppressor by inhibiting cell growth and

inducing apoptosis. In sum, REDD1 appears to be a key player the intersection between immunity and cancer.

**BIBLIOGRAPHY**

1. Fiore AE, Shay DK, Broder K, Iskander JK, Uyeki TM, Mootrey G, et al. Prevention and control of influenza: recommendations of the Advisory Committee on Immunization Practices (ACIP), 2008. MMWR Recomm Rep. 2008;57(RR-7):1-60.
2. Johnson NP, Mueller J. Updating the accounts: global mortality of the 1918-1920 "Spanish" influenza pandemic. Bull Hist Med. 2002;76(1):105-15.
3. Reed C, Angulo FJ, Swerdlow DL, Lipsitch M, Meltzer MI, Jernigan D, et al. Estimates of the prevalence of pandemic (H1N1) 2009, United States, April-July 2009. Emerg Infect Dis. 2009;15(12):2004-7. PMCID: 3375879.
4. Palese P, Shaw ML. *Orthomyxovididae*: the viruses and their replication. 5th ed. D.M. K, P.M. H, editors. Philadelphia: Lippincott Williams & Wilkins; 2007.
5. Wang TT, Palese P. Unraveling the mystery of swine influenza virus. Cell. 2009;137(6):983-5.
6. Yewdell J, Garcia-Sastre A. Influenza virus still surprises. Curr Opin Microbiol. 2002;5(4):414-8.
7. Layne SP, Monto AS, Taubenberger JK. Pandemic influenza: an inconvenient mutation. Science. 2009;323(5921):1560-1. PMCID: 2778479.
8. Molinari NA, Ortega-Sanchez IR, Messonnier ML, Thompson WW, Wortley PM, Weintraub E, et al. The annual impact of seasonal influenza in the US: measuring disease burden and costs. Vaccine. 2007;25(27):5086-96.
9. Oshansky CM, Thomas PG. The human side of influenza. J Leukoc Biol. 2012;92(1):83-96. PMCID: 3382310.
10. Davies WL, Grunert RR, Haff RF, McGahen JW, Neumayer EM, Paulshock M, et al. Antiviral Activity of 1-Adamantanamine (Amantadine). Science. 1964;144(3620):862-3.
11. Sansom MS, Kerr ID. Influenza virus M2 protein: a molecular modelling study of the ion channel. Protein Eng. 1993;6(1):65-74.
12. De Clercq E. Antiviral agents active against influenza A viruses. Nat Rev Drug Discov. 2006;5(12):1015-25.
13. Moscona A. Neuraminidase inhibitors for influenza. N Engl J Med. 2005;353(13):1363-73.
14. Karlas A, Machuy N, Shin Y, Pleissner KP, Artarini A, Heuer D, et al. Genome-wide RNAi screen identifies human host factors crucial for influenza virus replication. Nature. 2010;463(7282):818-22.
15. Konig R, Stertz S, Zhou Y, Inoue A, Hoffmann HH, Bhattacharyya S, et al. Human host factors required for influenza virus replication. Nature. 2010;463(7282):813-7. PMCID: 2862546.

16. Carette JE, Guimaraes CP, Varadarajan M, Park AS, Wuethrich I, Godarova A, et al. Haploid genetic screens in human cells identify host factors used by pathogens. Science. 2009;326(5957):1231-5.
17. Wullschleger S, Loewith R, Hall MN. TOR signaling in growth and metabolism. Cell. 2006;124(3):471-84.
18. Heitman J, Movva NR, Hall MN. Targets for cell cycle arrest by the immunosuppressant rapamycin in yeast. Science. 1991;253(5022):905-9.
19. Laplante M, Sabatini DM. mTOR signaling at a glance. J Cell Sci. 2009;122(Pt 20):3589-94. PMCID: 2758797.
20. Pause A, Methot N, Svitkin Y, Merrick WC, Sonenberg N. Dominant negative mutants of mammalian translation initiation factor eIF-4A define a critical role for eIF-4F in cap-dependent and cap-independent initiation of translation. EMBO J. 1994;13(5):1205-15. PMCID: 394930.
21. Dorrello NV, Peschiaroli A, Guardavaccaro D, Colburn NH, Sherman NE, Pagano M. S6K1- and betaTRCP-mediated degradation of PDCD4 promotes protein translation and cell growth. Science. 2006;314(5798):467-71.
22. Ma XM, Yoon SO, Richardson CJ, Julich K, Blenis J. SKAR links pre-mRNA splicing to mTOR/S6K1-mediated enhanced translation efficiency of spliced mRNAs. Cell. 2008;133(2):303-13.
23. Richardson CJ, Broenstrup M, Fingar DC, Julich K, Ballif BA, Gygi S, et al. SKAR is a specific target of S6 kinase 1 in cell growth control. Curr Biol. 2004;14(17):1540-9.
24. Hornstein E, Tang H, Meyuhas O. Mitogenic and nutritional signals are transduced into translational efficiency of TOP mRNAs. Cold Spring Harb Symp Quant Biol. 2001;66:477-84.
25. Shintani T, Klionsky DJ. Autophagy in health and disease: A double-edged sword. Science. 2004;306(5698):990-5.
26. Alers S, Loffler AS, Wesselborg S, Stork B. Role of AMPK-mTOR-Ulk1/2 in the regulation of autophagy: cross talk, shortcuts, and feedbacks. Mol Cell Biol. 2012;32(1):2-11. PMCID: 3255710.
27. Manning BD, Cantley LC. AKT/PKB signaling: navigating downstream. Cell. 2007;129(7):1261-74. PMCID: 2756685.
28. Inoki K, Li Y, Zhu T, Wu J, Guan KL. TSC2 is phosphorylated and inhibited by Akt and suppresses mTOR signalling. Nat Cell Biol. 2002;4(9):648-57.
29. Inoki K, Li Y, Xu T, Guan KL. Rheb GTPase is a direct target of TSC2 GAP activity and regulates mTOR signaling. Genes Dev. 2003;17(15):1829-34. PMCID: 196227.
30. Long X, Lin Y, Ortiz-Vega S, Yonezawa K, Avruch J. Rheb binds and regulates the mTOR kinase. Curr Biol. 2005;15(8):702-13.

31. Efeyan A, Zoncu R, Sabatini DM. Amino acids and mTORC1: from lysosomes to disease. Trends Mol Med. 2012;18(9):524-33. PMCID: 3432651.
32. Sancak Y, Peterson TR, Shaul YD, Lindquist RA, Thoreen CC, Bar-Peled L, et al. The Rag GTPases bind raptor and mediate amino acid signaling to mTORC1. Science. 2008;320(5882):1496-501. PMCID: 2475333.
33. Sancak Y, Bar-Peled L, Zoncu R, Markhard AL, Nada S, Sabatini DM. Ragulator-Rag complex targets mTORC1 to the lysosomal surface and is necessary for its activation by amino acids. Cell. 2010;141(2):290-303. PMCID: 3024592.
34. Arsham AM, Howell JJ, Simon MC. A novel hypoxia-inducible factor-independent hypoxic response regulating mammalian target of rapamycin and its targets. J Biol Chem. 2003;278(32):29655-60.
35. Brugarolas J, Lei K, Hurley RL, Manning BD, Reiling JH, Hafen E, et al. Regulation of mTOR function in response to hypoxia by REDD1 and the TSC1/TSC2 tumor suppressor complex. Genes Dev. 2004;18(23):2893-904. PMCID: 534650.
36. Corradetti MN, Inoki K, Guan KL. The stress-inducted proteins RTP801 and RTP801L are negative regulators of the mammalian target of rapamycin pathway. J Biol Chem. 2005;280(11):9769-72.
37. Brugarolas J, editor. mTORC1 Signaling and Hypoxia: Humana Press; 2010.
38. Guertin DA, Sabatini DM. An expanding role for mTOR in cancer. Trends Mol Med. 2005;11(8):353-61.
39. Guertin DA, Sabatini DM. Defining the role of mTOR in cancer. Cancer Cell. 2007;12(1):9-22.
40. Bjornsti MA, Houghton PJ. The TOR pathway: a target for cancer therapy. Nat Rev Cancer. 2004;4(5):335-48.
41. Vignot S, Faivre S, Aguirre D, Raymond E. mTOR-targeted therapy of cancer with rapamycin derivatives. Ann Oncol. 2005;16(4):525-37.
42. Buchkovich NJ, Yu Y, Zampieri CA, Alwine JC. The TORrid affairs of viruses: effects of mammalian DNA viruses on the PI3K-Akt-mTOR signalling pathway. Nat Rev Microbiol. 2008;6(4):266-75. PMCID: 2597498.
43. Cooray S. The pivotal role of phosphatidylinositol 3-kinase-Akt signal transduction in virus survival. J Gen Virol. 2004;85(Pt 5):1065-76.
44. Dawson CW, Tramountanis G, Eliopoulos AG, Young LS. Epstein-Barr virus latent membrane protein 1 (LMP1) activates the phosphatidylinositol 3-kinase/Akt pathway to promote cell survival and induce actin filament remodeling. J Biol Chem. 2003;278(6):3694-704.
45. O'Shea C, Klupsch K, Choi S, Bagus B, Soria C, Shen J, et al. Adenoviral proteins mimic nutrient/growth signals to activate the mTOR pathway for viral replication. EMBO J. 2005;24(6):1211-21. PMCID: 556401.

46. Hasan M, Koch J, Rakheja D, Pattnaik AK, Brugarolas J, Dozmorov I, et al. Trex1 regulates lysosomal biogenesis and interferon-independent activation of antiviral genes. Nat Immunol. 2013;14(1):61-71. PMCID: 3522772.
47. Shoshani T, Faerman A, Mett I, Zelin E, Tenne T, Gorodin S, et al. Identification of a novel hypoxia-inducible factor 1-responsive gene, RTP801, involved in apoptosis. Mol Cell Biol. 2002;22(7):2283-93. PMCID: 133671.
48. Ellisen LW, Ramsayer KD, Johannessen CM, Yang A, Beppu H, Minda K, et al. REDD1, a developmentally regulated transcriptional target of p63 and p53, links p63 to regulation of reactive oxygen species. Mol Cell. 2002;10(5):995-1005.
49. Kimball SR, Do AN, Kutzler L, Cavener DR, Jefferson LS. Rapid turnover of the mTOR complex 1 (mTORC1) repressor REDD1 and activation of mTORC1 signaling following inhibition of protein synthesis. J Biol Chem. 2008;283(6):3465-75. PMCID: 2654224.
50. Horak P, Crawford AR, Vadysirisack DD, Nash ZM, DeYoung MP, Sgroi D, et al. Negative feedback control of HIF-1 through REDD1-regulated ROS suppresses tumorigenesis. Proc Natl Acad Sci U S A. 2010;107(10):4675-80. PMCID: 2842042.
51. Katiyar S, Liu E, Knutzen CA, Lang ES, Lombardo CR, Sankar S, et al. REDD1, an inhibitor of mTOR signalling, is regulated by the CUL4A-DDB1 ubiquitin ligase. EMBO Rep. 2009;10(8):866-72. PMCID: 2726664.
52. Gery S, Park DJ, Vuong PT, Virk RK, Muller CI, Hofmann WK, et al. RTP801 is a novel retinoic acid-responsive gene associated with myeloid differentiation. Exp Hematol. 2007;35(4):572-8. PMCID: 1922386.
53. Wang Z, Malone MH, Thomenius MJ, Zhong F, Xu F, Distelhorst CW. Dexamethasone-induced gene 2 (dig2) is a novel pro-survival stress gene induced rapidly by diverse apoptotic signals. J Biol Chem. 2003;278(29):27053-8.
54. Brafman A, Mett I, Shafir M, Gottlieb H, Damari G, Gozlan-Kelner S, et al. Inhibition of oxygen-induced retinopathy in RTP801-deficient mice. Invest Ophthalmol Vis Sci. 2004;45(10):3796-805.
55. Wolff NC, Vega-Rubin-de-Celis S, Xie XJ, Castrillon DH, Kabbani W, Brugarolas J. Cell-type-dependent regulation of mTORC1 by REDD1 and the tumor suppressors TSC1/TSC2 and LKB1 in response to hypoxia. Mol Cell Biol. 2011;31(9):1870-84. PMCID: 3133225.
56. Giaccia A, Siim BG, Johnson RS. HIF-1 as a target for drug development. Nat Rev Drug Discov. 2003;2(10):803-11.
57. Jin HO, Seo SK, Woo SH, Kim ES, Lee HC, Yoo DH, et al. Activating transcription factor 4 and CCAAT/enhancer-binding protein-beta negatively regulate the mammalian target of rapamycin via Redd1 expression in response to oxidative and endoplasmic reticulum stress. Free Radic Biol Med. 2009;46(8):1158-67.

58. Jin HO, An S, Lee HC, Woo SH, Seo SK, Choe TB, et al. Hypoxic condition- and high cell density-induced expression of Redd1 is regulated by activation of hypoxia-inducible factor-1alpha and Sp1 through the phosphatidylinositol 3-kinase/Akt signaling pathway. Cell Signal. 2007;19(7):1393-403.
59. Vega-Rubin-de-Celis S, Abdallah Z, Kinch L, Grishin NV, Brugarolas J, Zhang X. Structural analysis and functional implications of the negative mTORC1 regulator REDD1. Biochemistry. 2010;49(11):2491-501. PMCID: 3046781.
60. Reiling JH, Hafen E. The hypoxia-induced paralogs Scylla and Charybdis inhibit growth by down-regulating S6K activity upstream of TSC in Drosophila. Genes Dev. 2004;18(23):2879-92. PMCID: 534649.
61. DeYoung MP, Horak P, Sofer A, Sgroi D, Ellisen LW. Hypoxia regulates TSC1/2-mTOR signaling and tumor suppression through REDD1-mediated 14-3-3 shuttling. Genes Dev. 2008;22(2):239-51. PMCID: 2192757.
62. Cai SL, Tee AR, Short JD, Bergeron JM, Kim J, Shen J, et al. Activity of TSC2 is inhibited by AKT-mediated phosphorylation and membrane partitioning. J Cell Biol. 2006;173(2):279-89. PMCID: 2063818.
63. Kimball SR, Jefferson LS. Induction of REDD1 gene expression in the liver in response to endoplasmic reticulum stress is mediated through a PERK, eIF2alpha phosphorylation, ATF4-dependent cascade. Biochem Biophys Res Commun. 2012;427(3):485-9. PMCID: 3482272.
64. Ray PD, Huang BW, Tsuji Y. Reactive oxygen species (ROS) homeostasis and redox regulation in cellular signaling. Cell Signal. 2012;24(5):981-90. PMCID: 3454471.
65. Lanford RE, Guerra B, Lee H, Chavez D, Brasky KM, Bigger CB. Genomic response to interferon-alpha in chimpanzees: implications of rapid downregulation for hepatitis C kinetics. Hepatology. 2006;43(5):961-72.
66. Platanias LC. Mechanisms of type-I- and type-II-interferon-mediated signalling. Nat Rev Immunol. 2005;5(5):375-86.
67. Schoggins JW, Wilson SJ, Panis M, Murphy MY, Jones CT, Bieniasz P, et al. A diverse range of gene products are effectors of the type I interferon antiviral response. Nature. 2011;472(7344):481-5. PMCID: 3409588.
68. Cuaz-Perolin C, Furman C, Larigauderie G, Legedz L, Lasselin C, Copin C, et al. REDD2 gene is upregulated by modified LDL or hypoxia and mediates human macrophage cell death. Arterioscler Thromb Vasc Biol. 2004;24(10):1830-5.
69. Harvey KF, Mattila J, Sofer A, Bennett FC, Ramsey MR, Ellisen LW, et al. FOXO-regulated transcription restricts overgrowth of Tsc mutant organs. J Cell Biol. 2008;180(4):691-6. PMCID: 2265581.

70. Safran M, Kaelin WG, Jr. HIF hydroxylation and the mammalian oxygen-sensing pathway. J Clin Invest. 2003;111(6):779-83. PMCID: 153778.
71. Kumar H, Kawai T, Akira S. Pathogen recognition by the innate immune system. Int Rev Immunol. 2011;30(1):16-34.
72. Thompson AJ, Locarnini SA. Toll-like receptors, RIG-I-like RNA helicases and the antiviral innate immune response. Immunol Cell Biol. 2007;85(6):435-45.
73. Saito T, Hirai R, Loo YM, Owen D, Johnson CL, Sinha SC, et al. Regulation of innate antiviral defenses through a shared repressor domain in RIG-I and LGP2. Proc Natl Acad Sci U S A. 2007;104(2):582-7. PMCID: 1766428.
74. Loo YM, Gale M, Jr. Immune signaling by RIG-I-like receptors. Immunity. 2011;34(5):680-92. PMCID: 3177755.
75. Hofmann K. The modular nature of apoptotic signaling proteins. Cell Mol Life Sci. 1999;55(8-9):1113-28.
76. Yoneyama M, Kikuchi M, Natsukawa T, Shinobu N, Imaizumi T, Miyagishi M, et al. The RNA helicase RIG-I has an essential function in double-stranded RNA-induced innate antiviral responses. Nat Immunol. 2004;5(7):730-7.
77. Hornung V, Ellegast J, Kim S, Brzozka K, Jung A, Kato H, et al. 5'-Triphosphate RNA is the ligand for RIG-I. Science. 2006;314(5801):994-7.
78. Kato H, Takeuchi O, Sato S, Yoneyama M, Yamamoto M, Matsui K, et al. Differential roles of MDA5 and RIG-I helicases in the recognition of RNA viruses. Nature. 2006;441(7089):101-5.
79. Yoneyama M, Kikuchi M, Matsumoto K, Imaizumi T, Miyagishi M, Taira K, et al. Shared and unique functions of the DExD/H-box helicases RIG-I, MDA5, and LGP2 in antiviral innate immunity. J Immunol. 2005;175(5):2851-8.
80. Rehwinkel J, Tan CP, Goubau D, Schulz O, Pichlmair A, Bier K, et al. RIG-I detects viral genomic RNA during negative-strand RNA virus infection. Cell. 2010;140(3):397-408.
81. Sumpter R, Jr., Loo YM, Foy E, Li K, Yoneyama M, Fujita T, et al. Regulating intracellular antiviral defense and permissiveness to hepatitis C virus RNA replication through a cellular RNA helicase, RIG-I. J Virol. 2005;79(5):2689-99. PMCID: 548482.
82. Loo YM, Fornek J, Crochet N, Bajwa G, Perwitasari O, Martinez-Sobrido L, et al. Distinct RIG-I and MDA5 signaling by RNA viruses in innate immunity. J Virol. 2008;82(1):335-45. PMCID: 2224404.
83. Tasaka M, Sakamoto N, Itakura Y, Nakagawa M, Itsui Y, Sekine-Osajima Y, et al. Hepatitis C virus non-structural proteins responsible for suppression of the RIG-I/Cardif-induced interferon response. J Gen Virol. 2007;88(Pt 12):3323-33.
84. Mibayashi M, Martinez-Sobrido L, Loo YM, Cardenas WB, Gale M, Jr., Garcia-Sastre A. Inhibition of retinoic acid-inducible gene I-mediated induction

of beta interferon by the NS1 protein of influenza A virus. J Virol. 2007;81(2):514-24. PMCID: 1797471.
85. Kovacsovics M, Martinon F, Micheau O, Bodmer JL, Hofmann K, Tschopp J. Overexpression of Helicard, a CARD-containing helicase cleaved during apoptosis, accelerates DNA degradation. Curr Biol. 2002;12(10):838-43.
86. Kang DC, Gopalkrishnan RV, Wu Q, Jankowsky E, Pyle AM, Fisher PB. mda-5: An interferon-inducible putative RNA helicase with double-stranded RNA-dependent ATPase activity and melanoma growth-suppressive properties. Proc Natl Acad Sci U S A. 2002;99(2):637-42. PMCID: 117358.
87. Gitlin L, Barchet W, Gilfillan S, Cella M, Beutler B, Flavell RA, et al. Essential role of mda-5 in type I IFN responses to polyriboinosinic:polyribocytidylic acid and encephalomyocarditis picornavirus. Proc Natl Acad Sci U S A. 2006;103(22):8459-64. PMCID: 1464000.
88. Kato H, Takeuchi O, Mikamo-Satoh E, Hirai R, Kawai T, Matsushita K, et al. Length-dependent recognition of double-stranded ribonucleic acids by retinoic acid-inducible gene-I and melanoma differentiation-associated gene 5. J Exp Med. 2008;205(7):1601-10. PMCID: 2442638.
89. Andrejeva J, Childs KS, Young DF, Carlos TS, Stock N, Goodbourn S, et al. The V proteins of paramyxoviruses bind the IFN-inducible RNA helicase, mda-5, and inhibit its activation of the IFN-beta promoter. Proc Natl Acad Sci U S A. 2004;101(49):17264-9. PMCID: 535396.
90. Childs K, Stock N, Ross C, Andrejeva J, Hilton L, Skinner M, et al. mda-5, but not RIG-I, is a common target for paramyxovirus V proteins. Virology. 2007;359(1):190-200.
91. Satoh T, Kato H, Kumagai Y, Yoneyama M, Sato S, Matsushita K, et al. LGP2 is a positive regulator of RIG-I- and MDA5-mediated antiviral responses. Proc Natl Acad Sci U S A. 2010;107(4):1512-7. PMCID: 2824407.
92. Seth RB, Sun L, Ea CK, Chen ZJ. Identification and characterization of MAVS, a mitochondrial antiviral signaling protein that activates NF-kappaB and IRF 3. Cell. 2005;122(5):669-82.
93. Kawai T, Takahashi K, Sato S, Coban C, Kumar H, Kato H, et al. IPS-1, an adaptor triggering RIG-I- and Mda5-mediated type I interferon induction. Nat Immunol. 2005;6(10):981-8.
94. Meylan E, Curran J, Hofmann K, Moradpour D, Binder M, Bartenschlager R, et al. Cardif is an adaptor protein in the RIG-I antiviral pathway and is targeted by hepatitis C virus. Nature. 2005;437(7062):1167-72.
95. Xu LG, Wang YY, Han KJ, Li LY, Zhai Z, Shu HB. VISA is an adapter protein required for virus-triggered IFN-beta signaling. Mol Cell. 2005;19(6):727-40.
96. West AP, Shadel GS, Ghosh S. Mitochondria in innate immune responses. Nat Rev Immunol. 2011;11(6):389-402.

97. Fitzgerald KA, McWhirter SM, Faia KL, Rowe DC, Latz E, Golenbock DT, et al. IKKepsilon and TBK1 are essential components of the IRF3 signaling pathway. Nat Immunol. 2003;4(5):491-6.
98. Sharma S, tenOever BR, Grandvaux N, Zhou GP, Lin R, Hiscott J. Triggering the interferon antiviral response through an IKK-related pathway. Science. 2003;300(5622):1148-51.
99. Weaver BK, Kumar KP, Reich NC. Interferon regulatory factor 3 and CREB-binding protein/p300 are subunits of double-stranded RNA-activated transcription factor DRAF1. Mol Cell Biol. 1998;18(3):1359-68. PMCID: 108849.
100. Lin R, Heylbroeck C, Pitha PM, Hiscott J. Virus-dependent phosphorylation of the IRF-3 transcription factor regulates nuclear translocation, transactivation potential, and proteasome-mediated degradation. Mol Cell Biol. 1998;18(5):2986-96. PMCID: 110678.
101. Yoneyama M, Suhara W, Fukuhara Y, Fukuda M, Nishida E, Fujita T. Direct triggering of the type I interferon system by virus infection: activation of a transcription factor complex containing IRF-3 and CBP/p300. EMBO J. 1998;17(4):1087-95. PMCID: 1170457.
102. Sato M, Tanaka N, Hata N, Oda E, Taniguchi T. Involvement of the IRF family transcription factor IRF-3 in virus-induced activation of the IFN-beta gene. FEBS Lett. 1998;425(1):112-6.
103. Suhara W, Yoneyama M, Iwamura T, Yoshimura S, Tamura K, Namiki H, et al. Analyses of virus-induced homomeric and heteromeric protein associations between IRF-3 and coactivator CBP/p300. J Biochem. 2000;128(2):301-7.
104. Honda K, Yanai H, Negishi H, Asagiri M, Sato M, Mizutani T, et al. IRF-7 is the master regulator of type-I interferon-dependent immune responses. Nature. 2005;434(7034):772-7.
105. Schindler C, Shuai K, Prezioso VR, Darnell JE, Jr. Interferon-dependent tyrosine phosphorylation of a latent cytoplasmic transcription factor. Science. 1992;257(5071):809-13.
106. Silvennoinen O, Ihle JN, Schlessinger J, Levy DE. Interferon-induced nuclear signalling by Jak protein tyrosine kinases. Nature. 1993;366(6455):583-5.
107. Fu XY, Schindler C, Improta T, Aebersold R, Darnell JE, Jr. The proteins of ISGF-3, the interferon alpha-induced transcriptional activator, define a gene family involved in signal transduction. Proc Natl Acad Sci U S A. 1992;89(16):7840-3. PMCID: 49807.
108. Der SD, Zhou A, Williams BR, Silverman RH. Identification of genes differentially regulated by interferon alpha, beta, or gamma using oligonucleotide arrays. Proc Natl Acad Sci U S A. 1998;95(26):15623-8. PMCID: 28094.
109. Sun Z, Andersson R. NF-kappaB activation and inhibition: a review. Shock. 2002;18(2):99-106.

110. Hayden MS, West AP, Ghosh S. NF-kappaB and the immune response. Oncogene. 2006;25(51):6758-80.
111. Ghosh S, Hayden MS. New regulators of NF-kappaB in inflammation. Nat Rev Immunol. 2008;8(11):837-48.
112. Balachandran S, Thomas E, Barber GN. A FADD-dependent innate immune mechanism in mammalian cells. Nature. 2004;432(7015):401-5.
113. Takahashi K, Kawai T, Kumar H, Sato S, Yonehara S, Akira S. Roles of caspase-8 and caspase-10 in innate immune responses to double-stranded RNA. J Immunol. 2006;176(8):4520-4.
114. Lund JM, Alexopoulou L, Sato A, Karow M, Adams NC, Gale NW, et al. Recognition of single-stranded RNA viruses by Toll-like receptor 7. Proc Natl Acad Sci U S A. 2004;101(15):5598-603. PMCID: 397437.
115. Diebold SS, Kaisho T, Hemmi H, Akira S, Reis e Sousa C. Innate antiviral responses by means of TLR7-mediated recognition of single-stranded RNA. Science. 2004;303(5663):1529-31.
116. Oshiumi H, Matsumoto M, Funami K, Akazawa T, Seya T. TICAM-1, an adaptor molecule that participates in Toll-like receptor 3-mediated interferon-beta induction. Nat Immunol. 2003;4(2):161-7.
117. Yamamoto M, Sato S, Mori K, Hoshino K, Takeuchi O, Takeda K, et al. Cutting edge: a novel Toll/IL-1 receptor domain-containing adapter that preferentially activates the IFN-beta promoter in the Toll-like receptor signaling. J Immunol. 2002;169(12):6668-72.
118. Li S, Strelow A, Fontana EJ, Wesche H. IRAK-4: a novel member of the IRAK family with the properties of an IRAK-kinase. Proc Natl Acad Sci U S A. 2002;99(8):5567-72. PMCID: 122810.
119. Deng L, Wang C, Spencer E, Yang L, Braun A, You J, et al. Activation of the IkappaB kinase complex by TRAF6 requires a dimeric ubiquitin-conjugating enzyme complex and a unique polyubiquitin chain. Cell. 2000;103(2):351-61.
120. Wang C, Deng L, Hong M, Akkaraju GR, Inoue J, Chen ZJ. TAK1 is a ubiquitin-dependent kinase of MKK and IKK. Nature. 2001;412(6844):346-51.
121. Akira S, Uematsu S, Takeuchi O. Pathogen recognition and innate immunity. Cell. 2006;124(4):783-801.
122. Colonna M, Trinchieri G, Liu YJ. Plasmacytoid dendritic cells in immunity. Nat Immunol. 2004;5(12):1219-26.
123. Dai J, Megjugorac NJ, Amrute SB, Fitzgerald-Bocarsly P. Regulation of IFN regulatory factor-7 and IFN-alpha production by enveloped virus and lipopolysaccharide in human plasmacytoid dendritic cells. J Immunol. 2004;173(3):1535-48.
124. Izaguirre A, Barnes BJ, Amrute S, Yeow WS, Megjugorac N, Dai J, et al. Comparative analysis of IRF and IFN-alpha expression in human plasmacytoid and monocyte-derived dendritic cells. J Leukoc Biol. 2003;74(6):1125-38.

125. Kawai T, Sato S, Ishii KJ, Coban C, Hemmi H, Yamamoto M, et al. Interferon-alpha induction through Toll-like receptors involves a direct interaction of IRF7 with MyD88 and TRAF6. Nat Immunol. 2004;5(10):1061-8.
126. Honda K, Yanai H, Mizutani T, Negishi H, Shimada N, Suzuki N, et al. Role of a transductional-transcriptional processor complex involving MyD88 and IRF-7 in Toll-like receptor signaling. Proc Natl Acad Sci U S A. 2004;101(43):15416-21. PMCID: 523464.
127. Uematsu S, Sato S, Yamamoto M, Hirotani T, Kato H, Takeshita F, et al. Interleukin-1 receptor-associated kinase-1 plays an essential role for Toll-like receptor (TLR)7- and TLR9-mediated interferon-{alpha} induction. J Exp Med. 2005;201(6):915-23. PMCID: 2213113.
128. Hoshino K, Sugiyama T, Matsumoto M, Tanaka T, Saito M, Hemmi H, et al. IkappaB kinase-alpha is critical for interferon-alpha production induced by Toll-like receptors 7 and 9. Nature. 2006;440(7086):949-53.
129. Cao W, Manicassamy S, Tang H, Kasturi SP, Pirani A, Murthy N, et al. Toll-like receptor-mediated induction of type I interferon in plasmacytoid dendritic cells requires the rapamycin-sensitive PI(3)K-mTOR-p70S6K pathway. Nat Immunol. 2008;9(10):1157-64.
130. Colina R, Costa-Mattioli M, Dowling RJ, Jaramillo M, Tai LH, Breitbach CJ, et al. Translational control of the innate immune response through IRF-7. Nature. 2008;452(7185):323-8.
131. Alain T, Lun X, Martineau Y, Sean P, Pulendran B, Petroulakis E, et al. Vesicular stomatitis virus oncolysis is potentiated by impairing mTORC1-dependent type I IFN production. Proc Natl Acad Sci U S A. 2010;107(4):1576-81. PMCID: 2824402.
132. Bouvier NM, Palese P. The biology of influenza viruses. Vaccine. 2008;26 Suppl 4:D49-53. PMCID: 3074182.
133. Portela A, Digard P. The influenza virus nucleoprotein: a multifunctional RNA-binding protein pivotal to virus replication. J Gen Virol. 2002;83(Pt 4):723-34.
134. Chen W, Calvo PA, Malide D, Gibbs J, Schubert U, Bacik I, et al. A novel influenza A virus mitochondrial protein that induces cell death. Nat Med. 2001;7(12):1306-12.
135. Lamb RA, Choppin PW, Chanock RM, Lai CJ. Mapping of the two overlapping genes for polypeptides NS1 and NS2 on RNA segment 8 of influenza virus genome. Proc Natl Acad Sci U S A. 1980;77(4):1857-61. PMCID: 348607.
136. Matlin KS, Reggio H, Helenius A, Simons K. Infectious entry pathway of influenza virus in a canine kidney cell line. J Cell Biol. 1981;91(3 Pt 1):601-13. PMCID: 2112819.
137. Maeda T, Kawasaki K, Ohnishi S. Interaction of influenza virus hemagglutinin with target membrane lipids is a key step in virus-induced

hemolysis and fusion at pH 5.2. Proc Natl Acad Sci U S A. 1981;78(7):4133-7. PMCID: 319742.
138. O'Neill RE, Jaskunas R, Blobel G, Palese P, Moroianu J. Nuclear import of influenza virus RNA can be mediated by viral nucleoprotein and transport factors required for protein import. J Biol Chem. 1995;270(39):22701-4.
139. Herz C, Stavnezer E, Krug R, Gurney T, Jr. Influenza virus, an RNA virus, synthesizes its messenger RNA in the nucleus of infected cells. Cell. 1981;26(3 Pt 1):391-400.
140. Plotch SJ, Bouloy M, Ulmanen I, Krug RM. A unique cap(m7GpppXm)-dependent influenza virion endonuclease cleaves capped RNAs to generate the primers that initiate viral RNA transcription. Cell. 1981;23(3):847-58.
141. Dias A, Bouvier D, Crepin T, McCarthy AA, Hart DJ, Baudin F, et al. The cap-snatching endonuclease of influenza virus polymerase resides in the PA subunit. Nature. 2009;458(7240):914-8.
142. Li X, Palese P. Characterization of the polyadenylation signal of influenza virus RNA. J Virol. 1994;68(2):1245-9. PMCID: 236570.
143. Linding R, Jensen LJ, Ostheimer GJ, van Vugt MA, Jorgensen C, Miron IM, et al. Systematic discovery of in vivo phosphorylation networks. Cell. 2007;129(7):1415-26. PMCID: 2692296.
144. Whittaker G, Bui M, Helenius A. Nuclear trafficking of influenza virus ribonuleoproteins in heterokaryons. J Virol. 1996;70(5):2743-56. PMCID: 190131.
145. Pawson T, Linding R. Network medicine. FEBS Lett. 2008;582(8):1266-70.
146. Fujii Y, Goto H, Watanabe T, Yoshida T, Kawaoka Y. Selective incorporation of influenza virus RNA segments into virions. Proc Natl Acad Sci U S A. 2003;100(4):2002-7. PMCID: 149948.
147. Lutz G. Virology of Human Influenza. Influenza Report 2006: Flying Publisher; 2006.
148. Hale BG, Randall RE, Ortin J, Jackson D. The multifunctional NS1 protein of influenza A viruses. J Gen Virol. 2008;89(Pt 10):2359-76.
149. Greenspan D, Palese P, Krystal M. Two nuclear location signals in the influenza virus NS1 nonstructural protein. J Virol. 1988;62(8):3020-6. PMCID: 253741.
150. Melen K, Kinnunen L, Fagerlund R, Ikonen N, Twu KY, Krug RM, et al. Nuclear and nucleolar targeting of influenza A virus NS1 protein: striking differences between different virus subtypes. J Virol. 2007;81(11):5995-6006. PMCID: 1900311.
151. Li Y, Yamakita Y, Krug RM. Regulation of a nuclear export signal by an adjacent inhibitory sequence: the effector domain of the influenza virus NS1 protein. Proc Natl Acad Sci U S A. 1998;95(9):4864-9. PMCID: 20179.

152. Nemeroff ME, Barabino SM, Li Y, Keller W, Krug RM. Influenza virus NS1 protein interacts with the cellular 30 kDa subunit of CPSF and inhibits 3'end formation of cellular pre-mRNAs. Mol Cell. 1998;1(7):991-1000.
153. Li Y, Chen ZY, Wang W, Baker CC, Krug RM. The 3'-end-processing factor CPSF is required for the splicing of single-intron pre-mRNAs in vivo. RNA. 2001;7(6):920-31. PMCID: 1370139.
154. Chen Z, Li Y, Krug RM. Influenza A virus NS1 protein targets poly(A)-binding protein II of the cellular 3'-end processing machinery. EMBO J. 1999;18(8):2273-83. PMCID: 1171310.
155. Poon LL, Pritlove DC, Fodor E, Brownlee GG. Direct evidence that the poly(A) tail of influenza A virus mRNA is synthesized by reiterative copying of a U track in the virion RNA template. J Virol. 1999;73(4):3473-6. PMCID: 104115.
156. Robertson JS, Schubert M, Lazzarini RA. Polyadenylation sites for influenza virus mRNA. J Virol. 1981;38(1):157-63. PMCID: 171135.
157. Satterly N, Tsai PL, van Deursen J, Nussenzveig DR, Wang Y, Faria PA, et al. Influenza virus targets the mRNA export machinery and the nuclear pore complex. Proc Natl Acad Sci U S A. 2007;104(6):1853-8. PMCID: 1794296.
158. Donelan NR, Basler CF, Garcia-Sastre A. A recombinant influenza A virus expressing an RNA-binding-defective NS1 protein induces high levels of beta interferon and is attenuated in mice. J Virol. 2003;77(24):13257-66. PMCID: 296096.
159. Hatada E, Fukuda R. Binding of influenza A virus NS1 protein to dsRNA in vitro. J Gen Virol. 1992;73 ( Pt 12):3325-9.
160. Hatada E, Takizawa T, Fukuda R. Specific binding of influenza A virus NS1 protein to the virus minus-sense RNA in vitro. J Gen Virol. 1992;73 ( Pt 1):17-25.
161. Gack MU, Albrecht RA, Urano T, Inn KS, Huang IC, Carnero E, et al. Influenza A virus NS1 targets the ubiquitin ligase TRIM25 to evade recognition by the host viral RNA sensor RIG-I. Cell Host Microbe. 2009;5(5):439-49. PMCID: 2737813.
162. Min JY, Krug RM. The primary function of RNA binding by the influenza A virus NS1 protein in infected cells: Inhibiting the 2'-5' oligo (A) synthetase/RNase L pathway. Proc Natl Acad Sci U S A. 2006;103(18):7100-5. PMCID: 1459024.
163. Min JY, Li S, Sen GC, Krug RM. A site on the influenza A virus NS1 protein mediates both inhibition of PKR activation and temporal regulation of viral RNA synthesis. Virology. 2007;363(1):236-43.
164. Ehrhardt C, Marjuki H, Wolff T, Nurnberg B, Planz O, Pleschka S, et al. Bivalent role of the phosphatidylinositol-3-kinase (PI3K) during influenza virus infection and host cell defence. Cell Microbiol. 2006;8(8):1336-48.

165. Hale BG, Jackson D, Chen YH, Lamb RA, Randall RE. Influenza A virus NS1 protein binds p85beta and activates phosphatidylinositol-3-kinase signaling. Proc Natl Acad Sci U S A. 2006;103(38):14194-9. PMCID: 1599933.
166. Ehrhardt C, Wolff T, Pleschka S, Planz O, Beermann W, Bode JG, et al. Influenza A virus NS1 protein activates the PI3K/Akt pathway to mediate antiapoptotic signaling responses. J Virol. 2007;81(7):3058-67. PMCID: 1866065.
167. Zhang L, Das P, Schmolke M, Manicassamy B, Wang Y, Deng X, et al. Inhibition of pyrimidine synthesis reverses viral virulence factor-mediated block of mRNA nuclear export. J Cell Biol. 2012;196(3):315-26. PMCID: 3275370.
168. Garcia-Sastre A, Egorov A, Matassov D, Brandt S, Levy DE, Durbin JE, et al. Influenza A virus lacking the NS1 gene replicates in interferon-deficient systems. Virology. 1998;252(2):324-30.
169. Talon J, Horvath CM, Polley R, Basler CF, Muster T, Palese P, et al. Activation of interferon regulatory factor 3 is inhibited by the influenza A virus NS1 protein. J Virol. 2000;74(17):7989-96. PMCID: 112330.
170. Wang X, Li M, Zheng H, Muster T, Palese P, Beg AA, et al. Influenza A virus NS1 protein prevents activation of NF-kappaB and induction of alpha/beta interferon. J Virol. 2000;74(24):11566-73. PMCID: 112437.
171. McNaney CA, Drexler DM, Hnatyshyn SY, Zvyaga TA, Knipe JO, Belcastro JV, et al. An automated liquid chromatography-mass spectrometry process to determine metabolic stability half-life and intrinsic clearance of drug candidates by substrate depletion. Assay Drug Dev Technol. 2008;6(1):121-9.
172. Ramirez RD, Sheridan S, Girard L, Sato M, Kim Y, Pollack J, et al. Immortalization of human bronchial epithelial cells in the absence of viral oncoproteins. Cancer Res. 2004;64(24):9027-34.
173. Yuen T, Wurmbach E, Pfeffer RL, Ebersole BJ, Sealfon SC. Accuracy and calibration of commercial oligonucleotide and custom cDNA microarrays. Nucleic Acids Res. 2002;30(10):e48. PMCID: 115302.
174. Kanehisa M, Araki M, Goto S, Hattori M, Hirakawa M, Itoh M, et al. KEGG for linking genomes to life and the environment. Nucleic Acids Res. 2008;36(Database issue):D480-4. PMCID: 2238879.
175. Kerrien S, Alam-Faruque Y, Aranda B, Bancarz I, Bridge A, Derow C, et al. IntAct--open source resource for molecular interaction data. Nucleic Acids Res. 2007;35(Database issue):D561-5. PMCID: 1751531.
176. Prasad TS, Kandasamy K, Pandey A. Human Protein Reference Database and Human Proteinpedia as discovery tools for systems biology. Methods Mol Biol. 2009;577:67-79.
177. http://www.reactome.org.
178. Hoffmann R, Valencia A. A gene network for navigating the literature. Nat Genet. 2004;36(7):664.

179. Stumpf MP, Thorne T, de Silva E, Stewart R, An HJ, Lappe M, et al. Estimating the size of the human interactome. Proc Natl Acad Sci U S A. 2008;105(19):6959-64. PMCID: 2383957.
180. Cabusora L, Sutton E, Fulmer A, Forst CV. Differential network expression during drug and stress response. Bioinformatics. 2005;21(12):2898-905.
181. Mawuenyega KG, Forst CV, Dobos KM, Belisle JT, Chen J, Bradbury EM, et al. Mycobacterium tuberculosis functional network analysis by global subcellular protein profiling. Mol Biol Cell. 2005;16(1):396-404. PMCID: 539182.
182. Eppstein D. Finding the k shortest paths. SIAM J Computing. 1998;28:652-73.
183. Hershberger J, Maxel M, Suri S, editors. Finding the k shortest simple paths: A new algorithm and its implementation. 5th Workshop on Algorithm Engineering and Experiments; 2003; SIAM Conferences.
184. Chakraborty P, Wang Y, Wei JH, van Deursen J, Yu H, Malureanu L, et al. Nucleoporin levels regulate cell cycle progression and phase-specific gene expression. Dev Cell. 2008;15(5):657-67. PMCID: 2835575.
185. Levy DE, Garcia-Sastre A. The virus battles: IFN induction of the antiviral state and mechanisms of viral evasion. Cytokine Growth Factor Rev. 2001;12(2-3):143-56.
186. Zhao M, Zhang J, Phatnani H, Scheu S, Maniatis T. Stochastic expression of the interferon-beta gene. PLoS Biol. 2012;10(1):e1001249. PMCID: 3265471.
187. Randall RE, Goodbourn S. Interferons and viruses: an interplay between induction, signalling, antiviral responses and virus countermeasures. J Gen Virol. 2008;89(Pt 1):1-47.
188. Desmyter J, Melnick JL, Rawls WE. Defectiveness of interferon production and of rubella virus interference in a line of African green monkey kidney cells (Vero). J Virol. 1968;2(10):955-61. PMCID: 375423.
189. Durbin JE, Hackenmiller R, Simon MC, Levy DE. Targeted disruption of the mouse Stat1 gene results in compromised innate immunity to viral disease. Cell. 1996;84(3):443-50.
190. Ludwig S, Planz O, Pleschka S, Wolff T. Influenza-virus-induced signaling cascades: targets for antiviral therapy? Trends Mol Med. 2003;9(2):46-52.
191. Hara K, Maruki Y, Long X, Yoshino K, Oshiro N, Hidayat S, et al. Raptor, a binding partner of target of rapamycin (TOR), mediates TOR action. Cell. 2002;110(2):177-89.
192. Kim DH, Sarbassov DD, Ali SM, King JE, Latek RR, Erdjument-Bromage H, et al. mTOR interacts with raptor to form a nutrient-sensitive complex that signals to the cell growth machinery. Cell. 2002;110(2):163-75.

193. Sarbassov DD, Ali SM, Kim DH, Guertin DA, Latek RR, Erdjument-Bromage H, et al. Rictor, a novel binding partner of mTOR, defines a rapamycin-insensitive and raptor-independent pathway that regulates the cytoskeleton. Curr Biol. 2004;14(14):1296-302.
194. Harris TE, Lawrence JC, Jr. TOR signaling. Sci STKE. 2003;2003(212):re15.
195. Memmott RM, Dennis PA. Akt-dependent and -independent mechanisms of mTOR regulation in cancer. Cell Signal. 2009;21(5):656-64. PMCID: 2650010.
196. Zhirnov OP, Klenk HD. Control of apoptosis in influenza virus-infected cells by up-regulation of Akt and p53 signaling. Apoptosis. 2007;12(8):1419-32.
197. Ma XM, Blenis J. Molecular mechanisms of mTOR-mediated translational control. Nat Rev Mol Cell Biol. 2009;10(5):307-18.
198. Hresko RC, Mueckler M. mTOR.RICTOR is the Ser473 kinase for Akt/protein kinase B in 3T3-L1 adipocytes. J Biol Chem. 2005;280(49):40406-16.
199. Sarbassov DD, Guertin DA, Ali SM, Sabatini DM. Phosphorylation and regulation of Akt/PKB by the rictor-mTOR complex. Science. 2005;307(5712):1098-101.
200. Stokoe D, Stephens LR, Copeland T, Gaffney PR, Reese CB, Painter GF, et al. Dual role of phosphatidylinositol-3,4,5-trisphosphate in the activation of protein kinase B. Science. 1997;277(5325):567-70.
201. Ellisen LW. Growth control under stress: mTOR regulation through the REDD1-TSC pathway. Cell Cycle. 2005;4(11):1500-02.
202. Sarbassov DD, Ali SM, Sabatini DM. Growing roles for the mTOR pathway. Curr Opin Cell Biol. 2005;17(6):596-603.
203. Yang Z, Klionsky DJ. Mammalian autophagy: core molecular machinery and signaling regulation. Curr Opin Cell Biol. 2010;22(2):124-31. PMCID: 2854249.
204. Kabeya Y, Mizushima N, Ueno T, Yamamoto A, Kirisako T, Noda T, et al. LC3, a mammalian homologue of yeast Apg8p, is localized in autophagosome membranes after processing. EMBO J. 2000;19(21):5720-8. PMCID: 305793.
205. Zhang Y, Gao X, Saucedo LJ, Ru B, Edgar BA, Pan D. Rheb is a direct target of the tuberous sclerosis tumour suppressor proteins. Nat Cell Biol. 2003;5(6):578-81.
206. Zoncu R, Efeyan A, Sabatini DM. mTOR: from growth signal integration to cancer, diabetes and ageing. Nat Rev Mol Cell Biol. 2011;12(1):21-35.
207. Kudchodkar SB, Levine B. Viruses and autophagy. Rev Med Virol. 2009;19(6):359-78.
208. Braciale TJ, Sun J, Kim TS. Regulating the adaptive immune response to respiratory virus infection. Nat Rev Immunol. 2012;12(4):295-305. PMCID: 3364025.

209. Holt PG, Strickland DH, Wikstrom ME, Jahnsen FL. Regulation of immunological homeostasis in the respiratory tract. Nat Rev Immunol. 2008;8(2):142-52.
210. Lin KL, Suzuki Y, Nakano H, Ramsburg E, Gunn MD. CCR2+ monocyte-derived dendritic cells and exudate macrophages produce influenza-induced pulmonary immune pathology and mortality. J Immunol. 2008;180(4):2562-72.
211. Becker S, Quay J, Soukup J. Cytokine (tumor necrosis factor, IL-6, and IL-8) production by respiratory syncytial virus-infected human alveolar macrophages. J Immunol. 1991;147(12):4307-12.
212. Tumpey TM, Garcia-Sastre A, Taubenberger JK, Palese P, Swayne DE, Pantin-Jackwood MJ, et al. Pathogenicity of influenza viruses with genes from the 1918 pandemic virus: functional roles of alveolar macrophages and neutrophils in limiting virus replication and mortality in mice. J Virol. 2005;79(23):14933-44. PMCID: 1287592.
213. Kim HM, Lee YW, Lee KJ, Kim HS, Cho SW, van Rooijen N, et al. Alveolar macrophages are indispensable for controlling influenza viruses in lungs of pigs. J Virol. 2008;82(9):4265-74. PMCID: 2293066.
214. Beaty SR, Rose CE, Jr., Sung SS. Diverse and potent chemokine production by lung CD11bhigh dendritic cells in homeostasis and in allergic lung inflammation. J Immunol. 2007;178(3):1882-95.
215. Moltedo B, Li W, Yount JS, Moran TM. Unique type I interferon responses determine the functional fate of migratory lung dendritic cells during influenza virus infection. PLoS Pathog. 2011;7(11):e1002345. PMCID: 3207893.
216. McGill J, Heusel JW, Legge KL. Innate immune control and regulation of influenza virus infections. J Leukoc Biol. 2009;86(4):803-12. PMCID: 2752015.
217. Kim TS, Braciale TJ. Respiratory dendritic cell subsets differ in their capacity to support the induction of virus-specific cytotoxic CD8+ T cell responses. PLoS One. 2009;4(1):e4204. PMCID: 2615220.
218. Ballesteros-Tato A, Leon B, Lund FE, Randall TD. Temporal changes in dendritic cell subsets, cross-priming and costimulation via CD70 control CD8(+) T cell responses to influenza. Nat Immunol. 2010;11(3):216-24. PMCID: 2822886.
219. Waithman J, Mintern JD. Dendritic cells and influenza A virus infection. Virulence. 2012;3(7):603-8. PMCID: 3545942.
220. Nakano H, Lin KL, Yanagita M, Charbonneau C, Cook DN, Kakiuchi T, et al. Blood-derived inflammatory dendritic cells in lymph nodes stimulate acute T helper type 1 immune responses. Nat Immunol. 2009;10(4):394-402. PMCID: 2668134.
221. Larsson M, Messmer D, Somersan S, Fonteneau JF, Donahoe SM, Lee M, et al. Requirement of mature dendritic cells for efficient activation of influenza A-specific memory CD8+ T cells. J Immunol. 2000;165(3):1182-90.

222. Sun J, Madan R, Karp CL, Braciale TJ. Effector T cells control lung inflammation during acute influenza virus infection by producing IL-10. Nat Med. 2009;15(3):277-84. PMCID: 2693210.
223. Billiau A. Interferon-gamma: biology and role in pathogenesis. Adv Immunol. 1996;62:61-130.
224. Baumgarth N, Kelso A. In vivo blockade of gamma interferon affects the influenza virus-induced humoral and the local cellular immune response in lung tissue. J Virol. 1996;70(7):4411-8. PMCID: 190374.
225. Moskophidis D, Kioussis D. Contribution of virus-specific CD8+ cytotoxic T cells to virus clearance or pathologic manifestations of influenza virus infection in a T cell receptor transgenic mouse model. J Exp Med. 1998;188(2):223-32. PMCID: 2212460.
226. Guermonprez P, Valladeau J, Zitvogel L, Thery C, Amigorena S. Antigen presentation and T cell stimulation by dendritic cells. Annu Rev Immunol. 2002;20:621-67.
227. Hennet T, Ziltener HJ, Frei K, Peterhans E. A kinetic study of immune mediators in the lungs of mice infected with influenza A virus. J Immunol. 1992;149(3):932-9.
228. Tamura S, Kurata T. Defense mechanisms against influenza virus infection in the respiratory tract mucosa. Jpn J Infect Dis. 2004;57(6):236-47.
229. Monteiro JM, Harvey C, Trinchieri G. Role of interleukin-12 in primary influenza virus infection. J Virol. 1998;72(6):4825-31. PMCID: 110027.
230. Yoshida T, Mett I, Bhunia AK, Bowman J, Perez M, Zhang L, et al. Rtp801, a suppressor of mTOR signaling, is an essential mediator of cigarette smoke-induced pulmonary injury and emphysema. Nat Med. 2010;16(7):767-73.
231. Vlahos R, Bozinovski S, Jones JE, Powell J, Gras J, Lilja A, et al. Differential protease, innate immunity, and NF-kappaB induction profiles during lung inflammation induced by subchronic cigarette smoke exposure in mice. Am J Physiol Lung Cell Mol Physiol. 2006;290(5):L931-45.
232. Almeida M, Han L, Ambrogini E, Bartell SM, Manolagas SC. Oxidative stress stimulates apoptosis and activates NF-kappaB in osteoblastic cells via a PKCbeta/p66shc signaling cascade: counter regulation by estrogens or androgens. Mol Endocrinol. 2010;24(10):2030-7. PMCID: 2954638.
233. Reiterer G, Toborek M, Hennig B. Quercetin protects against linoleic acid-induced porcine endothelial cell dysfunction. J Nutr. 2004;134(4):771-5.
234. Shi MM, Chong I, Godleski JJ, Paulauskis JD. Regulation of macrophage inflammatory protein-2 gene expression by oxidative stress in rat alveolar macrophages. Immunology. 1999;97(2):309-15. PMCID: 2326837.
235. Fujita T, Kohno S. Studies on interferon priming: cellular response to viral and nonviral inducers and requirement of protein synthesis. Virology. 1981;112(1):62-9.

236. Servant MJ, Grandvaux N, tenOever BR, Duguay D, Lin R, Hiscott J. Identification of the minimal phosphoacceptor site required for in vivo activation of interferon regulatory factor 3 in response to virus and double-stranded RNA. J Biol Chem. 2003;278(11):9441-7.
237. Dunn GP, Koebel CM, Schreiber RD. Interferons, immunity and cancer immunoediting. Nat Rev Immunol. 2006;6(11):836-48.
238. Sheehan KC, Lai KS, Dunn GP, Bruce AT, Diamond MS, Heutel JD, et al. Blocking monoclonal antibodies specific for mouse IFN-alpha/beta receptor subunit 1 (IFNAR-1) from mice immunized by in vivo hydrodynamic transfection. J Interferon Cytokine Res. 2006;26(11):804-19.
239. Takaoka A, Hayakawa S, Yanai H, Stoiber D, Negishi H, Kikuchi H, et al. Integration of interferon-alpha/beta signalling to p53 responses in tumour suppression and antiviral defence. Nature. 2003;424(6948):516-23.
240. Silverman RH. Implications for RNase L in prostate cancer biology. Biochemistry. 2003;42(7):1805-12.
241. Munoz-Fontela C, Macip S, Martinez-Sobrido L, Brown L, Ashour J, Garcia-Sastre A, et al. Transcriptional role of p53 in interferon-mediated antiviral immunity. J Exp Med. 2008;205(8):1929-38. PMCID: 2525597.
242. Ahuja D, Saenz-Robles MT, Pipas JM. SV40 large T antigen targets multiple cellular pathways to elicit cellular transformation. Oncogene. 2005;24(52):7729-45.